PHASE I Final Report for VRA Modeling Contract NAS8-38250-18

Louis M. Kindt
Michael E. Mullins, PhD.
David W. Hand, PhD.
Andrew A. Kline, PhD.

Michigan Technological University
Departments of Chemical and Civil/Environmental Engineering
1400 Townsend Dr.
Houghton, MI 49931

Submitted to:

John Garr
ION Electronics
6767 Madison Pike
Huntsville, AL 35803

The Peclet numbers determined for the differential test reaction on every trial indicates that the flow through the differential test reactor satisfies the plug flow criteria. However, the extremely small catalyst volume in this reactor makes it susceptible to very small changes in the packing. This is demonstrated by the difference in tests 1-3 versus 4 and 5, which were conducted on different days upon changing the reactors in and out of service.

The criteria for the use of reactor Peclet numbers are as follows :

$Pe_r > 10$: Assume plug flow

$2 < Pe_r < 10$: Axial dispersion significant

$Pe_r < 2$: Model as CSTR

On the other hand, the residence times determined for the VRA covered a fairly wide range of approximately 9 to 17 minutes. The corresponding Peclet numbers range from 3.84 to 6.64, also a rather large range. Both results point to a highly non-ideal reactor flow pattern; certainly outside the range of plug flow. One possibility is that the oxygen flow rate may be the source of these problems due to buildup of gas pockets, or channeling. However, four RTD trials with the VRA with no oxygen flow produced the following values shown in Table II:

TABLE II - RTD analysis for VRA with no oxygen flow

Trial	t_m (min)	σ^2	Pe_r
1	10.04	19.09	13.62
2	10.89	38.74	8.87
3	13.41	141.65	4.70
4	13.75	124.69	5.32
AVERAGE	12.02±1.59	81.04±52.93	8.13±3.55

The absence of gas in the column did increase the value of the reactor Peclet number; however, the large deviation in the Peclet number shows that the oxygen flow had no effect

TABLE OF CONTENTS

LIST OF FIGURES

LIST OF TABLES

ABSTRACT

The destruction of organic contaminants in waste water for closed systems, such as that of Space Station, is crucial due to the need for recycling the waste water. A co-current upflow bubble column using oxygen as the gas phase oxidant and packed with catalyst particles consisting of a noble metal on an alumina substrate is being developed for this process. The objective of this study is to develop a plug-flow model that will predict the performance of this three phase reactor system in destroying a multicomponent mixture of organic contaminants in water. Mass balances on a series of contaminants and oxygen in both the liquid and gas phases are used to develop this model. These mass balances incorporate the gas-to-liquid and liquid-to-particle mass transfer coefficients, the catalyst effectiveness factor, and intrinsic reaction rate. To validate this model, a bench scale reactor has been tested at Michigan Technological University at elevated pressures (50-83 psig) and a temperature range of 200 to 290°F. Feeds consisting of five dilute solutions of ethanol (~10 ppm), chlorobenzene (~20 ppb), formaldehyde (~ 100 ppb), dimethyl sulfoxide (DMSO ~300 ppb), and urea (~20 ppm) in water were tested individually with an oxygen mass flow rate of 0.009 lb/h. The results from these individual tests were used to develop the kinetic parameter inputs necessary for the computer model. The computer simulated results are compared to the experimental data obtained for all 5 components run in a mixture on the differential test column for a range of reactor contact times.

INTRODUCTION

Recovery of waste water streams for potable use on board space-based installations, such as the International Space Station (ISS), is paramount for long term missions in space. Although carbon adsorption and ion exchange can remove a large majority of the pollutants in such streams, weakly adsorbing organic compounds must still be removed in order to make the water potable. One method of removing these organic compounds is via catalytic oxidation. A catalytic reactor system known as the Volatile Removal Assembly (VRA) is

being designed to perform such an operation. The VRA is a co-current bubble column which uses gas-phase oxygen as the oxidant over a catalyst consisting of a noble metal on an alumina substrate. In the earth based testing, the VRA is run in an upflow mode. In zero gravity the gas phase will be moved only under the influence of the water's drag forces. Therefore, the residence time of the gas and liquid phases may be slightly altered. Before the design and operating conditions for the VRA are finalized, a numerical model incorporating mass transfer, contacting patterns, and the multicomponent reaction kinetics should be developed and tested in order to predict the reactor's performance. This report focuses on the model derivation and validation for a five component dilute aqueous solution.

Heterogeneous catalysts can be used effectively in oxygen purged packed bed reactors to remove aqueous organics at elevated temperatures. Goto and Smith [1] have shown that conversions of formic acid are quite high in a trickle bed reactor. Goto and Mabuchi [2] have shown that ethanol can be readily oxidized to acetic acid in either an upflow or downflow packed bed reactor. Numerous studies have been reported for oxidation of single components through packed beds, mostly in downflow trickle bed reactors [1], [2], [3],[4]. A thorough review revealed no studies on the multiphase oxidation of multicomponent streams. A small number of studies were found on the mass transfer characteristics of co-current upflow packed bubble columns (also known as flooded bed reactors). The extension of earlier models to a multicomponent mixture and the determination of the necessary parameters are described below.

BACKGROUND

A flooded bed reactor is a reactor in which a continuous liquid phase and a disperse gas phase flow co-currently through a fixed bed of catalyst particles while a reaction takes place. The rate at which this reaction occurs is a function of the mass transfer rates for the reactants, internal (pore) mass transfer, and the actual surface reaction rate. Figure 1 represents the external mass transfer processes occurring for a single catalyst particle within the reactor.

As the continuous phase, the liquid generally covers the catalyst particle. The gas phase

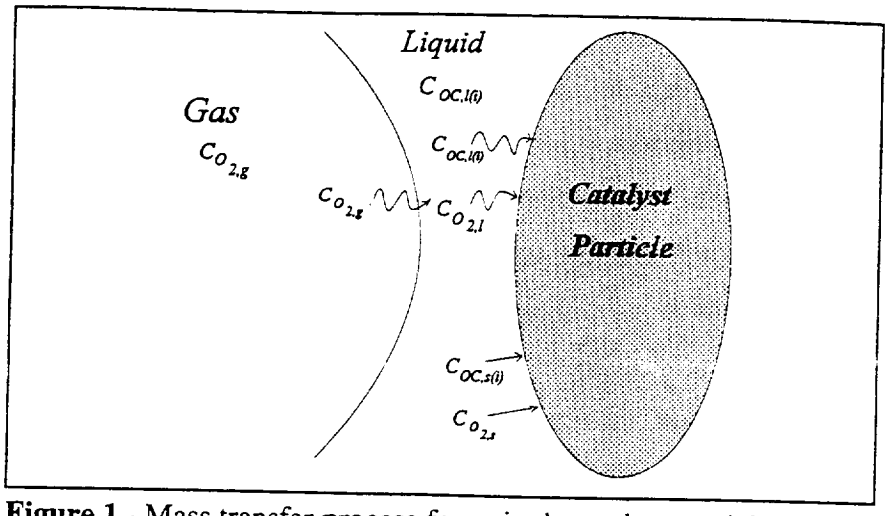

Figure 1 - Mass transfer process for a single catalyst particle.

(in the form of bubbles) forces its way between the liquid covered particles. The key steps in the mass transfer process are the transfer of the reactant (oxygen) from the gas to the liquid and of all the reactants from the liquid to the catalyst particle surface. The other reactants in the aqueous phase are the dilute aqueous organic contaminants (OC's). The basic transport and reaction steps in this three phase reaction are as follows:

1. Transport of oxygen from the bulk gas phase to the gas-liquid interface.
2. Equilibrium partitioning of oxygen at the gas-liquid interface.
3. Transport of oxygen from the interface to the bulk liquid.
4. Transport of the OC's and oxygen from the bulk liquid to the catalyst surface.
5. Diffusion and reaction of the reactants inside the catalyst pellet.

By taking these basic transport and reaction steps into account along with an appropriate reactor model, the behavior of a flooded bed reactor can be determined.

Before the behavior of a flooded bed reactor can be determined, an appropriate model must first be derived. The primary assumptions for the model are :

1. Isothermal reactor operation - Since the concentration of the contaminants is very low, the heat generated by the oxidation reactions has a negligible effect on the water temperature.
2. Axial dispersion in the gas phase is negligible - The bubbles would tend to move forward as self-contained units. Little backmixing would be possible.
3. Conditions are uniform in the radial direction - The liquid is evenly dispersed in the radial direction.
4. Gas and liquid flow rates are constant throughout the reactor - This is the standard steady state assumption (no accumulation).
5. Mass transfer resistances in the gas phase are negligible so that equilibrium exists at the gas-liquid interface - The diffusion rate in the gas phase is several orders of magnitude higher than the liquid phase.

Axial dispersion models take into account the diffusion of the components in the axial direction, whereas plug flow models typically assume axial dispersion is negligible. The following differential mass balances for the organic contaminants (OC) and oxygen in the liquid and gas phases are as Goto and Smith derived [1] for both axial dispersion and plug flow models.

Axial Dispersion Model

If plug flow cannot be assumed, then the more general axial dispersion model should be used. This model is derived from the molar material balances on each reactant in each phase. For a tubular reactor these take on the form of differential material balances over each increment of length, z, of the reactor. If we assume the principal reactions occur over the surface of the catalyst, the equations below result.

Material balance on oxygen in the gas phase - The only mechanism by which oxygen is removed from the gas phase is via mass transfer to the water. Since we are neglecting axial

dispersion in the gas phase, the plug flow balance is:

$$V_g \frac{dC_{O_2,g}}{dz} - (k_l a)_{O_2} A\left(C^{*}_{O_2,l} - C_{O_2,l}\right) = 0 \qquad (1)$$

Oxygen in the liquid phase - For disperse flow, a second order differential term in the equation to account for this dispersion results. Oxygen is added to the liquid via mass transfer from the gas phase (second term), and removed by transport to the catalyst surface (last term).

$$D_a A \frac{d^2 C_{O_2,l}}{dz^2} - V_l \frac{dC_{O_2,l}}{dz} - (k_l a)_{O_2} A\left(C^{*}_{O_2,l} - C_{O_2,l}\right) - (k_s a)_{O_2} A\left(C_{O_2,l} - C_{O_2,s}\right) = 0 \qquad (2)$$

Organic contaminants in the liquid phase - The disperse flow equation for each contaminant, i, shows the depletion of organic from the liquid by transfer to the surface.

$$D_{a_{(i)}} A \frac{d^2 C_{OC,l_{(i)}}}{dz^2} - V_l \frac{dC_{OC,l_{(i)}}}{dz} - (k_s a)_{OC_{(i)}} A\left(C_{OC,l_{(i)}} - C_{OC,s_{(i)}}\right) = 0 \qquad (3)$$

Consideration of the flux balances at the entrance and exit conditions leads to the following boundary conditions, known as the "Danckwerts boundary conditions" [5].

At the inlet conditions (z = 0),

$$C_{O_2,g} = \left(C_{O_2,g}\right)_f \qquad (4)$$

$$-D_a A \frac{dC_{O_2,l}}{dz} = V_l \left[\left(C_{O_2,l}\right)_f - C_{O_2,l}\right] \qquad (5)$$

$$D_{a_{(i)}} A \frac{dC_{OC,l_{(i)}}}{dz} = V_l \left[\left(C_{OC,l_{(i)}} \right)_f - C_{OC,l_{(i)}} \right] \quad (6)$$

At the outlet conditions (z = L)

$$\frac{dC_{O_2,l}}{dz} = 0 \quad (7)$$

$$\frac{dC_{OC,l_{(i)}}}{dz} = 0 \quad (8)$$

Using the above equations and boundary conditions, a "predictor-corrector" numerical method can be used to fit the equations to an experimental data set.

Plug Flow Model

If plug flow conditions can be assumed, the axial dispersion is negligible and the second order terms in the above equations may be removed. The axial dispersion equations reduce to the following simplified equations.

Oxygen in the gas phase :

$$V_g \frac{dC_{O_2,g}}{dz} + (k_l a)_{O_2} A \left(C^*_{O_2,l} - C_{O_2,l} \right) = 0 \quad (9)$$

Oxygen in the liquid phase :

$$- V_l \frac{dC_{O_2,l}}{dz} + (k_l a)_{O_2} A \left(C^*_{O_2,l} - C_{O_2,l} \right) - (k_s a)_{O_2} A \left(C_{O_2,l} - C_{O_2,s} \right) = 0 \quad (10)$$

Organic contaminants in the liquid phase :

$$- V_l \frac{dC_{OC,l_{(i)}}}{dz} - (k_s a)_{OC_{(i)}} A\left(C_{OC,l_{(i)}} - C_{OC,s_{(i)}}\right) = 0 \qquad (11)$$

The boundary conditions in for the plug flow model are known at z = 0 :

$$C_{OC,l} = \left(C_{OC,l_i}\right)_f \qquad (12)$$

$$C_{O_2,l} = \left(C_{O_2,l}\right)_f \qquad (13)$$

Surface Concentrations

The overall reaction on the surface of the catalyst is

$$OC_i - \alpha_i O_2 \rightarrow \beta_i CO_2 - \gamma_i H_2O \qquad (14)$$

Before any of the above equations can be solved, the surface concentration C_s must be related to the bulk liquid concentration C_l. Since the rate of reaction is limited by the rate of mass transfer of the components to the surface and the rate of mass transfer from the surface is limited by the rate of reaction, at steady state, these two terms are equal. By incorporating an effectiveness factor, the equality between mass transfer and reaction rates can be expressed as follows :

$$(k_s a)_{O_2}\left[\left(C_{O_2,l}\right) - \left(C_{O_2,s}\right)\right] = r_{O_2} = \rho_{cat} \sum \eta_i f\left[\left(C_{O_2,s}\right), \left(C_{OC,s_i}\right)\right] \qquad (15)$$

$$(k_s a)_{OC_{(i)}}\left[(C_{OC,l_{(i)}}) - (C_{OC,s_{(i)}})\right] = r_{OC_{(i)}} = \frac{\rho_{cat}}{\alpha_i}\eta_i f\left[(C_{O_2,s}), (C_{OC,s_{(i)}})\right] \quad (16)$$

These equations for both the axial dispersion and the plug flow models must be solved simultaneously . For Phase I of the project, we are examining very dilute contaminant mixtures, so a reasonable starting assumption is a simple kinetic rate expression which is first order with respect to the organic contaminants and oxygen :

$$f\left[(C_{O_2,s}), (C_{OC,s_i})\right] = k_{OC_i}(C_{O_2,s})(C_{OC,s_i}) \quad (17)$$

This kinetic rate expression is the usage rate of oxygen for each individual organic contaminant. The test of whether this is a valid approach or if a more sophisticated reaction rate model is required, is the match between the combined contaminant model results and the experimental data for that mixture. Competitive adsorption effects would cause the model to deviate significantly if they are important. If this is the case one would use a competitive adsorption model such as the Mars-van Krevelan model to account for such effects. However, this is a two parameter rate law, requiring more extensive experimental studies to determine the values of both rate constants.

For plug flow, the model used is based on an Fortran based ordinary differential equation solving algorithm (LSODE) coupled with a Newton-Raphson's method for nonlinear equation solving. The LSODE algorithm, which is based on the Adam's method, solves the given set of plug flow differential equations and returns the values of the dependent variables. The algorithm is set up to return the results as a function of empty bed contact time. This approach is more robust than determining the concentrations as a function of bed length, in that contact time allows scaling of the model to many different reactor geometries. The model also employs Newton-Raphson's method for computing the values for the surface concentration of the components. The equations are constrained so that the roots are always positive. These values are substituted into the differential equations along with the other known parameters, to obtain the values of the derivatives. This model was validated by comparing the output to actual data obtained for acetic acid and formic acid [1].

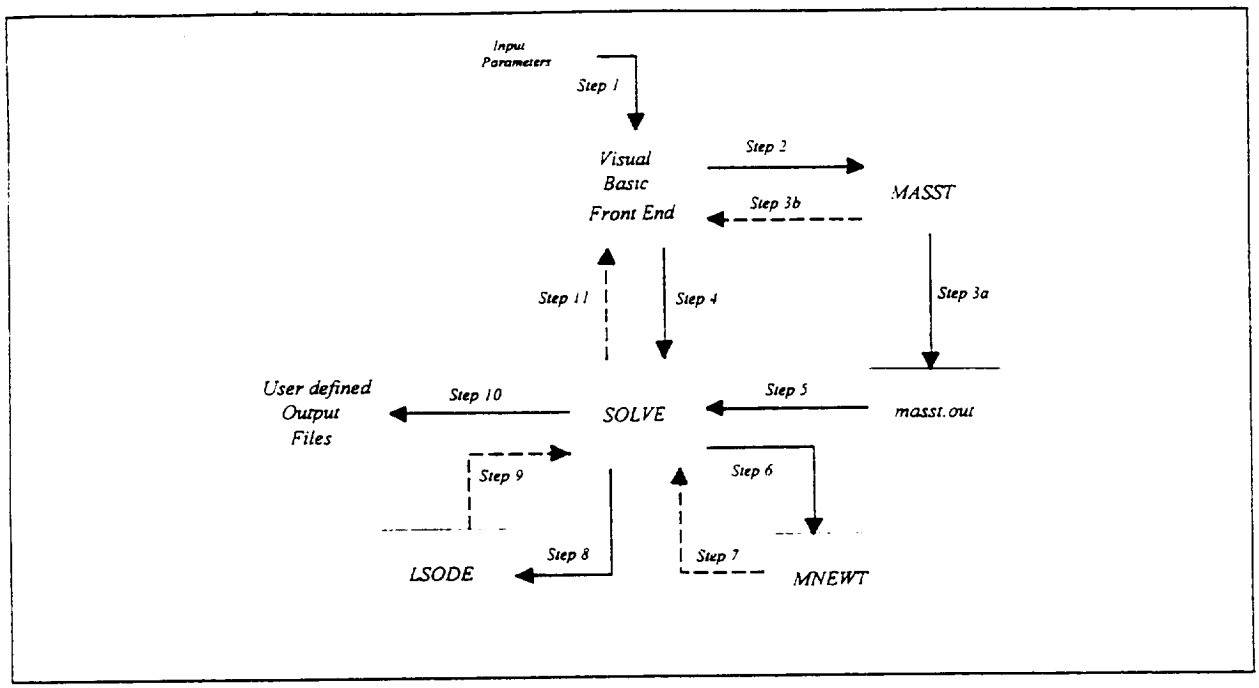

Figure 2- Flow diagram for computer model *

* - Step 1 : Input necessary parameters

Step 2 : Visual Basic writes parameters to 'mass-p.out' an executes MASST.EXE

Step 3a : MASST writes calculated quantities to output file 'masst.out'

Step 3b : Visual Basic reads 'masst.out' and displays output

Step 4 : Visual Basic writes necessary parameters to 'solve-p.out' and executes SOLVE.EXE

Step 5 : 'mass-p.out' and 'masst.out' are read into SOLVE

Step 6 : MNEWT is called and calculates surface concentrations

Step 7 : MNEWT returns surface concentrations to SOLVE

Step 8 : LSODE is called to solve plug flow equations

Step 9 : LSODE returns solution to plug flow equations to SOLVE

Step 10 : SOLVE writes solution to user defined output files and 'fconc.out'

Step 11 : 'fconc.out' is read into Visual Basic and the final concentration and conversion is displayed

Figure 2 shows the flow diagram for the computer model. The sequence begins with the user entering the necessary inputs into the visual basic front end. These input include diameter of the column, volumetric flow rate of the liquid, volumetric flow rate of oxygen at standard conditions, desired contact time, output files, and tolerances for LSODE and the non-linear equation solver. Because of problems with transferring variables between Visual Basic® and Fortran, the Visual Basic® front end writes these parameters to an output file 'mass-p.out' and executes MASST.EXE where all of the mass transfer and kinetic properties

are calculated. MASST then writes these variables to an output file called 'masst.out'. For user reference, the Visual Basic® front end also reads this file and displays them on the screen. Once the mass transfer properties are calculated, the front end writes the necessary parameters to 'solve-p.out' and executes SOLVE.EXE where remaining calculations are performed. After the initial parameters are read into from 'solve-p.out' into SOLVE, the mass transfer and kinetic properties are read into SOLVE from 'masst.out'. SOLVE then calls MNEWT, which calculates the surface concentrations of the components using the above mentioned Newton-Raphson algorithm for finding roots of systems of non-linear equations. MNEWT then returns the surface concentrations to SOLVE. The nonlinear differential equation solver LSODE is then called, which solves the plug flow equations for each of the components. These values are returned to SOLVE where they are printed to user defined output files. One of the files is an ASCII file and the other is a comma delimited file for use in spreadsheet programs such as Quattro-Pro or Lotus. Once the integration is completed, SOLVE writes the final concentrations to an output file called 'solve.out' which the Visual Basic front end reads and displays the final concentration and calculated conversion of the components.

RESIDENCE TIME DISTRIBUTIONS

In a flooded bed reactor, the reaction media usually does not flow through the bed uniformly. Often times there will exist sections in the packed catalyst which offer little resistance to flow and as a result a major portion of the liquid will flow through this section. Consequently, the molecules flowing through this section do not spend as much time in the reactor as those molecules subjected to the high resistance areas. The time that the molecules spend in the reactor is called the residence time. Since all of the molecules do not spend the same amount of time in the reactor, as would be the case for ideal reactors, a residence time distribution (RTD) is used to determine the characteristics specific to each individual reactor.

RTD's are determined experimentally by injecting an inert chemical called a tracer into the reactor at some initial time (t=0) and then measuring the tracer concentration, C, in the

effluent stream as a function of time. The good tracer must be nonreactive, easily detectible, soluble in the mixture, and should have properties similar to those of the reacting mixture. It also should not absorb on any of the surfaces within the reactor. A pulse input is one of the most common methods to determine RTD's.

In a pulse input, a given amount of tracer is suddenly injected into the feed stream entering the reactor. The outlet concentration is then measured as a function of time. Figure 3 shows the injection/response curves for a pulse injection.

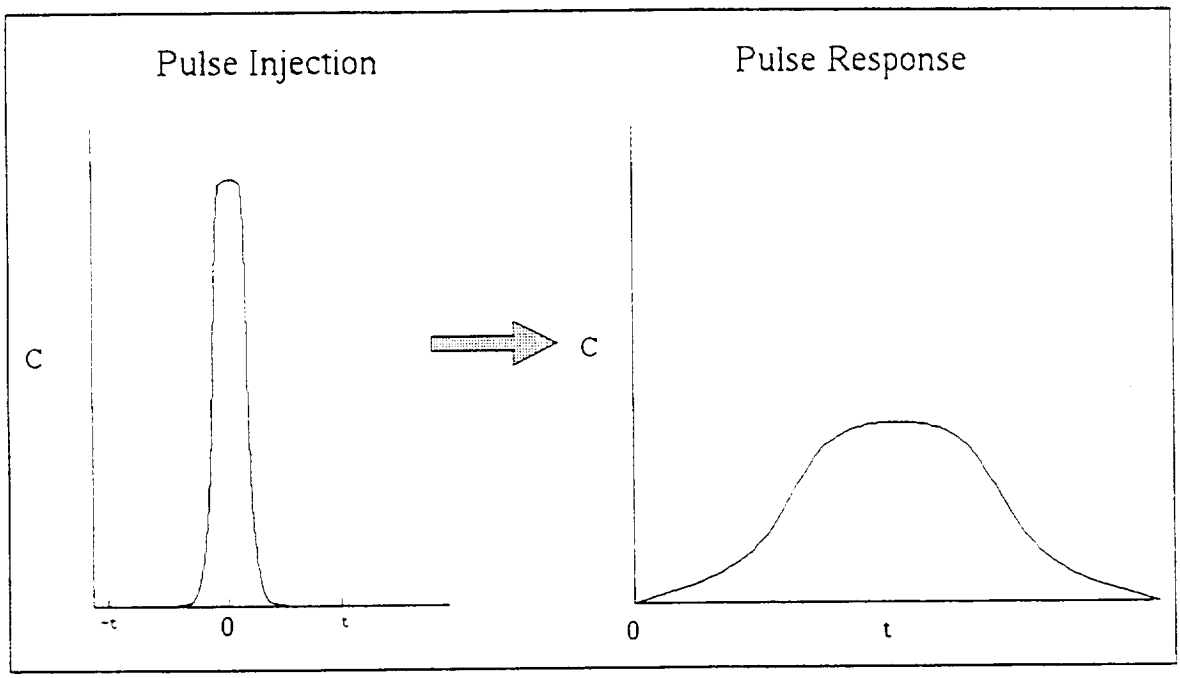

Figure 3 - RTD Measurements for Pulse Input

The residence time distribution function, E(t), describes in a quantitative manner how much time different fluid elements have spent in the reactor. For pulse inputs with constant volumetric flow rate, E(t), is defined by equation 18 [6].

$$E(t)=\frac{C(t)}{\int_0^\infty C(t)dt} \tag{18}$$

Since this is not an ideal reactor system, the space time cannot be used for the residence time. Because of this, a mean residence time, t_m, must be determined. This quantity is simply the first moment of the RTD function, E(t). This moment is defined by equation 19 [6].

$$t_m = \int_0^\infty t\ E(t)\ dt \tag{19}$$

The second moment of the RTD function is also an important parameter needed to evaluate the RTD. This moment is known as the variance, or square of the standard deviation, σ^2. It is defined by equation 20 [6].

$$\sigma^2 = \int_0^\infty (t - t_m)^2 E(t) dt \tag{20}$$

From concentration-time data, all of the above parameters can be determined.

Axial Dispersion Coefficient

Axial dispersion is the process by which components mix and diffuse in the axial direction. The axial dispersion coefficient takes these effects into account and is a required parameter in the axial dispersion model of the trickle bed reactor design equations. The Peclet number is used to determine the axial dispersion coefficient. Two different forms of the Peclet number are in common use - the reactor Peclet number, Pe_r, and the fluid Peclet number Pe_f. These two quantities are defined by equations 21 and 22 respectively [6].

$$Pe_r = \frac{u_f L}{D_a} \tag{21}$$

$$Pe_f = \frac{u_f d_p}{D_a} \tag{22}$$

The fluid Peclet number is given in all correlations relating the Reynolds number to the Peclet number because both depend on fluid mechanics. Although many correlations are available that relate the Peclet number to the Reynolds and Schmidt numbers, experimental determination of the Peclet number is considered more accurate.

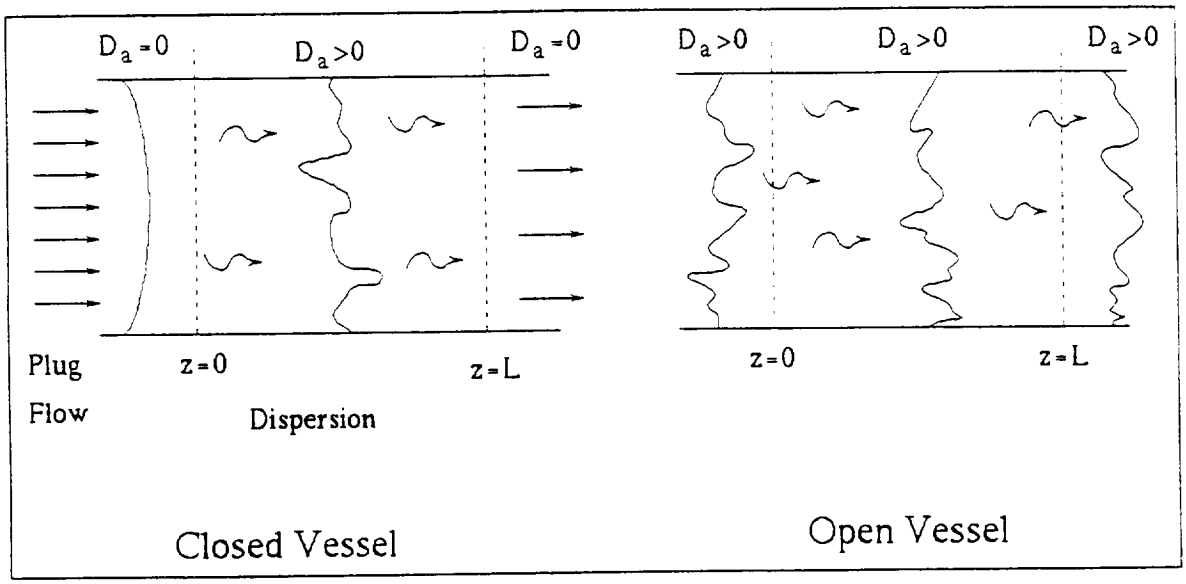

Figure 4 - Axial Dispersion Models

For a closed-closed vessel, dispersion takes place only in the packed bed - the entrance and exit voids have no dispersion, as indicated by Figure 4. In an open-open vessel, dispersion exists in both of the entrance and exit voids as well as in the packed bed. Since there are two different models, two different equations must be used to determine the Peclet number. For the closed-closed vessel, equation 23 defines the Peclet number in terms of mean residence time and variance. Equation 24 defines the same parameters for an open-open system.

$$\frac{\sigma^2}{t_m^2} = \frac{2}{Pe_r} - \frac{2}{Pe_r^2}\left(1 - e^{-Pe_r}\right) \tag{23}$$

$$\frac{\sigma^2}{t_m^2} = \frac{2}{Pe_r} - \frac{8}{Pe_r^2} \qquad (24)$$

Examination of the VRA and differential test reactor revealed open volumes at either end of the reactor, thus the open-open model was used for both calculations. The Peclet number can consequently be solved for by using the RTD data described previously.

Axial or Plug Flow

In order to determine which model to use, the criteria suggested by Satterfield [7] was used. This correlation relates the reactor length L and particle diameter d_p to the fluid Peclet number. Axial dispersion is negligible and the plug flow model can be used if :

$$\frac{L}{d_p} > \frac{20}{Pe_f} \cdot n \cdot \ln \frac{1}{1-X} \qquad (25)$$

Initial RTD studies on the differential reactor indicated that it did indeed satisfy the above criteria and is operating in plug flow. However, RTD studies on the VRA did not satisfy this criteria indicating dispersion must be taken into account (see Appendix A for calculations)

Residence Time Data

A variety of tracer compounds including several organic dyes were tested as pulsed inputs. Even at ambient conditions these dyes were either decolorized or destroyed by the reactor bed. Finally, an ammonium hydroxide solution was used and the outlet concentration monitored by connecting a pH meter to the data acquisition system. Four trials were conducted on the VRA with a liquid flow rate of ≈ 120 ml/min and a gas flow rate of ≈ 50 ml/min. The test reactor was also run at conditions comparable to the VRA. From this data, the residence time distribution function was determined (shown in Figures 5 and 6 for the

VRA and test column respectively). From these quantities, the Peclet number was determined using the nonideal open-open system model. Table I lists the parameters obtained from the RTD analysis.

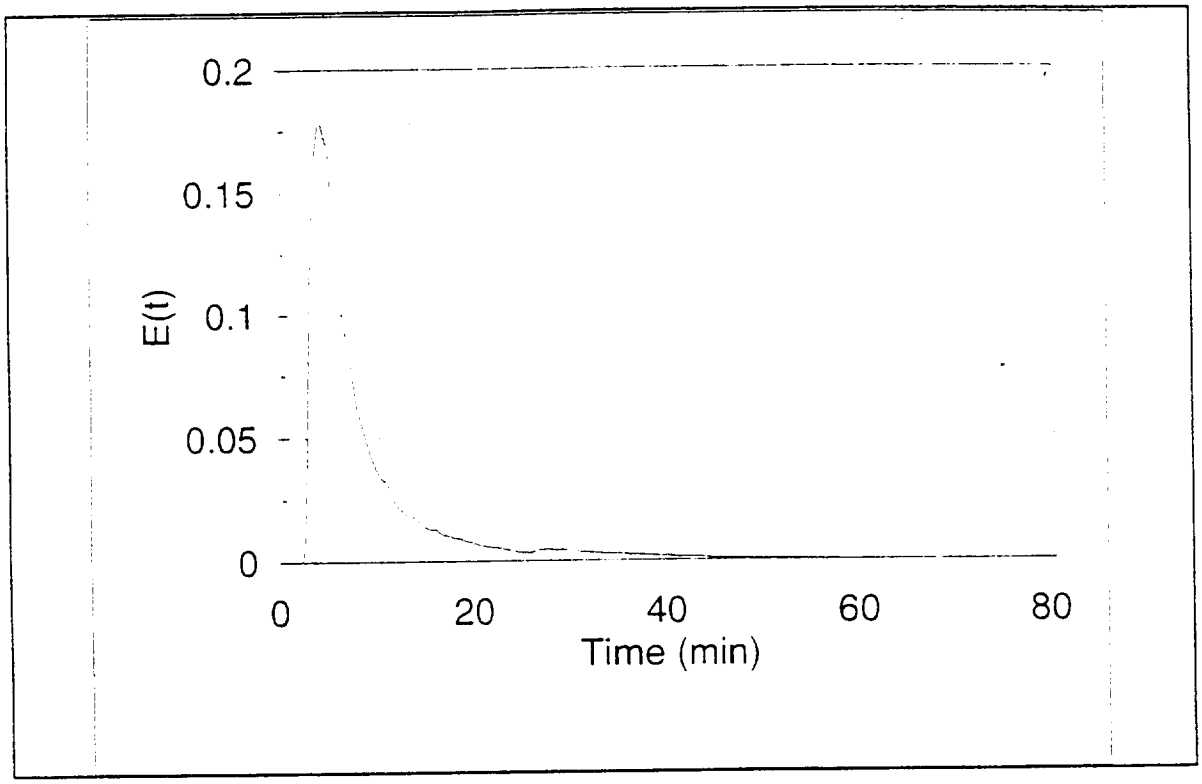

Figure 5 - RTD analysis of VRA

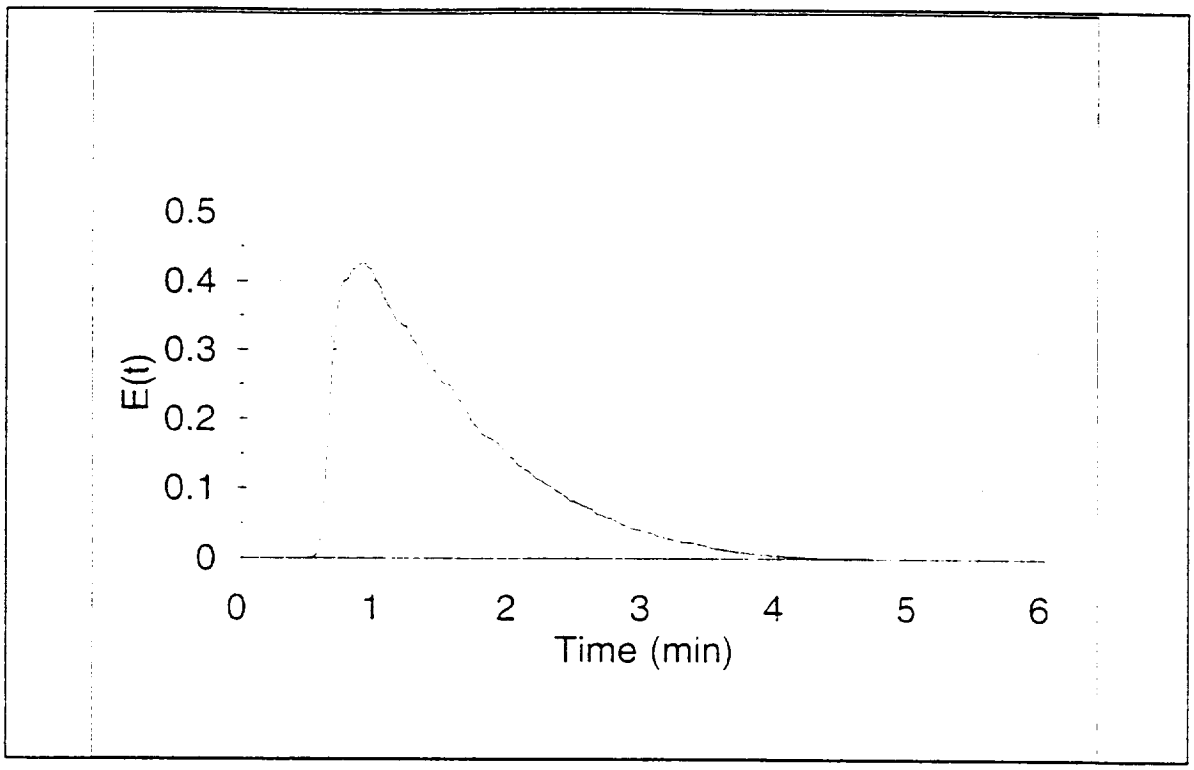

Figure 6 - RTD analysis for differential reactor

TABLE I - RTD Analysis with oxygen flow

Trial	VRA REACTOR			TEST REACTOR		
	t_m (min)	σ^2	Pe_r	t_m(min)	σ^2	Pe_r
1	9.02	73.68	4.27	1.52	0.48	12.60
2	11.68	65.85	6.64	1.51	0.49	12.28
3	17.11	310.43	3.84	1.49	0.46	12.64
4	15.40	241.70	3.95	1.03	0.15	17
5	---	---	---	0.98	0.15	16.05
AVERAGE	13.30 ±3.16	172.92 ±106.01	4.67±1.14	1.30 ±0.25	0.35 ±0.16	14.11 ±1.99

The Peclet numbers determined for the differential test reaction on every trial indicates that the flow through the differential test reactor satisfies the plug flow criteria. However, the extremely small catalyst volume in this reactor makes it susceptible to very small changes in the packing. This is demonstrated by the difference in tests 1-3 versus 4 and 5, which were conducted on different days upon changing the reactors in and out of service.

The criteria for the use of reactor Peclet numbers are as follows :

$Pe_r > 10$: Assume plug flow

$2 < Pe_r < 10$: Axial dispersion significant

$Pe_r < 2$: Model as CSTR

On the other hand, the residence times determined for the VRA covered a fairly wide range of approximately 9 to 17 minutes. The corresponding Peclet numbers range from 3.84 to 6.64, also a rather large range. Both results point to a highly non-ideal reactor flow pattern; certainly outside the range of plug flow. One possibility is that the oxygen flow rate may be the source of these problems due to buildup of gas pockets, or channeling. However, four RTD trials with the VRA with no oxygen flow produced the following values shown in Table II:

TABLE II - RTD analysis for VRA with no oxygen flow

Trial	t_m (min)	σ^2	Pe_r
1	10.04	19.09	13.62
2	10.89	38.74	8.87
3	13.41	141.65	4.70
4	13.75	124.69	5.32
AVERAGE	12.02±1.59	81.04±52.93	8.13±3.55

The absence of gas in the column did increase the value of the reactor Peclet number; however, the large deviation in the Peclet number shows that the oxygen flow had no effect

on the reproducability of these variables. Disassembly of the VRA proved that the catalyst bed was packed tightly, so no attempt was made to repack the reactor. The dead space that existed on each end of the packed bed might contribute to the axial dispersion, but not enough to account for the observed behavior. The only major contributing factors which might account for the observed behavior is either adsorption/desorption in the bed, or channeling around the reactor fittings. The ammonium hydroxide tracer was the only one of 5 different tracers (four others were organic dyes) which produced a "clean" peak at the exit, so the adsorption effects were small compared to the organic dyes. However, fairly small adsorption effects may cause the RTD to deviate considerably from the ideal performance. Inorganic ion tracers were not used for fear of "fouling" the catalyst surface; but perhaps low concentrations of chloride ion could be used as an alternative tracer material with minimal detrimental effects on the catalyst.

MODEL PARAMETERS

Prior to executing the model, parameters such as the solid to liquid mass transfer coefficients, gas to liquid mass transfer coefficients, rate constants, and gas-liquid equilibrium concentrations had to be determined. The mass transfer coefficients were estimated using techniques from various authors. Table III lists examples of the parameters and physical constants used in the model for ethanol, chlorobenzene, and oxygen. A complete list of parameters for all five contaminants as a function of temperature and flowrate are listed in Appendix A.

The gas to liquid mass transfer coefficient was estimated using the correlation recommended by Alexander and Shah [8]. An exhaustive search found this to be the empirical correlation which most closely matched the operation of the VRA. The correlation was adjusted to our particle size by multiplying the ratio of the particle surface area, a, used in their study to the particle surface area used in this study. The equation is listed as equation number 26.

TABLE III - Sample parameters used in computer model

T : 200 °F	Henry's Constant for O_2 : 42.189 (dimensionless)		
	Flow Rate (ml/min)		
	100	80	60
$(k_x a)_{Ethanol}$ (1/s)	0.165	0.167	0.17
$(k_x a)_{Chlorobenzene}$ (1/s)	0.068	0.069	0.07
$(k_x a)_{DMSO}$ (1/s)	0.101	0.102	0.104
$(k_x a)_{Formaldehyde}$ (1/s)	0.128	0.13	0.132
$(k_x a)_{Urea}$ (1/s)	0.145	0.147	0.149
$(k_x a)_{Oxygen}$ (1/s)	0.547	0.489	0.423
$(k_l a)_{Oxygen}$ (1/s)	0.024	0.0224	0.0206
$k_{Ethanol}$: 547300 $cm^6/(gmol \cdot g_{catalyst} \cdot s)$		$k_{chlorobenzene}$: $5.257 \times 10^7 cm^6/(gmol \cdot g_{catalyst} \cdot s)$	
k_{DMSO} : 737260$cm^6/(gmol \cdot g_{catalyst} \cdot s)$		$k_{Formaldehyde}$: $1.00 \times 10^{15} cm^6/(gmol \cdot g_{catalyst} \cdot s)$	
k_{Urea} : 223900$cm^6/(gmol \cdot g_{catalyst} \cdot s)$			

$$k_l a = 0.06371 \left(\frac{3.17}{1.03} \right) \left(V_l' \right)^{0.3014} \left(V_g' \right)^{0.4484} \quad \sec^{(-1)} \tag{26}$$

The liquid to solid mass transfer coefficient was estimated using the technique recommended by Mochizuki [9]. For our conditions, the final working equation is

$$\frac{Sh}{Sc^{1/3}} = 0.75 Re_l^{0.5} \tag{27}$$

The Reynold's number in this case is defined as:

$$Re_l = \frac{d_h u_l}{\epsilon_l \nu_l} \tag{28}$$

Where the liquid hold-up is estimated by

$$\epsilon_l = \frac{V_l}{V_l + V_g}$$

and the hydraulic diameter, d_h, used in the dimensionless numbers is based on liquid hold-up, ϵ_l, as

$$d_h = \frac{\epsilon_l d_p}{1.5(1-\epsilon_l)} \tag{30}$$

and the average actual liquid velocity (u_l) is also used in the dimensionless numbers. The mass transfer coefficient is related to the Sherwood number, which is defined as

$$Sh = \frac{k_s u_l}{D_l} \tag{31}$$

and the effective external surface area available for mass transfer is defined as

$$a = \frac{6(1-\epsilon)}{d_p} \tag{32}$$

The Henry's law constant for oxygen in water was taken from Himmelblau [10]. Since in the temperature regime of interest, the Henry' law constant is not a simple function of temperature, this value was found by solving the roots of the nonlinear equations for the temperature of interest. The diffusion coefficient for oxygen, urea, and ethanol was taken from Perry's [11] and adjusted accordingly using temperature and viscosity. Diffusion coefficients for chlorobenzene, DMSO, and formaldehyde were estimated using the Hayduk and Minhas method [12]. Details of the calculations may be found in Appendix A.

The surface reaction rate constants were obtained from the computer model by fitting the data for each individual component. Using the parameters in Table III and a second order

rate expression (1st order in organic contaminant and 1st order in oxygen), the kinetic rate constant was adjusted until the model prediction agreed with the experimental effluent concentrations over a range of contact times. A"Golden Section" computer algorithm was written for this optimization. This algorithm takes output from the VRA computer model and optimizes the rate constant until the predicted effluent concentration converges to the experimental effluent concentration. This calculated rate constant also incorporates the particle effectiveness factor. A more detailed description of this process is discussed later.

Experimental Mass Transfer Coefficients

To qualitatively verify the validity of the mass transfer correlations being employed, it is desirable to have experimental estimates of these rates. This may be done semi-empirically for the liquid - solid mass transfer coefficient by examining the rate of reaction for a range of flowrates. Extension of this technique to three phase systems is more uncertain. At any point in the column, the overall rate of transport is at steady state. Because of this, the rate of transport from the bubble to the liquid is equal to the rate of transport to the catalyst surface which is equal to the rate of reaction on the catalyst pellet (equation 33).

$$r_{overall} = (k_s a)_{OC_{(i)}} \left(C_{OC,l_{(i)}} - C_{OC,s_{(i)}}\right) = \frac{\eta_i}{\alpha_i} k_{OC_{(i)}} C_{O_2,s} C_{OC,s_{(i)}} \qquad (33)$$

By rearranging the above equations and adding, we arrive at the following equation:

$$\frac{C_{OC,l}}{r_{overall}} = \frac{\alpha}{k_{OC} \eta C_{O_2,s}} + \frac{1}{k_s a} \qquad (34)$$

By using Colburn "j" correlations for mass transfer, the volumetric flowrate, Q, can be related to $k_s a$ at constant particle diameter according to equation 34, where the empirical exponent γ is usually varied between, 0.25 and 0.45 to give the straightest line [13].

$$k_s a \propto Q^{\gamma} \tag{35}$$

If the surface concentration of oxygen does not vary significantly over the range of flowrates examined (e.g. - a large excess of oxygen exists) equation 34 can be reduced to a linear form which can then be plotted and the variables easily solved according to equation 36.

$$\frac{C_{OC,l}}{r_{overall}} = b_n - \frac{A_n}{Q^{\gamma}} \tag{36}$$

Where,

A_n = the slope of the line for particle size n

b_n = the y-intercept of particle size n, $1/k_{OC}\eta_i C_{O2,s}$

The resulting graph is similar to Figure 7.

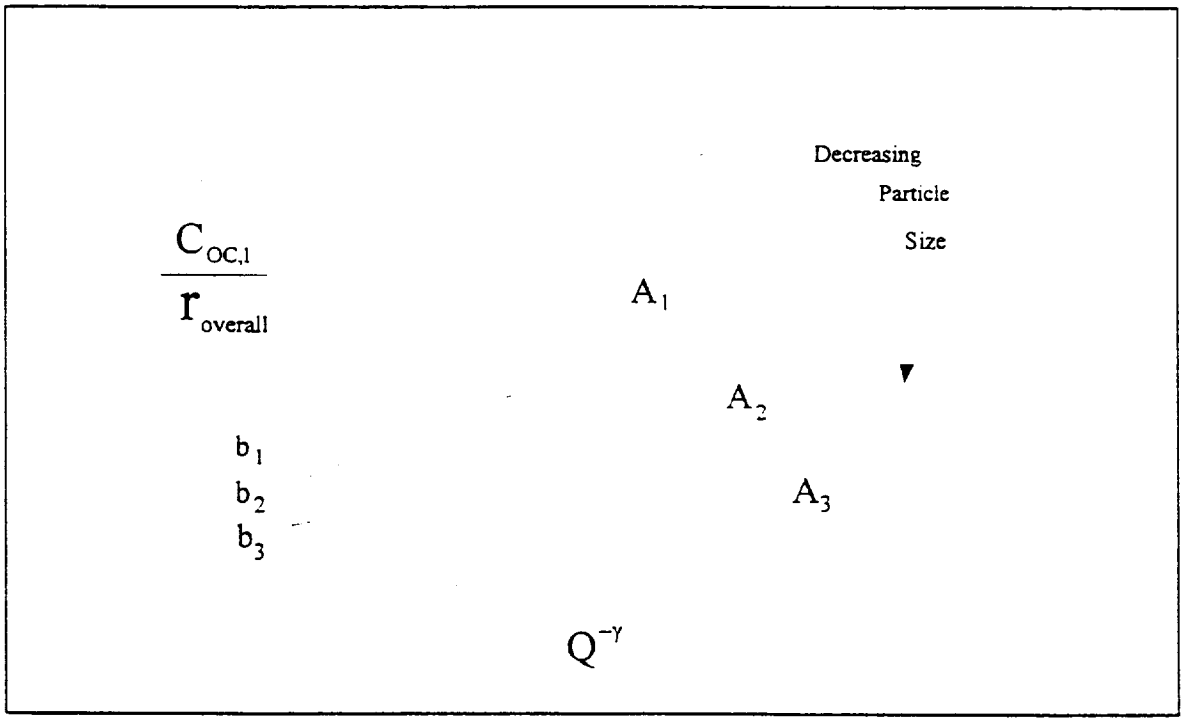

Figure 7 - Effect of Particle Size on Reaction Rate

The liquid solid mass transfer coefficient is subsequently obtained from the absolute difference between the intercept and the point on the plot for the desired flowrate. As the

particle size decreases, the external mass transfer resistance decreases due to the increasing particle surface area. If the surface oxygen concentration is not present in large excess the plot may not be linear. In the limit (e.g. - very high flowrates) the value of the intercept does indeed represent the surface concentration. However, at lower flowrate (in range measured), the actual surface concentration may be lower. To account for this one may algebraically estimate the external mass transfer coefficient by iteratively solving equation 32 for the values of surface concentration which linearize the plot. In this fashion, values of the mass transfer coefficient for ethanol at 60 ml/min and 100 ml/min of 0.13 sec^{-1} and 0.08 sec^{-1}, respectively, were determined over the raw catalyst. These are slightly lower than those predicted via the correlation, but are representative of the range of values seen for our entire range of operating conditions. In light of the several experimental uncertainties with the above process, the data seems in line with the correlation for modelling purposes.

Internal Effectiveness Factor and Rate Constant

Since a highly porous catalyst is being used, the entire surface of the catalyst is not accessible to the same concentration of reactants. To account for this variation, the rate law is modified to include an internal effectiveness factor, η. This effectiveness factor may be lumped together with the intrinsic rate constant if a constant catalyst size is used. However, to predict the reaction rates over different size catalysts it is essential. Although this is not directly used in our model for the VRA, extensions to different catalyst sizes may be desirable, and thus the effectiveness factor of the present system should be evaluated. The modified rate law takes into account the rate of reaction and the rate of diffusion into the catalyst and is written as equation 37.

$$-\frac{dC_{OC_i}}{dt} = -r_{OC_i} = \frac{\rho_{cat}}{\alpha_i}\eta k_{OC} C_{O_2,s} C_{OC,s_i} \qquad (37)$$

The effectiveness factor for the catalyst under consideration has been determined using three different methods: theoretical determination from the catalyst pellet physical properties

using the Thiele modulus approach [13], analysis of the value of ηk_{α} for 2 different catalyst particle sizes (as from the intercepts above)[14], and an iterative solution of the Thiele moduli for one experimental data point [14]. The first approach is based totally upon the physical characteristics of the catalyst pellet (see Table III), and the use of the second order Theile moduli equations. Uncertainties arise in this analysis based upon the surface reaction rate constants (effective rates) employed. Appendix A shows the details of this standard calculation. An effectiveness factor for ethanol over the raw catalyst particle of 0.012 is calculated via this method. The second technique is based upon knowing the reaction rate over two different catalyst sizes, and finding the two values of the Theile modulus which satisfies those conditions. Since the ratio of the particle radii is equal to the ratio of their Theile moduli, the analytical relationship between the Theile moduli and the effectiveness factors should provide unique solutions. Finding these values entails using a non-linear fitting technique for comparing experimental data for 2 particle sizes. The actual calculations are detailed in Appendix A. This method requires that the effectiveness factor for the two catalyst sizes be sufficiently different. This fitting technique yields an effectiveness factor value of 0.008.

Finally, in the third technique, the effectiveness factor can be calculated from one experimental condition by a trial and error iterative solution using the same relationships between the particle radius, Theile modulus, and effectiveness factors described above. Since for isothermal conditions, the effectiveness factor is bounded by 0 and 1, it is easiest to iterate on the effectiveness factor. This last approach may be the strongest, in that it makes no assumptions about the surface reaction conditions. The effectiveness factor calculated via this final technique (ethanol at 200° F) is 0.007. This value is in close agreement with the two point estimate (0.008). Details of this calculation are shown in Appendix A.

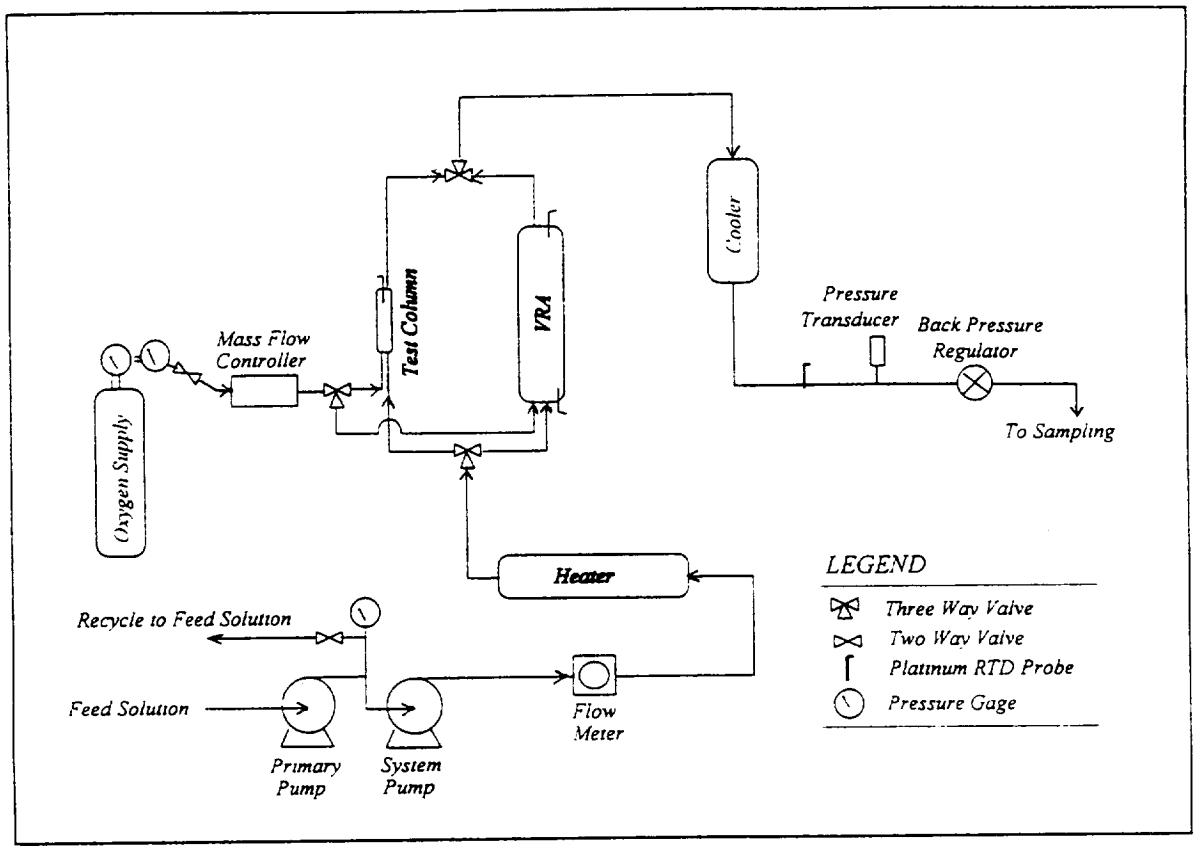

Figure 8- Schematic diagram of reactor set-up

EXPERIMENTAL SECTION

Equipment Description

Figure 8 shows a schematic diagram of the bench scale reactor system. The feed solutions were prepared in 12 gallon glass carboys, and supplied to the reactor system using pulseless rotary gear pump heads. Two pumps were used - a primary pump to raise the inlet conditions of the system to about 30-40 psig and a secondary system pump which maintained the desired system pressure. The flow rate was monitored using a stainless steel rotary flow meter. The feed was heated in a large heat exchanger and then routed via a three way valve to either the bench scale VRA or a small differential test reactor. The majority of the model parameters were obtained on the differential reactor which consisted of a section of

0.5"diameter by 3.25" length stainless steel pipe. The length of the catalyst packed bed was 2.8", and the remaining volume at the ends of the reactor were packed with glass wool. The VRA consists of 1.5" diameter 1.5' length stainless steel pipe packed with catalyst. Heat tape is wrapped on the exterior to maintain the VRA at constant temperature. Platinum RTD probes are placed at the inlet and outlet of the VRA to monitor the temperature. The tubing was insulated from the heater to the differential reactor and VRA. To monitor the temperature of the differential reactor, a platinum RTD probe was inserted into the top of the reactor. The oxygen flow rate was controlled by a mass flow controller, and entered the bottom of the reactors via 1/16 " stainless steel tubing. The effluent stream was cooled to ambient temperature via tap water in a counter-current heat exchanger. At this point the pressure was monitored via a pressure transducer and subsequently controlled via a back pressure regulator, which maintained the system at a constant pressure. All temperatures, pressures, and flow rates were fed to a data acquisition system where they were continuously monitored via Labview for Windows on a desktop computer.

The test solutions were made by dissolving enough ethanol, formaldehyde, urea, dimethyl sulfoxide, and/or chlorobenzene in the 12 gallon carboys to make the initial concentrations of 10 ppm, 100 ppb, 3 ppm, 300 ppb, or 20 ppb, respectively. The reactor assembly flow rate is first set via the primary pump and secondary system pump. Once the liquid has reached the back pressure regulator, the regulator and the throttle valve on the primary pump recycle can be adjusted to achieve the desired flow rate and pressure. The preheater was then adjusted to the desired operating temperature. Once enough data points were collected at steady state at one temperature, the temperature was increased to the next temperature while holding the flow rate constant. Preliminary studies indicated that a reactor steady state was reached within 1.5 hrs. After all the data was collected at each temperature for three flow rates, the assembly was allowed to cool down and the process was then repeated. To test for mass transfer effects, ethanol and chlorobenzene were separately run though the system at three different water flow rates (100ml/min, 80 ml/min, and 60 ml/min) at 200° F over three different sizes of catalyst particles. Extension to other components and temperatures will be discussed later. Three different operating pressures (50 psig, 67 psig, and 90 psig) were examined. Ethanol and chlorobenzene at concentrations of 10 ppm and 20 ppb respectively,

were first individually tested at all of the flow rates, temperatures, and pressures; and then a combination of the two components at similar concentrations in the feed were examined. Finally, the reaction over the raw catalyst (d_p~1 mm) was compared to that over a smaller size fraction (80 - 100 mesh). Kinetic data was obtained separately for the raw catalyst for all five components at five different temperatures (200°F, 220°F, 240°F, 250 °F, and 270°F) at a flow rate of 100 ml/min and pressure of 67 psig. Samples of the effluent were taken every 10 minutes in sealed vials for further analyses.

Analytical Chemistry

Samples for chlorobenzene were analyzed via the purge and trap method. The purge and trap used was a Tekmar ALS-10 controlled by a Tekmar LSC 2000 controller. The purge and trap was connected to a Hewlett Packard model 5840A gas chromatograph with a Volcol 105 meter by 0.53 mm ID capillary column with a 3 micron film thickness. The chlorobenzene was detected via an FID with nitrogen as the carrier gas at a flow rate of 60 ml/min. The temperature program started at 60°C and increased at a rate of 3°C/min to a final temperature of 132°C. With this temperature program, the chlorobenzene had a retention time of 23.5 minutes. To ensure an accurate calibration curve, standards for chlorobenzene were made from two different stock solutions. Samples of these stock solutions were diluted to make a range of standards from 0.5 ppb to 25 ppb. The resulting calibration curve was linear (see Appendix B for calibration curve for chlorobenzene and subsequent chemicals).

Dimethylsulfoxide (DMSO) analysis was also accomplished using the purge and trap. The purge and trap used is the same as used for chlorobenzene detection above. The temperature program, however, is different. No temperature program was used and the GC column was maintained at a constant 60°C. Under these conditions, the DMSO had a retention time of 5.75 min. During sampling, 2 drops of concentrated hydrochloric acid was added to the (40 ml) sample vials to stabilize the solution. A FID detector was used to detect the DMSO. In order to detect the DMSO, it first must be reduced to DMS by addition of sodium borohydride. The sample was first purged with argon for 10 minutes to remove any trace

amounts of DMS and other volatiles which have close to the same retention time as DMS. Twenty milliliters of the sample was then injected into the purge and trap vessel, followed by 2 ml of 4% $NaBH_4$ which reduced the DMSO to DMS. The purge gas was then sent through the trap, desorbed and sent to the GC where the DMS was detected. Likewise, to ensure accurate calibration curve, standards were made from two different stock solutions. The resulting calibration curve was linear. The detection limit for DMSO is <55 ppb.

The analysis for ethanol was done using the flame ionization detector (FID) on a Hewlett Packard 5890 series II gas chromatograph with a Supelco 2mm ID by a 10' glass column packed with 80/120 Carbopack B/3% SP-1500. The temperature of the column was maintained at a constant 60°C. Helium was used as the carrier gas at a flow rate of 5.4 ml/min. The retention time of ethanol with this arrangement was only 4.1 minutes. Likewise, to ensure an accurate calibration curve, standards for ethanol were made from two different stock solutions. Samples of these stock solutions were diluted to make standards ranging from 0.2 ppm to 30 ppm. The resulting calibration curve was linear.

Formaldehyde detection was accomplished by a derivatization technique which uses O-(2,3,4,5,6-pentafluorobenzyl)-hydroxylamine (PFBOA) as the derivatizing agent. A 10 ml sample was collected from the VRA effluent in a 20 ml screw cap vial with Teflon coated septa. To this sample, 4 drops of 0.1 M sodium sulfite was added along with 0.8 ml of a 1.0 mg/ml PFBOA solution. The solution was left at room temperature for two hours to allow the reaction to take place. The derivative was extracted using 2.5 ml n-hexane with 21.32 ppb decafluorobiphenyl as an internal standard by shaking for one minute. The hexane extract was then transferred to another 20 ml vial via polyethylene transfer pipets and shaken with 5 ml of 0.1 N sulfuric acid. After the last wash, the hexane extract was transferred to GC vials, again via the transfer pipets. Analysis for the formaldehyde derivative was done using the electron capture detector (ECD) on a Hewlett Packard 5890 series II gas chromatograph with a J&W Scientific DB624 0.53 mm ID by 30 m glass capillary column with a 3 micron film. Helium was used as the carrier gas at a flow rate of 5.4 ml/min. The detection limit for this procedure is <0.5 ppb. Since the detection limit is so low, any formaldehyde dissolved from the air in the derivatizing solutions had to first be subtracted as background noise from the resulting GC curve.

Urea analysis was accomplished via direct aqueous injection of 10 microliter samples into a Hewlett-Packard 1090 HPLC equipped with a column packed with VYDAC 201HS52 packing with water as the carrier fluid. A diode array detector was employed at a wavelength of 190 nanometers. An ultimate sensitivity for a urea concentration of 0.2 ppm was determined from calibration standards. Because of the low concentrations of urea in the effluent solutions (<3.0 ppm), we were operating close to the limits of detection. This may have lowered the overall accuracy of the HPLC measurements.

Quality Control

To ensure that the calibration plots were linear, any curves with a correlation coefficient less that 0.99 were rejected. To ensure that the standards for each component were made correctly, two stock solutions were used, and standards were made so that the concentrations of the standards made from different stock solutions overlapped. If the resulting calibration curve was linear, the standards were accepted. For ethanol and urea standards, a minimum of 3 samples for each concentration were analyzed. Before each sample analysis, representative calibration standards and blanks were run. If they did not fall within the calibration specifications, a new calibration set was analyzed (scince an internal standard was used for formaldehyde, no calibration curve was necessary). After all of the reactor samples were analyzed, representative standards were run to check for "base-line" drift. If the standards fell within the previous calibration curve, a new calibration curve was not deemed necessary. If they did not, a new calibration curve was run. For urea, the calibration was run before and after the reactor samples. Because of the length of the analysis, chlorobenzene standards were run only once per concentration. The resulting calibration curve showed correlation coefficients within the tolerances. In addition, an internal standard was used for formaldehyde detection to provide an extra quality assurance check on this component. The calibration plots for each component are given in Appendix B.

Catalyst Characterization

The reactor catalyst supplied by Hamilton Standard was physically characterized to determine the BET surface area, oxygen chemisorption surface area, pore radii, void volume, and bulk and pellet density. The results of these tests are summarized in Table IV. No chemical characterization of the catalyst composition was attempted. The BET analysis was performed both at Michigan Tech and at Quantachrome, Inc. Both labs reported a total BET surface area of approximately 212 square meters per gram of catalyst. However, it is interesting to note that the active area for oxidation as evidenced by the chemisorption behavior is approximately half the BET surface area. This would indicate a moderate degree of catalyst dispersion. The oxygen chemisorption surface area was determined by oxygen titration using a Cahn microbalance. After degassing and reducing the catalyst samples in the balance chamber, the surface uptake of oxygen was measured and related to the adsorption surface area. The pore volumes determined for this material are fairly high, and the average pore radii of 44 angstroms compares favorably with other catalysts of this type [14].

TABLE IV - Catalyst Characterization

Physical Properties of the VRA Catalyst	
BET surface area (m^2/gm catalyst)	212.3
Pellet porosity	0.61
Average pore radii (angstroms)	43.8
Pellet density (gram/cm^2)	2.61
Oxygen Chemisorption area (m^2/gm catalyst)	94.2
Void volume (cm^3/gm catalyst)	0.24

RESULTS

Component Testing on the VRA

Individual component solutions were tested in the VRA for all five components - chlorobenzene, DMSO, ethanol, formaldehyde, and urea. Table V shows the complete VRA test matrix. At the nominal reactor operating conditions (a temperature of 270°F, operating pressure of 67 psig, and a flow rate of 120 ml/min) the effluent concentrations for ethanol, formaldehyde, and urea were all below the analytical detection limits. Even at the mildest reaction conditions (200 °F) the destruction of ethanol was 100%. Only chlorobenzene and DMSO were not completely mineralized. Single contaminant conversions for these components at the above nominal operating conditions were 0.424 and 0.621 respectively. A combined matrix (combined 3) of all five components at their highest concentrations was run through the VRA at the nominal operating conditions listed. Again no ethanol, formaldehyde, or urea were detected in the effluent. The high conversion of the hydrocarbon constituents in both the individual and the combined matrix made the acquisition of multicomponent modeling data for the VRA itself difficult if not impossible. If complete destruction of the contaminant is obtained, we do not know if it was destroyed in the first 2 cm or the first 20 cm. This precludes us from obtaining kinetic rate constants from the data. Therefore, the remainder of the combined runs on the VRA were of relatively low priority in the model development, and subsequent experiments to derive the rate parameters focused on the differential test reactor. The fact that only 40 to 60 percent of the chlorobenzene and DMSO are being destroyed at the nominal reactor operating conditions is of some concern however; since this would indicate the effluent treatment objectives for these contaminants may not be satisfied by the current VRA design. A successful model should give us some quantification of these potential problems.

TABLE V - Contaminant Matrix for VRA Testing

Pressure : 67 psig	Temperature (°F)				
Influent	200	220	240	250	270
10 ppm Ethanol	--	--	--	--	✔
3 ppm Urea	--	--	--	--	✔
100 ppb Formaldehyde	--	--	--	--	✔
300 ppb DMSO	--	--	--	--	✔
20 ppb Chlorobenzene	--	--	--	--	✔
Combined 1*	✔	✔	✔	✔	✔
Combined 2*	✔	✔	✔	✔	✔
Combined 3*	✔	✔	✔	✔	✔
Combined 4*	✔	✔	✔	✔	✔
Combined 5*	✔	✔	✔	✔	✔

* - Combined 1 : 10 ppm Ethanol, 3 ppm Urea, 100 ppb Formaldehyde, 300 ppb DMSO, 20 ppb Chlorobenzene

Combined 2 : 1 ppm Ethanol, 3 ppm Urea, 100 ppb Formaldehyde, 300 ppb DMSO, 20 ppb Chlorobenzene

Combined 3 : 20 ppm Ethanol, 3 ppm Urea, 100 ppb Formaldehyde, 300 ppb DMSO, 20 ppb Chlorobenzene

Combined 4 : 10 ppm Ethanol, 1 ppm Urea, 100 ppb Formaldehyde, 300 ppb DMSO, 20 ppb Chlorobenzene

Combined 5 : 10 ppm Ethanol, 10 ppm Urea, 100 ppb Formaldehyde, 300 ppb DMSO, 20 ppb Chlorobenzene

Differential Test Reactor

Ethanol and Chlorobenzene Binary Tests

All of the parameter fitting data for the oxidation model were obtained in the smaller differential test reactor at steady state. Initial studies focused on a two component system of ethanol and chlorobenzene in which the effects of flowrate (from 60 to 100 ml/min.), particle size (three sizes), pressure (50 to 80 psig), and temperature (200 to 280°F) were all examined. With this parameter screening completed, later tests were expanded to incorporate all five components. In order to confirm steady state operation, the reactant

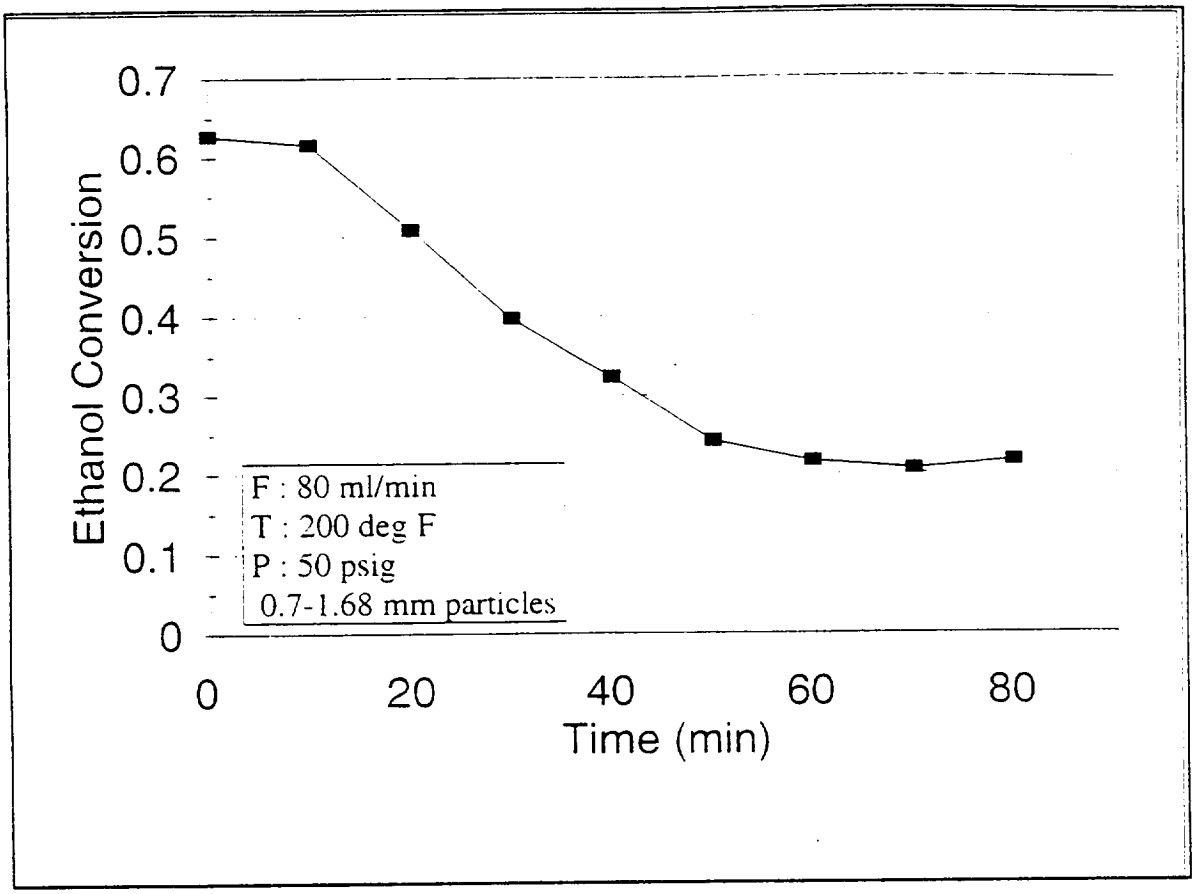

Figure 9 - Break-in Period for Ethanol

conversion as a function of time was monitored. Figure 9 shows the transient data plot from the reactor start up with ethanol. From this plot, we can see the differential reactor operates in a transient state for about 60 minutes prior to reaching steady state. Chlorobenzene also showed a similar break-in period. The source of this break-in phenomena may arise from two sources: either a large degree of adsorption on the alumina catalyst support prior to reaction, or surface enrichment on the catalyst. If adsorption is the key, it is difficult to understand such long breakthrough times (50 - 60 minutes) for the small quantities of catalyst used in the differential test reactor. The surface enrichment (or deactivation) of oxidation catalysts due to carbon deposits is a second possibility. Only a careful elemental analysis of the surface could verify this hypothesis. This break-in period would significantly affect later development of a transient model, and therefore should be examined more carefully in future studies. After an initial steady state was achieved, the system responded quickly to changes

in flow rate or temperature and steady state at the new flow rate/temperature was reached within the sampling period. The temperature stability of the heat exchanger feed to the reactor was excellent for nearly all conditions at ±2.5 °F.

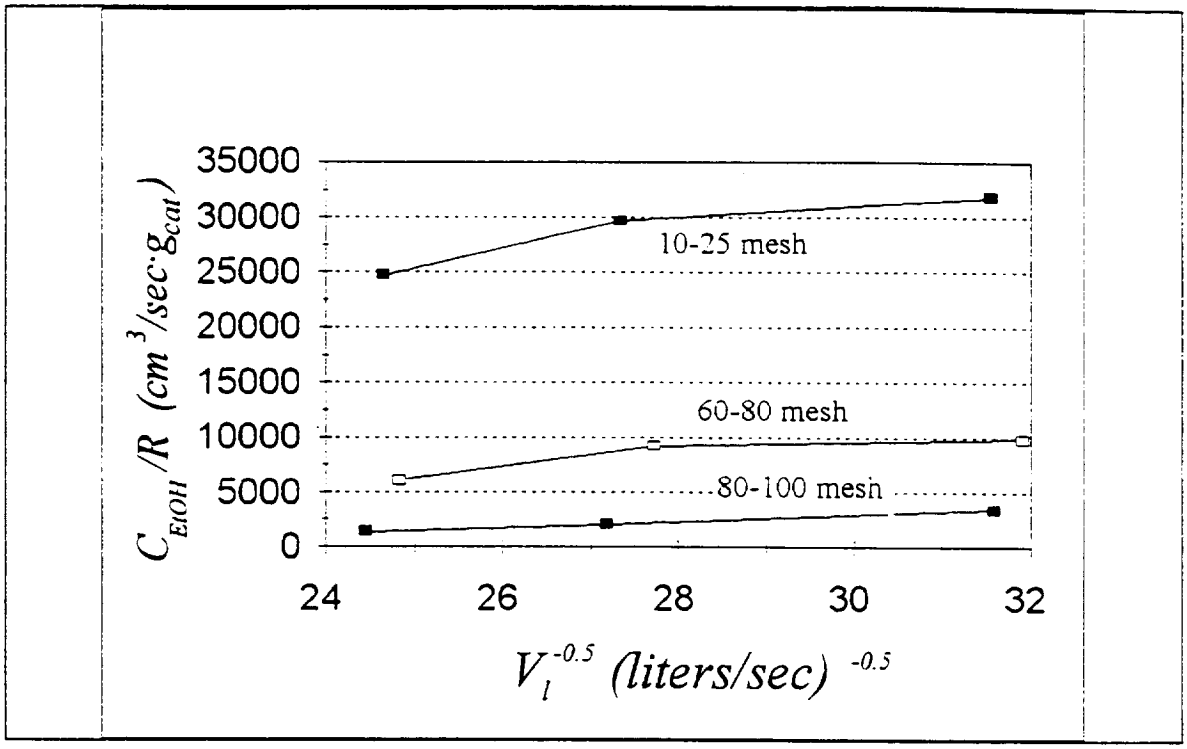

Figure 10- Effect of catalyst size on reaction rate

Another important aspect examined by this study is the role of mass transfer versus the intrinsic kinetics. To explore the relationship of these rates, the effect of catalyst size and liquid flow rate on the overall reaction rate of both ethanol and chlorobenzene was analyzed. Figure 10 shows the effect of liquid flow rate on the overall ethanol reaction rate normalized to the mass of catalyst for three catalyst particle sizes. For the smaller size catalyst (149 to 177 μ), the reaction rate is approximately an order of magnitude larger than that for the larger, raw particle size (~1mm). This indicates that the larger size particle has significant pore mass transfer limitations. Flow rate also has a significant effect on the contaminant conversions for each particle size. This would indicate that there remains a significant external mass transfer effect for both particle sizes and contaminants. Therefore, both of these reaction parameters may be significant in the model development.

Figure 11 shows the effects of pressure on the conversion of the contaminants. From this figure we see that there is no significant effect on the conversion of ethanol and only a very slight effect on the conversion of chlorobenzene after the break-in period. This slight effect is probably more influenced by stripping than by pressure. This would seem to indicate that the gas to liquid mass transfer coefficient does not change with pressure within our pressure range, and possibly that we have a considerable excess of oxygen.

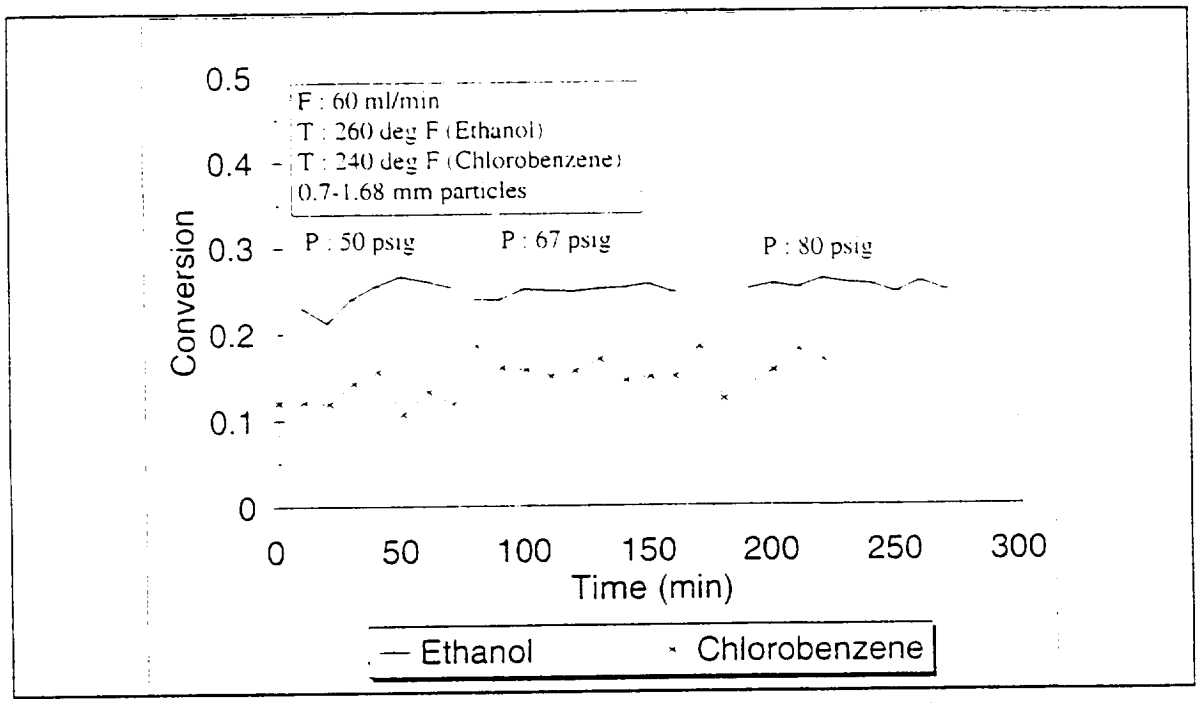

Figure 11- Pressure effects on contaminant conversion for separate matrices

Figure 12 illustrates the effect of temperature on conversion of contaminants through the differential reactor with the raw catalyst size (0.7 to 1.68 mm). Notice that a break in period of about 1 hour for the reactor and catalyst is also observed here. Figure 12 shows that the conversion of ethanol is highly dependent on temperature whereas the conversion of chlorobenzene is less sensitive to temperature. As expected one sees higher conversions at higher temperatures for both the chlorobenzene and ethanol. The results at 280°F showed more scatter. This is probably due to the proximity to the water boiling point at lower pressures (50 psig). The higher temperature data for 67 psig was not as erratic, thereby supporting this hypothesis.

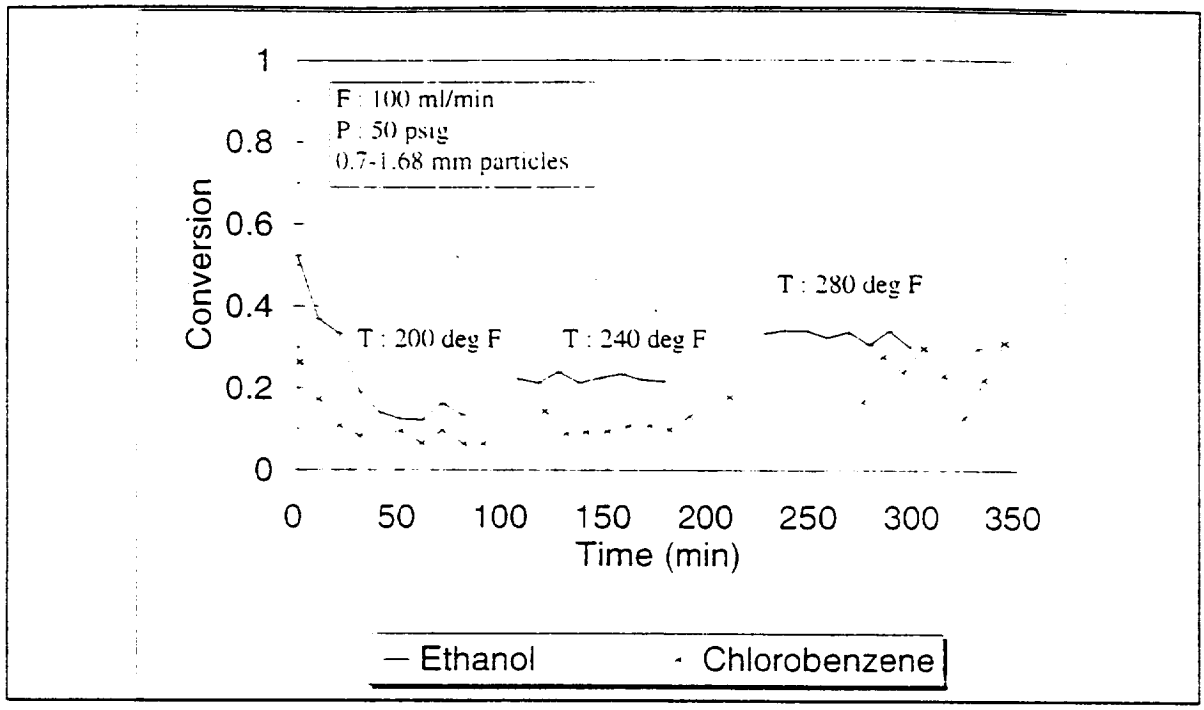

Figure 12-Temperature effect on conversion of contaminants

TABLE VI - Combined vs. Individual Matrices

Catalyst Size : 0.7-1.68 mm P : 50 psig T : 200°F		
Liquid Flow Rate (ml/min)	Individual Matrix Ethanol Conversion	Combined Matrix Ethanol Conversion
100	0.147±0.027	0.158±0.010
80	0.221±0.015	0.178±0.009
60	0.360±0.025	0.224±0.007
	Chlorobenzene Conversion	Chlorobenzene Conversion
100	0.077±0.017	0.097±0.007
80	0.063±0.013	0.122±0.029
60	0.154±0.026	0.137±0.022

A combined matrix with both chlorobenzene and ethanol and an individual matrix consisting of separate ethanol and chlorobenzene were tested. Table VI compares the results of conversion vs. flow rate for one temperature (200°F) and pressure (50 psig) over the raw catalyst. From Table VI we see that in general for ethanol the conversions are higher for the individual runs than the combined runs; whereas for the chlorobenzene the results are more ambiguous. This is probably not due to the competitive adsorption of the organics since the chlorobenzene in the system is very dilute. It is more likely that this reflects competition for oxygen on the surface of the catalyst. More demand → lower surface concentration $r = K_s a (C_s - C_e)$

Table VII shows the effect of flow rate and temperature on conversion for the individual reactants. As listed above, the conversion increases as the temperature increases, having a larger effect on ethanol than chlorobenzene. The conversion of ethanol follows the trend of increasing as contact time increases. On the other hand, chlorobenzene conversion follows the same trend at lower contact times, but demonstrates the opposite at higher contact times. The effect of mass transfer may thus outweigh the contact time at the faster surface reaction conditions of higher temperatures. As noted previously, the higher temperatures had considerably more scatter because of the proximity to the boiling point of water at these conditions. Subsequent runs were made at a minimum of 67 psig to mitigate this effect. The complexity of this data is an additional indication that an accurate, multivariable model is needed for the interpretation of this complex system.

Table VIII shows the effect of both temperature and flow rate on the conversion of the contaminants for the combined matrix over the smaller catalyst size. As for the individual contaminants over this smaller catalyst size (Figure 9), we see that flow rate still has an effect on the conversion; but is less pronounced than for the raw catalyst. This indicates that there are less external mass transfer limitations for the smaller catalyst due to the increased surface area, but they are still significant.

TABLE VII - Effect of temperature and flow rate on contaminant conversion for raw catalyst

Cat. Size : 0.7-1.68 mm P : 50 psig Reactor Volume : 5.08 cm^3				
Liquid Flow Rate (ml/min)	Contact Time (sec)	Temperature (°F)	Ethanol Conversion	Chlorobenzene Conversion
100	3.05	200	0.147±0.027	0.077±0.017
100	3.05	240	0.225±0.010	0.104±0.015
100	3.05	280	0.335±0.023	0.235±0.063
80	3.81	200	0.221±0.015	0.063±0.013
80	3.81	240	0.294±0.007	0.085±0.009
80	3.81	280	0.387±0.021	0.209±0.038
60	5.08	200	0.360±0.025	0.154±0.026
60	5.08	240	0.474±0.015	0.127±0.016
60	5.08	280	0.634±0.050	0.156±0.085

TABLE VIII - Effect of temperature and flow rate on conversion for crushed catalyst

Catalyst Size : 149-177 μ P : 50 psig Reactor Volume : 0.356 cm^3				
Liquid Flow Rate (ml/min)	Contact Time (sec)	Temperature (°F)	Ethanol Conversion	Chlorobenzene Conversion
100	0.214	200	0.198±0.007	0.159±0.042
100	0.214	240	0.357±0.008	0.178±0.009
100	0.214	280	0.565±0.015	0.437±0.064
80	0.267	200	0.158±0.016	0.094±0.018
80	0.267	240	0.281±0.007	0.105±0.014
80	0.267	280	0.667±0.056	0.557±0.150
60	0.356	200	0.144±0.013	0.083±0.037
60	0.356	240	0.295±0.015	0.080±0.027
60	0.356	280	0.590±0.157	0.301±0.088

Five component test series

Following the preliminary tests on the two component series, each of the 5 components were tested at 5 temperatures ranging from 200 to 270 °F and a pressure of 67 psig (to avoid possible steam generation problems). These tests were performed at a flowrate of 100 ml/min over the raw catalyst particle size. The objective of these studies was to develop the information for fitting the Arrhenius expressions for the rate constants for each component over the temperature range of interest. The conversions for each component at steady state are listed in Table IX.

Table IX - Effect of Temperature on conversion for the individual contaminants

Raw Catalyst particle; Flow rate - 100 ml/min; P: 67 psig.					
Temperature (°F)	Formaldehyde conversion	DMSO conversion	Urea conversion	Ethanol conversion	Chlorobenzene conversion
200	0.710±0.013	~0	0.118±0.18	0.106±0.003	0.043±0.017
220	0.710±0.021	~0	0.148±0.06	0.112±0.003	0.066±0.039
240	0.773±0.017	0.134±0.21	0.130±0.15	0.184±0.012	0.077±0.049
250	0.794±0.009	0.151±.28	0.243±0.13	0.209±0.008	0.090±0.021
270	0.814±0.014	0.254±.25	0.421±0.18	0.260±0.002	0.121±0.015

By far the most reactive of these compounds is formaldehyde, with over 70% destruction even at the lowest temperature at this high flowrate. This can be compared with DMSO for which no appreciable destruction was noted until 240° F. At higher temperatures, DMSO reacted quite well. This rather peculiar behavior might be explained by either strong chemisorption or mild poisoning of the catalyst by the DMSO. The sulfur group of this molecule would serve as such a poison over most noble metal catalyst. The higher temperatures could potentially desorb these groups. Further evidence of this mild poisoning is observed in the subsequent results for chlorobenzene and ethanol. The reaction rates for these compounds dropped as much as 50% following the testing of DMSO over the catalyst

bed. Further heating of the catalyst to the maximum reaction temperature (270°F) seemed to restore much of the original activity loss. This would indicate some reversibility of the process, but it would be wise to conduct further tests of this possible poisoning. The large deviations for the urea conversions (Table IX) are because the concentrations of the urea samples were so close to the detection limit of the HPLC. Because of the proximity to the detection limit, background noise was a significant factor which introduced a large amount of error. Reintegration of the results did not improve the precision. The tests shown for ethanol show a slightly higher conversion than during the two component tests. After the possible poisoning was discovered, a new catalyst bed was prepared and conditioned, and a small increase in the catalyst load and the fresh catalyst surface resulted in the higher conversion.

DISCUSSION

Many complex processes are happening within the reactor. Mass transfer from gas to liquid, mass transfer from liquid to solid, diffusion through the liquid, adsorption and desorption of chemicals, pore diffusion, and intrinsic kinetics are all occurring simultaneously. As a result a simple single variable analysis or data interpretation is impossible. For example, if the flow rate is decreased, the contact time in the reactor is increased proportionally, thus one might expect higher conversions; however, lower flow rates also may decrease the rate of mass transfer, thus lowering the expected conversion. In order to adequately analyze the results obtained from a three phase catalytic reactor. The appropriate model would then take into account all of the processes listed above into account. The simple plug flow model derived earlier was programmed to perform these tasks.

Individual Rate Constant Determination

In order to determine the overall rate constant for the organic contaminants and oxygen on the surface of the catalyst, the plug flow model was used for the individual components.

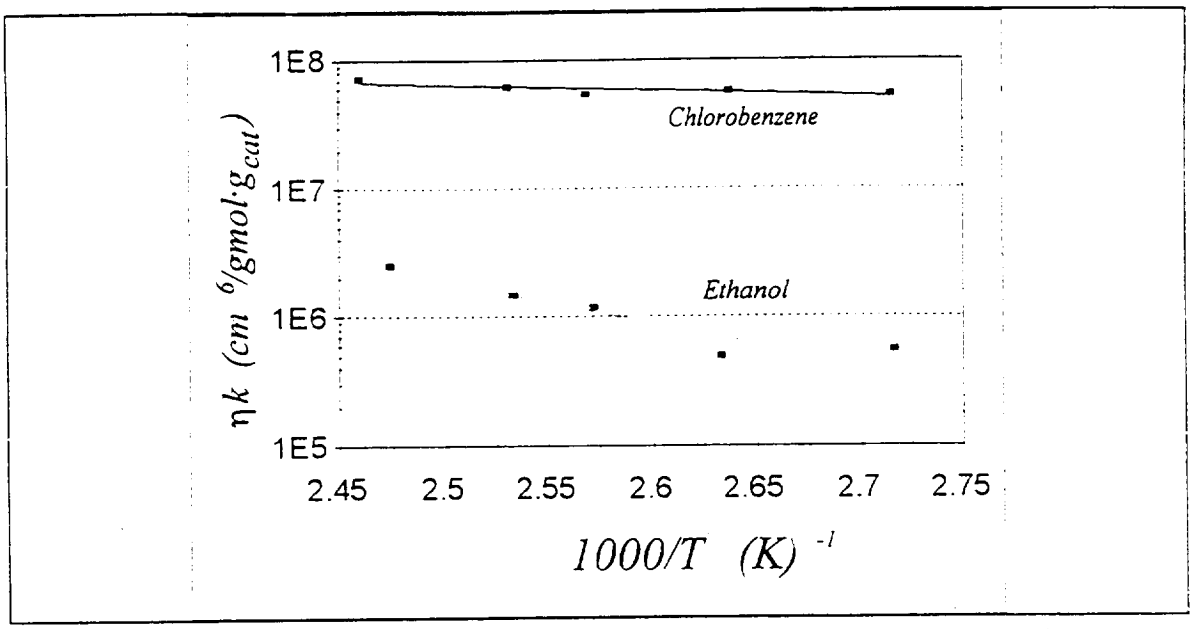

Figure 13 - Arrhenius plot of surface reaction rate constant for ethanol and chlorobenzene

This overall rate constant is the product of the effectiveness factor and the intrinsic surface reaction rate constant. The mass transfer coefficients as determined from the appropriate correlations and the other required parameters listed in Table I were put into the model and temperature dependent parameters were adjusted to the proper temperature. The rate was assumed to be second order (first with respect to oxygen and first with respect to the organic contaminants) due to the dilute nature of the reactants. Using the exit concentration obtained from experimental results, the overall reaction rate constant was determined by successive iteration until the predicted exit concentration was equal to the experimental exit concentration at one experimental flow rate and five different temperatures. From this data, we were able to produce an Arrhenius relationship for the overall surface rate constant. Figure 13 shows the results of this calculation for two of the components, chlorobenzene and ethanol. The data is linear, an indication that the Arrhenius expression provides a good fit over the experimental temperature range. From the slope of a linear regression on this data, we can obtain the values for the Arrhenius expression for both chlorobenzene and ethanol. The resulting expressions are shown in equations 38 and 39:

$i := 0..999 \qquad x_i := \frac{i}{1000}$

$$f(L, d_p, Pe_f, n, X) := \frac{d_p}{L} \cdot \frac{20}{Pe_f} \cdot n \cdot \ln\left(\frac{1}{1 - X}\right)$$

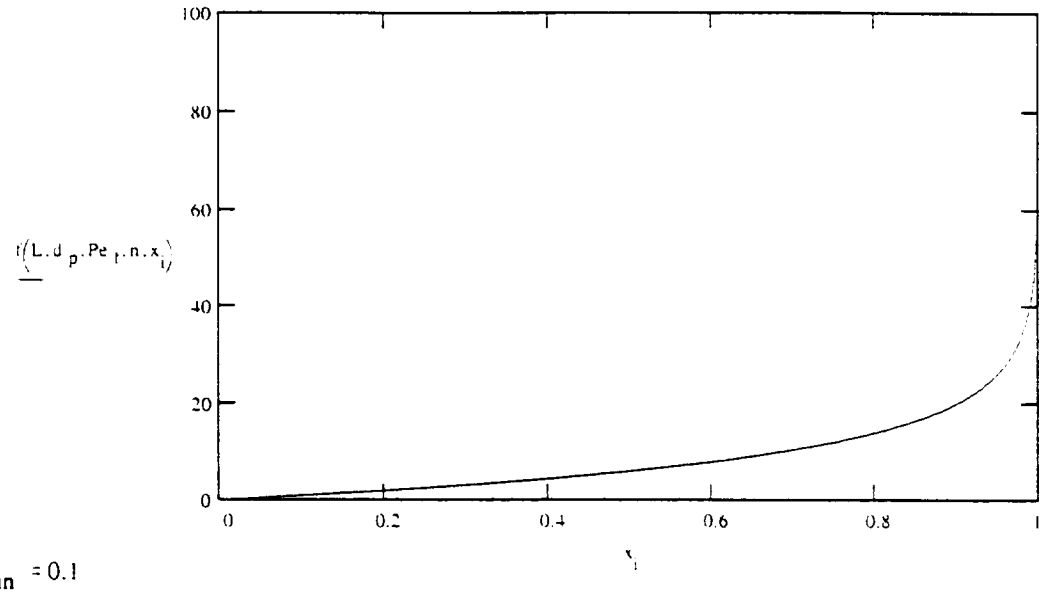

$Pe_{min} := 0.1$

Given

$f(L, d_p, Pe_{min}, n, 0.999) = 1$

$Pe_{min} := \text{find}(Pe_{min})$

$Pe_{min} = 0.619$

Therefore, we must have a fluid Peclet number above 0.619 for plug flow to be assumed. The fluid Peclet number for the VRA is well below this limit and axial dispersion must be taken into account

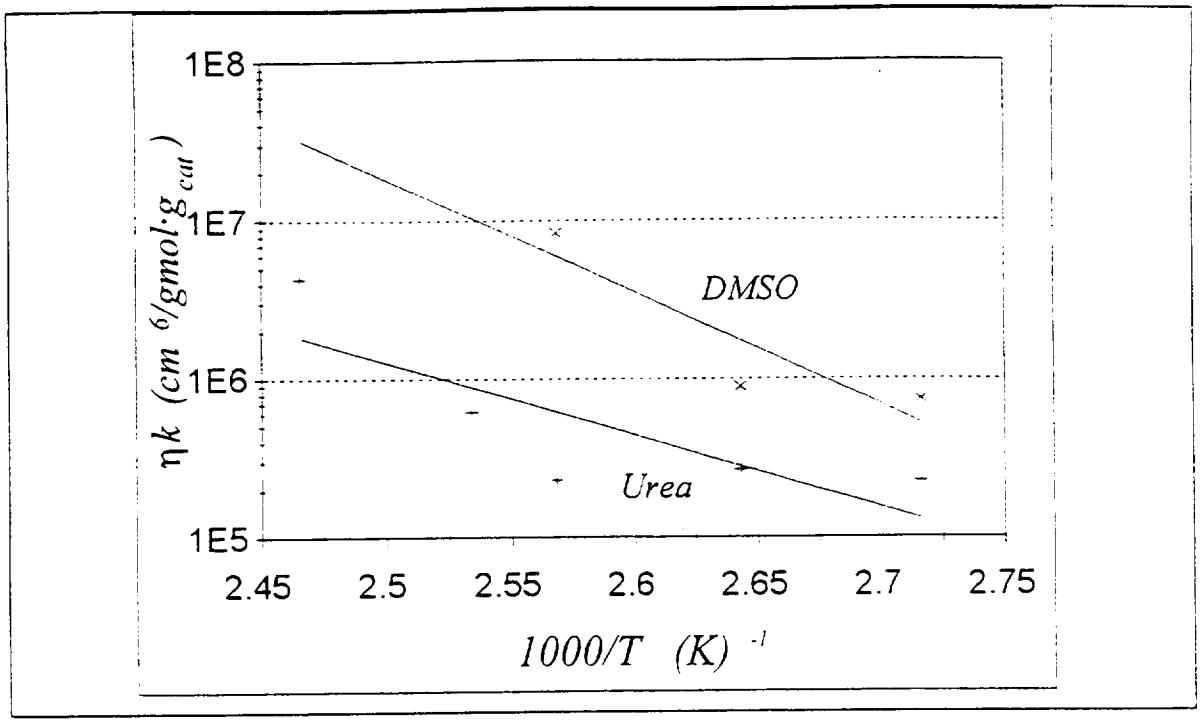

Figure 14 - Arrhenius plot of surface reaction rate constant for DMSO and urea

which noticeable conversion was observed, and may be somewhat suspect. Finally, the fitting exercise for the formaldehyde data was quite interesting. The experimental conversions were only approached for very large values of the rate constant. Further increasing the value proved the data fit to be relatively insensitive to the rate constant assumed. Ultimately, the reason for this insensitivity was determined to be complete mass transfer limitations in the liquid phase. Formaldehyde was by far the most reactive compound, therefore it is not surprising to observe this mass transfer control for the relatively low flowrates employed. In the case of formaldehyde, the overall reaction rate was set equal to the mass transfer rate. The overall rate of destruction was well below that which might be expected in a homogeneous reaction.

Multicomponent Plug Flow Model Validation

To validate the proposed model, the kinetic rate constants determined above for the individual components were used to predict the final concentration of a five component

combined matrix solution with three different contact times (flowrates) using the differential reactor. Table X shows the results for all five contaminants. Since the single component fitting was conducted for only one flowrate, its accuracy in predicting the effluent concentrations for three different contact times (flowrates) is a fairly rigorous test of the fundamental soundness of the proposed approach. The extension to a multicomponent solution is also a test of the assumption of a second order reaction. Although the dilute concentration range used for all of the contaminants would suggest that this is appropriate; any competitive adsorption effects would cause major deviations (probably several fold) in the model predictions. The model already reflects the overall competition for oxygen stoichiometrically.

The predictions for the first three chemicals in Table X are quite good, and the predictions for urea and ethanol fall within about 7 percent of the actual. The results for formaldehyde are not nearly as good. Since the formaldehyde is entirely mass transfer limited, the results largely depend upon the accuracy of the mass transfer correlations employed, which in turn are a sensitive function of flowrate, holdup, and catalyst geometry. The calculated effluent concentrations are extremely sensitive to the value used. In future work the reaction of formaldehyde might could be used as an experimental method for determining mass transfer coefficients and fine tuning the correlations employed. The major outlier in the predictions is for DMSO. This contaminant appears to be strongly chemisorbed on the surface of the catalyst. The result is either mild fouling or poisoning of the catalyst. Over the length of time the combined runs were performed, the effects on the other contaminants was not largely noticeable. However, for DMSO itself, the outlet concentrations are far above those predicted by the model. This is probably the result of a poor data quality, especially in the lower temperature range. The unusual behavior for DMSO may not actually be surprising, in that it is suggested by some researchers as a model poisoning compound for noble metal catalysts (usually in the gas phase). Further study will be necessary on this compound if it is allowed to enter the VRA reactor bed for long periods. The removal of DMSO prior to the reactor is probably a better alternative.

TABLE X - Experimental vs. Predicted Final Contaminant Concentrations for Combined Run

Catalyst Size : 0.7-1.68 mm T : 200°F P : 67 psig			
Contact Time (sec)	Experimental Final Concentration	Predicted Final Concentration	% error
	Ethanol (mol/cm^3)		
3.05	5.78×10^{-7}	5.49×10^{-7}	4.9
3.81	5.58×10^{-7}	5.37×10^{-7}	3.7
5.08	5.44×10^{-7}	5.17×10^{-7}	5.1
	Chlorobenzene (mol/cm^3)		
3.05	1.49×10^{-10}	1.24×10^{-10}	16.9
3.81	1.46×10^{-10}	1.20×10^{-10}	17.6
5.08	1.47×10^{-10}	1.6×10^{-10}	21.3
	Urea (mol/cm^3)		
3.05	4.73×10^{-8}	5.06×10^{-8}	7.1
3.81	4.70×10^{-8}	4.99×10^{-8}	6.3
5.08	4.55×10^{-8}	4.87×10^{-8}	6.9
	Formaldehyde (mol/cm^3)		
3.05	9.17×10^{-10}	5.11×10^{-10}	44.3
3.81	7.80×10^{-10}	3.65×10^{-10}	53.1
5.08	6.35×10^{-10}	2.26×10^{-10}	64.4
	DMSO (mol/cm^3)		
3.05	4.40×10^{-9}	1.91×10^{-9}	99
3.81	6.01×10^{-9}	1.90×10^{-9}	99
5.08	5.32×10^{-9}	1.90×10^{-9}	99

Application of the model to the VRA data

Direct comparison of the model results to the VRA data is difficult, since for nearly all of the experimental conditions, complete destruction of ethanol, urea, and formaldehyde were achieved. The model results for DMSO are suspect, therefore leaving chlorobenzene as the best test of whether the VRA can be modeled using the plug flow equations. Figure 15 shows the comparison of the model predictions for ethanol and chlorobenzene as a function of contact time to the actual effluent concentrations based upon plug flow assumptions. For ethanol, complete destruction is predicted and achieved experimentally. In fact, 99% destruction of the ethanol is approached after only 2.5 minutes of reactor contact time (as compared to 4.13 minutes theoretical plug flow contact time for the actual reactor.) However, for chlorobenzene the model predicts approximately 98% conversion for the VRA, versus 42 % actual conversion. The model would predict this degree of chlorobenzene conversion in less than 1 minute.

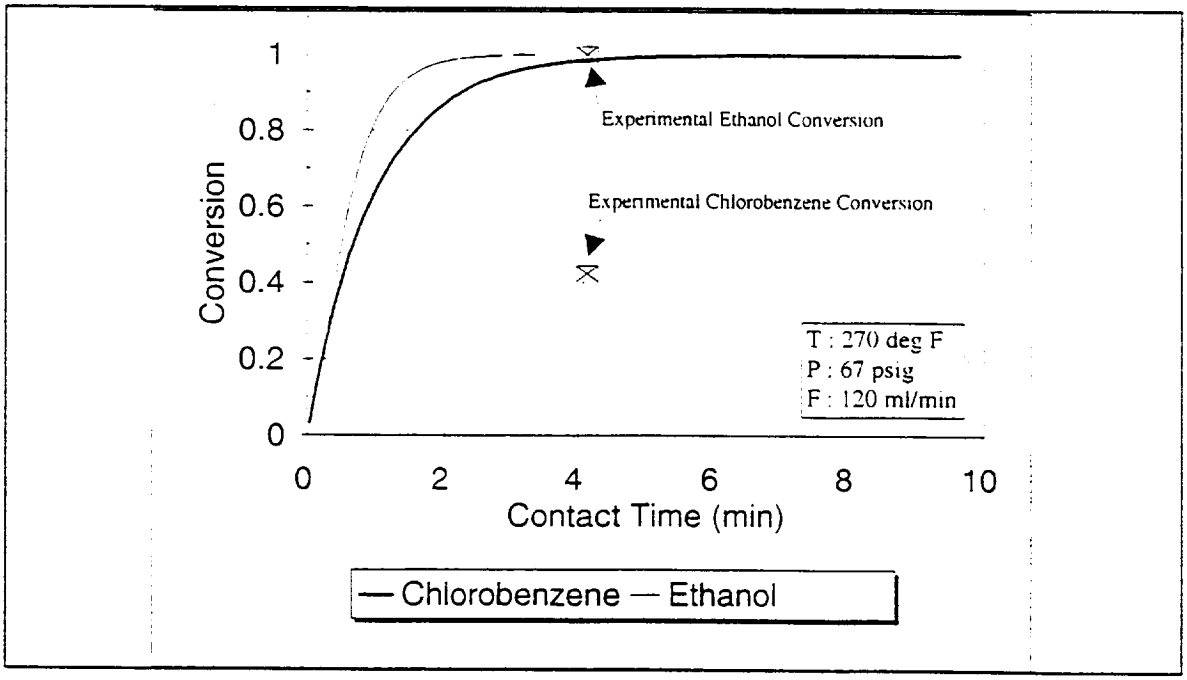

Figure 15 - Predicted conversion vs. experimental for VRA

The reasons for this discrepancy probably lie in the non-ideal flow characteristics of the VRA found during residence time studies. The RTD studies showed far less than ideal

plug flow dispersion in the reactor. The differential test reactor shows > 10% destruction of chlorobenzene for contact times of less than 5 seconds. Qualitatively, one would expect the VRA with a contact time almost 50 time greater to show a very high degree of destruction. If bypassing, mixing, or channeling occurs in the VRA bed, all of these factors would contribute to decreased destruction. Sputtering and bursts of oxygen periodically interrupted the liquid flow from the reactor during operation. This might be an indication that gas pockets are building up within the bed, "short circuiting" the liquid flow through the bed. The flow characteristics cannot be directly observed during operation, but perhaps a clear bed could be constructed to observe the reactor hydraulics more closely.

Overall, due to the high levels of destruction for most of the components, there is only a very limited set of data to compare the model to the VRA performance. However, the relatively high concentrations of chlorobenzene observed in the effluent as compared to the model predictions would seem to confirm that the VRA is operating at a very low efficiency. This would also appear to be confirmed by the RTD studies. DMSO also is passing through the VRA without adequate destruction. The DMSO may be acting as a mild poison, thereby decreasing the VRA performance. The source of these problems needs to be addressed before VRA can operate dependably.

CONCLUSIONS

A multiphase, multicomponent reactor model was developed for the oxidation of dilute contaminants in water. Over the range of temperatures and flow rates examined, the experimental data for the destruction of chlorobenzene, ethanol, DMSO, formaldehyde, and urea were used to calculate the single component overall reaction rate constants. The resulting data for each compound was fit to the Arrhenius equation and the individual activation energies determined. The activation energies obtained for the raw catalyst fell within the range which is generally ascribed to pore diffusion limited for ethanol, external mass transfer limited for formaldehyde and chlorobenzene, and surface reaction limited for urea and DMSO. By running the experiments at different particle sizes, we were able to

qualitatively identify that the bigger catalyst size is largely internal mass transfer limited, and this is directly lumped into the overall rate constant determined.

The multicomponent plug flow model developed was applied to a five component mixture and gave predicted results very close to actual experimental results for urea, chlorobenzene, and ethanol over the range of conditions. The deviations between the model and experiments fall well within the range of experimental error. The results for formaldehyde showed its reaction rate to be determined totally by the rate of mass transfer. This would confirm that the mass transfer correlations of Alexander and Shah [8] and Mochizuki [9] were adequate for the prediction of the desired mass transfer coefficients. DMSO has been determined to be a weak catalyst poison, and as a result the conversions were always much lower than predicted. It may in turn be affecting the results for other compounds. By incorporating the appropriate mass transfer correlations and scale up parameters, this model will allow the testing of other reactor configurations and contaminant mixtures.

Further extension of the model to incorporate a larger number of variables is needed. The model must be extended to incorporate a larger number of components representative of the entire range of contaminants encountered in the ISS. Potential poisoning by DMSO is of great concern. Finally, since the VRA may be operating outside the range of ideal plug flow, the model should be extended to incorporate axial dispersion and transient effects. Alternative catalysts (especially for the more electronegative compounds) and reactor designs to increase the energy, oxygen, and space efficiency of the reactor system should also be examined.

RECOMMENDATIONS

Experimental studies

The experimental measurements for contaminant destruction in the differential test reactor and the VRA were very successful for ethanol, formaldehyde, and chlorobenzene. Quantification of the potential partial oxidation products (e.g. - ketones, or organic acids)

should be attempted; however, such products appeared only as barely detectable traces in the tests conducted here. Even though the best current analytical techniques were employed for urea and DMSO, the results were not as satisfactory. Using the technique suggested by NASA/Boeing, the measurements for urea were too close to the limits of detection for the method. Even though a larger number of samples were analyzed, the standard deviation was greater than desired. For DMSO, the analytical technique was shown to be excellent in standards tests and with the VRA effluent, but transient or adsorptive effects made the test reactor results erratic. In the future, a better method might be to follow the sulfate/sulfite ion concentration in the effluent. This technique would be much more sensitive, and would only show the DMSO destroyed, not adsorbed.

The DMSO also poses a larger problem, in the potential poisoning threat it represents. Our initial study indicates that even at low concentrations and short durations, this contaminant may mildly foul the catalyst surface. Although this fouling appears mostly reversible at higher operating temperatures, the long term effects need to be examined closely.

The residence time distribution and axial dispersion studies also deserve added attention. Although great care was taken to minimize adsorptive effects, the role of adsorption/desorption on the catalyst surface needs to be examined in detail. Based upon the actual performance of the VRA, the dispersion would appear to be significantly affecting the destruction of the contaminants. Overall, the VRA demonstrates far from ideal performance. The apparent ineffectiveness of the reactor for the destruction of chlorobenzene and DMSO is probably a combined result of the dispersion and the use of an inappropriate catalyst.

Oxidation catalysts

The catalyst currently employed is adequate for the destruction of ethanol, urea, and formaldehyde. However, for the molecules with more electronegative groups (e.g. - DMSO and chlorobenzene) the current catalyst would seem the wrong choice for long term use. For example, carbon supported catalysts currently being examined under a different project at MTU show complete destruction of similar compounds with bed sizes more than an order of

magnitude smaller. A two catalyst bed system would be far more effective in size, energy efficiency, and oxygen utilization for the processes desired in water treatment for the ISS.

A second major problem is the internal catalyst mass transfer. Based upon the effectiveness factors calculated for the VRA catalyst (~0.007) internal mass transfer limitations are quite severe. This means that less than 1% of the internal catalyst surface is being utilized for the reaction. The experimental data on the different particle sizes indicate that smaller particle sizes would enable the bed size to be decreased by over an order of magnitude by taking better advantage of the catalyst's internal surface area.

Reactor modeling

The proposed modelling approach has shown promise in predicting the performance of the VRA system for oxidizing a multicomponent aqueous contaminant system. Several modifications to the model would enhance the predictive capability of this device.

1. Expansion of the model to more than five components. This would be essential to model the actual water entering the reactor. In order to predict the performance for other organics for which no test data is available, the only viable approach is to develop Quantitative Structure Activity Relationships (QSARs) for families of compounds over the VRA catalyst. QSARs use key physio-chemical properties of molecules (e.g. - polarizability, boiling point, etc.) in correlations to a set of reaction rate constant data for a class of compounds. QSARs such as the Hammet acidity have long been used in homogeneous catalysis. Applications to heterogeneous catalysis have been moderately successful for individual catalyst materials, but cannot take into account complex factors such as catalyst deactivation.

2. Incorporation of axial dispersion effects. Based upon the Peclet number calculations and the model results, the VRA would seem to be operating outside the plug flow regime.

3. Incorporation of transient influent effects. Until the role of adsorption/desorption is more clearly understood, this task would be difficult, if not impossible to complete. Combined with the axial dispersion equations, this represents a very formidable computational and experimental task.

4. Addition of catalyst deactivation kinetics. No catalyst is immune from deactivation. As a consequence, the results from experimental runs performed even under well defined conditions may vary considerably over time. The long term effects of highly electronegative moieties on the catalyst surface will determine the useful lifetimes of the bed. Traces of metals or other occasional materials may render the catalyst bed completely useless. These effects need to be understood for long term space applications.

The incorporation of competitive adsorption effects would not significantly enhance the model unless an exhaustive experimental study was performed to determine the multiple constants needed for such a model. (Probably an order of magnitude more experimental work.) For the dilute concentrations of contaminants oxidized in this reactor, such a rate model (e.g. - Mars-van Krevelan) would appear to be superfluous. Finally, the mass transfer correlations used might be "fine tuned" formaldehyde data or data on any other highly reactive compound. The predicted results for mass transfer limited reactions are quite sensitive to the calculated mass transfer coefficient.

Reactor Design

Overall, the current VRA performance is less than satisfactory for the proposed ISS water treatment design objectives. The basic tubular design does not make efficient use of space, energy, or oxygen. The short contact times observed to treat the contaminants in the differential test reactor do not translate to space or energy saving in the current VRA design. Increasing the length to diameter ratio of the reactor may reduce the degree of axial dispersion, but only at the cost of a greater pressure drop and higher energy utilization.

Three recommendations could be made to improve upon the current design:

- Use a mixed catalyst bed for the oxidation process to minimize the required bed contact time. The current catalyst used in conjucntion with a catalyst that is more effective on halogenated and sulfonated compounds would be a good start. The particle size employed now takes advantage of less than 1% of the internal surface area. Smaller particle sizes would utilize much more of the total surface. As a result, the reactor would be much more compact and energy efficient.

- Change the method for water/oxygen contacting. Although the rates of mass transfer from gas to liquid in the bed seem adequate, the passage of bubbles (even under normal gravity) may account for the poor flow pattern performance as evidenced by the RTD studies. Pre-oxygenating the water using membranes or other high surface area materials prior to entering the reactor would be one solution. Also, a large excess of gas phase oxygen is being employed in the VRA design. Much of this excess (> 90% of the influent in our reactors) may be seen escaping in the reactor effluent. This gas is probably contaminated and must be cleaned prior to further use. If conservation of oxygen is a concern, contacting the water and oxygen external to the reactor would allow much higher utilization of oxygen in the oxidation system. The oxygen saturated water would then be contacted with the catalyst. Intermediate additions of oxygen could be made to insure total organic destruction.

- Changing the reactor geometry to a low pressure drop, moderate superficial velocity reactor design should be considered. Decreased pressure drop would allow the use of a finer catalyst particle size thus significantly reducing mass transfer effects and reactor size. Obvious options include crossflow reactors or radial flow reactors. These systems operate with little change in performance over a wide range of influent conditions, and might offer less bubble retention and dispersion problems in space applications.

NOMENCLATURE

$a = 6(1-\epsilon)/d_p$: Effective external surface area for mass transfer (cm^{-1})

A Cross-sectional area of reactor tube (cm^2)

C Concentration ($gmol/cm^3$)

$C^* = C_g/H$: Concentration at gas-liquid interface ($gmol/cm^3$)

D_a Axial dispersion coefficient (cm^2/sec)

D_l Diffusivity (cm^2/sec)

$d_h = \epsilon_l d_p/1.5(1-\epsilon_l)$: Hydraulic diameter (cm)

d_p Equivalent particle diameter to a sphere having same surface area (cm)

H Dimensionless Henry's law constant

k_{OC} Second order rate constant ($gmol/cm^3 \cdot g_{cat} \cdot sec$)

k_l Mass transfer coefficient for gas to liquid (cm/sec)

k_s Mass transfer coefficient for liquid to the surface of the catalyst particle (cm/sec)

L Length of bed (cm)

n Reaction order

P Pressure (psig)

$Pe_l = d_p u_l/D_a$: Fluid Peclet number

$Pe_r = Lu_l/D_a$: Reactor Peclet number

r Reaction rate ($cm^6/gmol \cdot s \cdot g_{cat}$)

R Gas Constant (1.987 cal/gmol K)

$Re_l = d_h u_l/\epsilon_l \nu_l$: Reynolds number

$Sc = \mu_l/\rho_l D_l$: Schmidt number

$Sh = k_s u_l/D_l$: Sherwood number

t_m Mean residence time (min)

T Temperature (K - in equations; F in graphs)

u_l Liquid velocity (cm/sec)

V_g Gas volumetric flow rate (cm^3/sec)

V_l Liquid volumetric flow rate (cm^3/sec)

V_g' Gas superficial mass velocity ($kg/m \cdot sec$)

V_l' Liquid superficial mass velocity (kg/m·sec)

X $(C_f-C_e)/C_f$: Fractional conversion

z Axial coordinate of reactor tube (cm)

Greek Letters

α Stoichiometric coefficient

ϵ Void fraction in packed bed

ϵ_l Liquid hold up

η Internal effectiveness factor

ν Kinematic viscosity (cm^2/s)

ρ Density (g/cm^3)

σ^2 Variance

μ Viscosity (g/cm·sec) or micron (10^{-6} m)

Subscripts

cat Catalyst

e Exit

f Feed

g Gas

l Liquid

O_2 Oxygen

OC Organic contaminants

s external catalyst surface

Acronyms

DMSO Dimethyl Sulfoxide

LSODE Livermore Solver for Ordinary Differential Equations

PFBOA O (2,3,4,5,6-Pentafluorobenzyl)-hydroxylamine hydrochloride

QSAR Quantitative Structure Activity Relationships

VRA Volatile Removal Assembly

REFERENCES

1. Goto, S. and J.M. Smith, 1975. "Trickle Bed Reactor Performance," AIChE Journal, 21(4): 714-720.

2. Goto, S. and K. Mabuchi, 1984. "Oxidation of Ethanol in Gas-Liquid Concurrent Upflow and Downflow Reactors," The Canadian Journal of Chemical Engineering, 62(December): 865-869.

3. Levec, J. and J.M. Smith, 1976. "Oxidation of Acetic Acid Solutions is a Trickle Bed Reactor," AIChE Journal, 22(1): 159-168.

4. Baldi,G., S. Goto, C.-K.Chow, and J.M. Smith, 1974. "Catalytic Oxidation of Formic Acid in Water. Intraparticle Diffusion in Liquid Filled Pores," Industrial and Engineering Chemistry, Process Design and Development, 13(4): 447-452.

5. Froment,G.F, and K.B.Bischoff, 1990. Chemical Reactor Analysis and Design, John Wiley &Sons, New York.

6. Fogler, H.S., 1992. Elements of Chemical Reaction Engineering, 2nd ed., P T R Prentice Hall, New Jersey.

7. Satterfield, C.H., 1975. "Trickle Bed Reactors," AIChE Journal, 21(2): 209-227.

8. Alexander, B.F., Y.T. Shah, 1976. "Gas-Liquid Mass Transfer Coefficients for Concurrent Upflow in Packed Beds - Effect of Packing Shape at Low Flow Rates." The Canadian Journal of Chemical Engineering, 54(December) : 556-559.

9. Mochizuki, S., 1981. "Empirical Expressions of Liquid-Solid Mass Transfer in Concurrent Gas-Liquid Upflow Fixed Beds," Chemical Engineering Science, 37(9) : 1422-1424.

10. Himmelblau, D.M., 1960. "Solubilities of Inert Gases in Water," Journal of Chemical and Engineering Data, 5(January) : 10-15.

11. Perry's Chemical Engineering Handbook, 6th edition, McGraw Hill, Inc., 1984.

12. Hayduk,W. and B.S. Minhas, 1982. "Correlations for Prediction of Molecular Diffusivities in Liquids," The Canadian Journal of Chemical Engineering, 60: 295-299.

13. Smith, J.M., 1981. Chemical Engineering Kinetics, 3rd ed., McGraw-Hill Book Company.

14. Satterfield, C.H., 1977. Mass Transfer in Heterogeneous Catalysis, MIT Press.

15. Rase, H.F., 1990. Fixed-Bed Reactor Design and Diagnostics, Butterworth Publishers.

APPENDIX A - Mathcad Calculations

Effectiveness factor using Theile modulus approach

Effectiveness factor using experimental particle size data and Theile modulus

Effectivenss factor using iterative approach

Gas-liquid mass transfer coefficient

Liquid-solid mass transfer coefficient

Henry's constant

Plug Flow Validation

Theoretical calculation of catalyst effectiveness factors using the Theile modulus
(units: cm-g-gmol-sec-K)

Temperature $T = 377.6K$

Solvent/water data $MW = 46$ $V_b = 129$ $\mu = .00277$

Catalyst properties $R = .059$ $\varepsilon_p = .61$ $r_e = 4.4 \cdot 10^{-7}$ $\tau = 3$ $\rho_p = 2.605$

$S_p = 2.19 \cdot 10^{6}$

Reaction parameters $C_{O2s} = 6.022 \cdot 10^{-5}$ $k_1 = 5.5 \cdot 10^{6}$ Order $n = 2$

$C_{OCs} = 2.54 \cdot 10^{-7}$

Ordinary binary diffusion $D_{12} = 7.4 \cdot 10^{-10} \cdot \frac{T \cdot (2.6 \cdot MW)^{.5}}{\mu \cdot V_b^{.6}}$ Wilke-Chang Model

Knudsen pore diffusion $D_{Knudsen} = 9700 \cdot r_e \cdot \sqrt{\frac{T}{MW}}$

Total diffusion coefficient $D_{overall} = \frac{1}{\left(\frac{1}{D_{Knudsen}} + \frac{1}{D_{12}}\right)}$

Effective diffusivity $D_{eff} = \frac{D_{overall} \cdot \varepsilon_p}{\tau}$

nth-order effectiveness factor for large Theile moduli $\eta = \frac{3}{R} \cdot \sqrt{\frac{2}{n-1} \cdot \frac{D_{eff}}{\rho_p \cdot k_1 \cdot (C_{O2s})^{n-1}}}$

Theoretical effectiveness factor: $\eta = 0.0049$

MK

η

EXPERIMENTAL DETERMINATION OF EFFECTIVENESS FACTORS FOR HETEROGENEOUS CATALYSIS

This document calculates the experimental effectiveness factor of a solid catalyst via a non-linear fitting routine to the appropriate Thiele moduli. It uses the nth-order functions t determine the effectiveness factor from data for two different particle sizes, for either a sla or sphere.

Particle geometry (0 = slab, 1 = sphere) $pg := 1$ Order $n := 2$

	First experiment	Second experiment
Particle diameter (cm):	$d_1 := .0163$	$d_2 := .119$
Relative reaction rate:	$r_1 := .9 \cdot 10^{-5}$	$r_2 := 1.1 \cdot 10^{-4}$

$i := 0..30 \quad fi_i := 10^{\frac{i-10}{10}} \quad slab(\Phi) := \frac{\tanh(\Phi)}{\Phi} \quad sphere(\Phi) := \left(\frac{3}{n+1}\right)^{\frac{1}{2}} \cdot \frac{1}{\Phi} \cdot \left(\frac{1}{\tanh(3\cdot\Phi)}\right) - \left(\frac{1}{3\cdot\Phi}\right)$

$\eta(\Phi, pg) := if(pg=0, slab(\Phi), if(pg=1, sphere(\Phi), 0))$

$eta_i := \eta(fi_i, pg)$

Initial guess: $\Phi_1 := 1 \qquad \Phi_2 := \frac{d_2}{d_1}$

Given $\frac{\Phi_1}{d_1} = \frac{\Phi_2}{d_2} \qquad \frac{\eta(\Phi_1, pg)}{r_1} = \frac{\eta(\Phi_2, pg)}{r_2}$

$\begin{pmatrix} fi_1 \\ fi_2 \end{pmatrix} := Find(\Phi_1, \Phi_2)$

$E := \eta(fi_1, pg) \qquad e := \eta(fi_2, pg)$

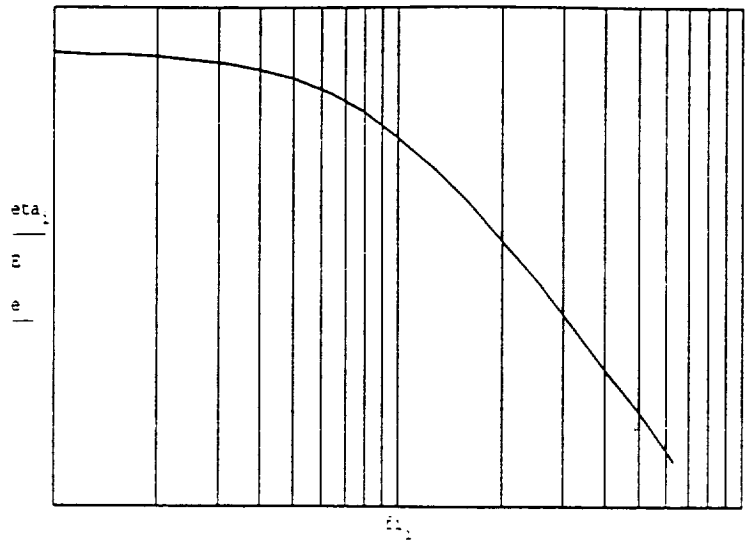

The effectiveness factors are:

E = 0.06 (small particles) e = 0.008 (large particles)

Determination of effectivenss factor using iterative approach for one catalyst size for ethanol over the raw catalyst.

Given : $i := 0..1$

$Rate := 1.9514 \cdot 10^{-8} \cdot \frac{mole}{sec \cdot gm}$

$T_{isothermal} := 366.48 \cdot K$

$V_l := 100 \cdot \frac{cm^3}{min}$

$t_{contact} := 3.08 \cdot sec$

$\varepsilon_{pellet} := 0.61$ (Pellet Porosity)

$\tau := 3$ (Tortuosity)

$MW_{EtOH} := 46.07$

$MW_{O2} := 32.0$

$a := 219.1 \cdot \frac{m^2}{gm}$ (External surface area)

$ksa_{EtOH} := 0.165 \cdot sec^{-1}$

$ksa_{O2} := 0.258 \cdot sec^{-1}$

$\rho_{cat} := 1.022 \cdot \frac{gm}{cm^3}$

$\rho_{pellet} := 2.6046 \cdot \frac{gm}{cm^3}$

$n := 2$ (Reaction Order)

$r_e := 4.382 \cdot 10^{-7} \cdot cm$ (Mean pore radius)

$D_{O2} := 1.167 \cdot 10^{-4} \cdot \frac{cm^2}{sec}$

$D_{EtOH} := 5.993 \cdot 10^{-5} \cdot \frac{cm^2}{sec}$

$d_p := 0.112 \cdot cm$

Liquid Phase Concentrations:

$C_{O2} := 7.0544 \cdot 10^{-5} \cdot \frac{mole}{cm^3}$

$C_{EtOH} := 4.8518 \cdot 10^{-5} \cdot \frac{mole}{cm^3}$

Provide initial guess for eta

$\eta_{guess} := .00771$

$C_{O2s} := 5.0 \cdot 10^{-6} \cdot \frac{mole}{cm^3}$

$C_{EtOHs} := 5.0 \cdot 10^{-6} \cdot \frac{mole}{cm^3}$

From experimental results:

$\eta k := 552650 \cdot \frac{cm^6}{mole \cdot gm \cdot sec}$

$k := \frac{\eta k}{\eta_{guess}}$

$k = 7.168 \cdot 10^{7} \cdot gm^{-1} \cdot cm^{6} \cdot sec^{-1}$

Surface Concentrations of Oxygen and Ethanol:

(Solved from boundary conditions at surface of the catalyst)

Given

$$C_{O2s} = \frac{C_{O2} \cdot ksa_{O2}}{\rho_{cat} \cdot \eta_{guess} \cdot k \cdot C_{EtOHs} - ksa_{O2}}$$

$$C_{EtOHs} = \frac{C_{EtOH} \cdot ksa_{EtOH}}{3 \cdot \rho_{cat} \cdot \eta_{guess} \cdot k \cdot C_{O2s} - ksa_{EtOH}}$$

$$C_s = \text{Find}(C_{O2s}, C_{EtOHs})$$

C_{s_1}

$6.022 \cdot 10^{-5} \cdot cm^{-3}$
$7.833 \cdot 10^{-8} \cdot cm^{-3}$

$C_{O2sf} = C_{s_0}$ $C_{EtOHsf} = C_{s_1}$

$C_{O2sf} = 6.022 \cdot 10^{-5} \cdot cm^{-3} \cdot mole$

$C_{EtOHsf} = 7.833 \cdot 10^{-8} \cdot cm^{-3} \cdot mole$

Calculate Knudsen Diffusivity:

$$D_{KO2} = 9700 \cdot r_e \cdot \sqrt{\frac{T_{isothermal}}{MW_{O2} \cdot K}} \cdot \frac{cm}{sec}$$

$D_{KO2} = 0.014 \cdot cm^2 \cdot sec^{-1}$

Calculate Overall Diffusivty

$$D_{OAO2} = \frac{1}{D_{KO2}^{-1} - D_{O2}^{-1}}$$

$D_{OAO2} = 1.158 \cdot 10^{-2} \cdot cm^2 \cdot sec^{-1}$

Calculate Effective Diffusivity

$$D_{effO2} = \frac{D_{OAO2} \cdot \varepsilon_{pellet}}{\tau}$$

$$D_{effO2} = 2.354 \cdot 10^{-5} \cdot cm^{2} \cdot sec^{-1}$$

Calculate Thiele Modulus

Initial Guess : $\Phi = 50$

$$\Phi = root\left(\eta_{guess} \cdot \Phi - \tanh(\Phi), \Phi\right)$$

$$\Phi = 129.702$$

$$k_s = \left(\frac{\Phi \cdot 2}{d_p} \cdot \left(\frac{n-1}{2}\right)^{-0.5^{-2}}\right) \cdot \frac{D_{effO2}}{\rho_{pellet} \cdot C_{O2sf}}$$

$$k_s = 5.367 \cdot 10^{5} \cdot gm^{-1} \cdot cm^{6} \cdot sec^{-1}$$

Check to see if equality holds (F1=F2 ?)

$$F1 = k_s \cdot \eta_{guess} \qquad F2 = \frac{Rate}{C_{O2sf} \cdot C_{EtOHsf}} \qquad \eta k = 5.527 \cdot 10^{5} \cdot gm^{-1} \cdot cm^{6} \cdot sec^{-1}$$

$$F1 = 4.138 \cdot 10^{3} \cdot gm^{-1} \cdot cm^{6} \cdot sec^{-1} \qquad F2 = 4.137 \cdot 10^{3} \cdot gm^{-1} \cdot cm^{6} \cdot sec^{-1}$$

Determination of gas to liquid overall mass transfer coefficient : (Alexander and Shah, 1976)

$i := 0..2 \quad j := 0..4$

$\alpha := 0.06371$
$B := 0.3014$
$Y := 0.4484$

$R := 8.206 \cdot 10^{-5} \cdot \frac{atm \cdot m^3}{mole \cdot K}$

$\varepsilon := 0.6076$
$D := 0.953 \cdot cm$
$L := 7.14 \cdot cm$

$\rho_{water} := 1000 \cdot \frac{kg}{m^3}$

$P_f := 81.7 \cdot psi$
$P_{stp} := 14.7 \cdot psi$
$T_{stp} := 298.15 \cdot K$

$V_{stp} := 0.793 \cdot \frac{cm^3}{sec}$

$d_1 := 1.68 \cdot mm \qquad d_2 := 0.707 \cdot mm$

$d_p := \frac{d_1 - d_2}{\ln\left(\frac{d_1}{d_2}\right)}$

$d_p = 1.12418 \cdot mm$

$T_{F_j} :=$

200
220
240
250
270

degrees F

$T_j := \left(\frac{T_{F_j} - 32}{1.8} - 273.15\right) \cdot K$

$V_{l_i} :=$

$100 \cdot \frac{cm^3}{min}$
$80 \cdot \frac{cm^3}{min}$
$60 \cdot \frac{cm^3}{min}$

$A := \pi \cdot \left(\frac{D}{2}\right)^2$

$A = 7.133 \cdot 10^{-5} \cdot m^2$

$MW_{O2} := 3.2 \cdot 10^{-2} \cdot \frac{kg}{mole}$

T_j

$366.483 \cdot K$
$377.594 \cdot K$
$388.706 \cdot K$
$394.261 \cdot K$
$405.372 \cdot K$

$V_{g_j} = \frac{T_j \cdot P_{stp} \cdot V_{stp}}{T_{stp} \cdot P_f}$

$u_g = \frac{V_g}{A \cdot \varepsilon}$

$u_{l_i} = \frac{V_{l_i}}{A \cdot \varepsilon}$

V_{g_j}

$1.754 \cdot 10^{-7} \cdot m^3 \cdot sec^{-1}$
$1.807 \cdot 10^{-7} \cdot m^3 \cdot sec^{-1}$
$1.86 \cdot 10^{-7} \cdot m^3 \cdot sec^{-1}$
$1.887 \cdot 10^{-7} \cdot m^3 \cdot sec^{-1}$
$1.94 \cdot 10^{-7} \cdot m^3 \cdot sec^{-1}$

u_{g_j}

$0.00405 \cdot m \cdot sec^{-1}$
$0.00417 \cdot m \cdot sec^{-1}$
$0.00429 \cdot m \cdot sec^{-1}$
$0.00435 \cdot m \cdot sec^{-1}$
$0.00448 \cdot m \cdot sec^{-1}$

u_{l_i}

$0.038 \cdot m \cdot sec^{-1}$
$0.031 \cdot m \cdot sec^{-1}$
$0.023 \cdot m \cdot sec^{-1}$

$\rho_{O2_j} = \frac{P_f}{T_j \cdot R} \cdot MW_{O2}$

$V_{G_j} = \rho_{O2_j} \cdot u_{g_j}$

$V_{L_i} = u_{l_i} \cdot \rho_{water}$

ρ_{O2_j}

$5.915 \cdot kg \cdot m^{-3}$
$5.741 \cdot kg \cdot m^{-3}$
$5.577 \cdot kg \cdot m^{-3}$
$5.499 \cdot kg \cdot m^{-3}$
$5.348 \cdot kg \cdot m^{-3}$

V_{G_j}

$0.024 \cdot kg \cdot m^{-2} \cdot sec^{-1}$
$0.024 \cdot kg \cdot m^{-2} \cdot sec^{-1}$
$0.024 \cdot kg \cdot m^{-2} \cdot sec^{-1}$
$0.024 \cdot kg \cdot m^{-2} \cdot sec^{-1}$
$0.024 \cdot kg \cdot m^{-2} \cdot sec^{-1}$

V_{L_i}

$38.455 \cdot kg \cdot m^{-2} \cdot sec^{-1}$
$30.764 \cdot kg \cdot m^{-2} \cdot sec^{-1}$
$23.073 \cdot kg \cdot m^{-2} \cdot sec^{-1}$

$Dim := 1 \cdot \frac{kg}{m^2 \cdot sec}$

$Kla_{i,j} = \frac{\alpha \cdot \left(V_{L_i}\right)^B \cdot \left(V_{G_j}\right)^Y}{Dim^B \cdot Dim^Y \cdot sec}$

$$Kla = \begin{pmatrix} 0.0359 & 0.0359 & 0.0359 & 0.0359 & 0.0359 \\ 0.03356 & 0.03356 & 0.03356 & 0.03356 & 0.03356 \\ 0.03078 & 0.03078 & 0.03078 & 0.03078 & 0.03078 \end{pmatrix} \cdot sec^{-1}$$

Determination of Liquid-Solid Mass Transfer Coefficients : (Mochizuki, 1981)

$i := 0..2$ $\quad j := 0..4$

$d_1 := 1.68 \cdot mm$ $\quad d_2 := 0.707 \cdot mm$

$$d_p := \frac{d_1 - d_2}{\ln\left(\frac{d_1}{d_2}\right)}$$

$d_p = 0.112 \cdot cm$

$V_{l_i} :=$

$100 \cdot \frac{cm^3}{min}$
$80 \cdot \frac{cm^3}{min}$
$60 \cdot \frac{cm^3}{min}$

$T_{F_j} :=$

200
220
240
250
270

degrees F

$$T_j := \left(\frac{T_{F_j} - 32}{1.8} - 273.15\right) \cdot K$$

$T_j =$

366.483·K
377.594·K
388.706·K
394.261·K
405.372·K

$P_f := 81.7 \cdot psi$

$P_{stp} := 14.7 \cdot psi$ $\quad T_{stp} := 298.15 \cdot K$

$\varepsilon := 0.6076$ $\quad V_{stp} := 0.793 \cdot \frac{cm^3}{sec}$

$D := 9.53 \cdot mm$

$L := 7.1 \cdot cm$ $\quad \mu_g := 0.000258 \cdot \frac{gm}{cm \cdot sec}$

$\Phi := 0.75$ $\quad \rho_l := 1.0 \cdot \frac{gm}{cm^3}$

$$V_{g_j} := \frac{T_j \cdot P_{stp} \cdot V_{stp}}{T_{stp} \cdot P_f}$$

$V_{g_j} =$

$0.175 \cdot cm^3 \cdot sec^{-1}$
$0.181 \cdot cm^3 \cdot sec^{-1}$
$0.186 \cdot cm^3 \cdot sec^{-1}$
$0.189 \cdot cm^3 \cdot sec^{-1}$
$0.194 \cdot cm^3 \cdot sec^{-1}$

$$\mu_j := \exp\left(-24.71 - \frac{4209 \cdot K}{T_j} - 0.04527 \cdot \frac{T_j}{1 \cdot K} - 0.00003376 \cdot \left(\frac{T_j}{1 \cdot K}\right)^2\right) \cdot 0.01 \cdot \frac{gm}{cm \cdot sec}$$

$$\nu_j := \frac{\mu_j}{\rho_l}$$

$\mu_j =$

$0.00311 \cdot gm \cdot cm^{-1} \cdot sec^{-1}$
$0.00277 \cdot gm \cdot cm^{-1} \cdot sec^{-1}$
$0.0025 \cdot gm \cdot cm^{-1} \cdot sec^{-1}$
$0.00238 \cdot gm \cdot cm^{-1} \cdot sec^{-1}$
$0.00218 \cdot gm \cdot cm^{-1} \cdot sec^{-1}$

$\nu_j =$

$0.00311 \cdot cm^2 \cdot sec^{-1}$
$0.00277 \cdot cm^2 \cdot sec^{-1}$
$0.0025 \cdot cm^2 \cdot sec^{-1}$
$0.00238 \cdot cm^2 \cdot sec^{-1}$
$0.00218 \cdot cm^2 \cdot sec^{-1}$

$$a_t := 6 \cdot \frac{1 - \varepsilon}{d_p}$$

$a_t = 20.943 \cdot cm^{-1}$

$$A := \pi \cdot \left(\frac{D}{2}\right)^2$$

$A = 0.713 \cdot cm^2$

$$u_g := \frac{V_g}{A \cdot \varepsilon}$$

$u_{g_j} =$

$0.405 \cdot cm \cdot sec^{-1}$
$0.417 \cdot cm \cdot sec^{-1}$
$0.429 \cdot cm \cdot sec^{-1}$
$0.435 \cdot cm \cdot sec^{-1}$
$0.448 \cdot cm \cdot sec^{-1}$

$$u_{l_i} := \frac{V_{l_i}}{A \cdot \varepsilon}$$

$u_{l_i} =$

$3.846 \cdot cm \cdot sec^{-1}$
$3.076 \cdot cm \cdot sec^{-1}$
$2.307 \cdot cm \cdot sec^{-1}$

$$\varepsilon_{g_{i,j}} := \frac{V_{g_j}}{V_{g_j} - V_{l_i}}$$

$$\varepsilon_{l_{i,j}} := \left(1 - \varepsilon_{g_{i,j}}\right)$$

$$\varepsilon_l = \begin{pmatrix} 0.905 & 0.902 & 0.9 & 0.898 & 0.896 \\ 0.884 & 0.881 & 0.878 & 0.876 & 0.873 \\ 0.851 & 0.847 & 0.843 & 0.841 & 0.838 \end{pmatrix}$$

$$A_p := 4 \cdot \pi \cdot \left(\frac{d_p}{2}\right)^2 \cdot \Phi$$

$A_p = 0.03 \cdot cm^2$

$$d_{pe} := \sqrt{\frac{A_p}{\pi}}$$

$d_{pe} = 0.097 \cdot cm$

$$\mu_{25} = \exp\left(24.71 - \frac{4209 \cdot K}{298.15 \cdot K} - 0.04527 \cdot \frac{298.15 \cdot K}{1 \cdot K} - 0.00003376 \cdot \left(\frac{298.15 \cdot K}{1 \cdot K}\right)^2\right) \cdot 0.01 \cdot \frac{gm}{cm \cdot sec}$$

$$d_{h_{i,j}} = \frac{\varepsilon_{l_{i,j}} \cdot d_{pe}}{1.5 \cdot \left(1 - \varepsilon_{l_{i,j}}\right)} \qquad \mu_{25} = 0.009 \cdot gm \cdot cm^{-1} \cdot sec^{-1}$$

$$d_h = \begin{pmatrix} 0.617 & 0.599 & 0.582 & 0.573 & 0.558 \\ 0.493 & 0.479 & 0.465 & 0.459 & 0.446 \\ 0.37 & 0.359 & 0.349 & 0.344 & 0.335 \end{pmatrix} \cdot cm$$

Literature Diffusion Coefficients at 25 degrees C

$$D_{O2} = 3.25 \cdot 10^{-5} \cdot \frac{cm^2}{sec} \qquad D_{O2_j} = \frac{D_{O2} \cdot \mu_{25} \cdot T_j}{298.15 \cdot K \cdot \mu_j}$$

$$D_{EtOH} = 1.669 \cdot 10^{-5} \cdot \frac{cm^2}{sec} \qquad D_{EtOH_j} = \frac{D_{EtOH} \cdot \mu_{25} \cdot T_j}{298.15 \cdot K \cdot \mu_j}$$

$$D_{Urea} = 1.37 \cdot 10^{-5} \cdot \frac{cm^2}{sec} \qquad D_{Urea_j} = \frac{D_{Urea} \cdot \mu_{25} \cdot T_j}{298.15 \cdot K \cdot \mu_j}$$

Predict Remaining Diffusivities using Hayduk and Minhas Method

$V_{CB} = 308.1$ cubic cm per mole $\qquad V_{DMSO} = 174.5 \qquad V_{Form} = 99.5$

$$\varepsilon_{CB} = \frac{9.58}{V_{CB}} - 1.12 \qquad \varepsilon_{DMSO} = \frac{9.58}{V_{DMSO}} - 1.12 \qquad \varepsilon_{Form} = \frac{9.58}{V_{Form}} - 1.12$$

$$D_{CB_j} = 1.25 \cdot 10^{-8} \cdot \left(V_{CB}^{-0.19} - 0.292\right) \cdot \left(\frac{\mu_j}{0.01} \cdot cm \cdot \frac{sec}{gm}\right)^{\varepsilon_{CB}} \cdot \left(\frac{T_j}{K}\right)^{1.52} \cdot \frac{cm^2}{sec}$$

$$D_{DMSO_j} = 1.25 \cdot 10^{-8} \cdot \left(V_{DMSO}^{-0.19} - 0.292\right) \cdot \left(\frac{\mu_j}{0.01} \cdot cm \cdot \frac{sec}{gm}\right)^{\varepsilon_{DMSO}} \cdot \left(\frac{T_j}{K}\right)^{1.52} \cdot \frac{cm^2}{sec}$$

$$D_{Form_j} = 1.25 \cdot 10^{-8} \cdot \left(V_{Form}^{-0.19} - 0.292\right) \cdot \left(\frac{\mu_j \cdot cm}{0.01} \cdot \frac{sec}{gm}\right)^{\varepsilon_{Form}} \cdot \left(\frac{T_j}{K}\right)^{1.52} \cdot \frac{cm^2}{sec}$$

D_{O2_j}	D_{EtOH_j}	D_{Urea_j}
$1.167 \cdot 10^{-4} \cdot cm^2 \cdot sec^{-1}$	$5.993 \cdot 10^{-5} \cdot cm^2 \cdot sec^{-1}$	$4.919 \cdot 10^{-5} \cdot cm^2 \cdot sec^{-1}$
$1.348 \cdot 10^{-4} \cdot cm^2 \cdot sec^{-1}$	$6.921 \cdot 10^{-5} \cdot cm^2 \cdot sec^{-1}$	$5.681 \cdot 10^{-5} \cdot cm^2 \cdot sec^{-1}$
$1.538 \cdot 10^{-4} \cdot cm^2 \cdot sec^{-1}$	$7.898 \cdot 10^{-5} \cdot cm^2 \cdot sec^{-1}$	$6.483 \cdot 10^{-5} \cdot cm^2 \cdot sec^{-1}$
$1.637 \cdot 10^{-4} \cdot cm^2 \cdot sec^{-1}$	$8.404 \cdot 10^{-5} \cdot cm^2 \cdot sec^{-1}$	$6.899 \cdot 10^{-5} \cdot cm^2 \cdot sec^{-1}$
$1.84 \cdot 10^{-4} \cdot cm^2 \cdot sec^{-1}$	$9.451 \cdot 10^{-5} \cdot cm^2 \cdot sec^{-1}$	$7.758 \cdot 10^{-5} \cdot cm^2 \cdot sec^{-1}$

D_{CB_j}	D_{DMSO_j}	D_{Form_j}
$1.57249 \cdot 10^{-5} \cdot cm^2 \cdot sec^{-1}$	$2.84519 \cdot 10^{-5} \cdot cm^2 \cdot sec^{-1}$	$4.09014 \cdot 10^{-5} \cdot cm^2 \cdot sec^{-1}$
$1.86314 \cdot 10^{-5} \cdot cm^2 \cdot sec^{-1}$	$3.36194 \cdot 10^{-5} \cdot cm^2 \cdot sec^{-1}$	$4.81025 \cdot 10^{-5} \cdot cm^2 \cdot sec^{-1}$
$2.1784 \cdot 10^{-5} \cdot cm^2 \cdot sec^{-1}$	$3.92118 \cdot 10^{-5} \cdot cm^2 \cdot sec^{-1}$	$5.58652 \cdot 10^{-5} \cdot cm^2 \cdot sec^{-1}$
$2.34516 \cdot 10^{-5} \cdot cm^2 \cdot sec^{-1}$	$4.21654 \cdot 10^{-5} \cdot cm^2 \cdot sec^{-1}$	$5.99542 \cdot 10^{-5} \cdot cm^2 \cdot sec^{-1}$
$2.69697 \cdot 10^{-5} \cdot cm^2 \cdot sec^{-1}$	$4.83875 \cdot 10^{-5} \cdot cm^2 \cdot sec^{-1}$	$6.85468 \cdot 10^{-5} \cdot cm^2 \cdot sec^{-1}$

$$Re_{i,j} = \frac{d_{h_{i,j}} \cdot u_{l_{i,j}}}{\varepsilon_{l_{i,j}} \cdot \nu_j}$$

$$Re_{Lc} = 0.312 \cdot e^{\left(0.341 \cdot \frac{d_{pe}}{1 \cdot cm}\right)}$$

$$Re_{Lc} = 0.323$$

$$Re_{Ls} = 7.77 \cdot e^{\left(0.334 \cdot \frac{d_{pe}}{1 \cdot cm}\right)}$$

$$Re_{Ls} = 8.027$$

$$Re = \begin{matrix} 843.6 & 920.353 & 993.974 & 1.03 \cdot 10^3 & 1.098 \cdot 10^3 \\ 552.755 & 603.43 & 652.111 & 675.669 & 721.236 \\ 322.973 & 352.933 & 381.782 & 395.769 & 422.872 \end{matrix}$$

Temperature Across
Flow Rate Down

$$Sc_{O2_j} = \frac{\mu_j}{\rho_l \cdot D_{O2_j}} \qquad Sc_{EtOH_j} = \frac{\mu_j}{\rho_l \cdot D_{EtOH_j}} \qquad Sc_{Urea_j} = \frac{\mu_j}{\rho_l \cdot D_{Urea_j}}$$

$$Sc_{CB_j} = \frac{\mu_j}{\rho_l \cdot D_{CB_j}} \qquad Sc_{DMSO_j} = \frac{\mu_j}{\rho_l \cdot D_{DMSO_j}} \qquad Sc_{Form_j} = \frac{\mu_j}{\rho_l \cdot D_{Form_j}}$$

Sc_{O2_j}	Sc_{EtOH_j}	Sc_{Urea_j}	Sc_{CB_j}	Sc_{DMSO_j}	Sc_{Form_j}
26.627	51.851	63.167	197.616	109.219	75.975
20.572	40.06	48.802	148.808	82.467	57.637
16.261	31.665	38.576	114.806	63.78	44.767
14.566	28.365	34.555	101.652	56.537	39.762
11.844	23.063	28.096	80.819	45.046	31.798

$$k_{O2_{i,j}} = 0.75 \cdot \left(Re_{i,j}\right)^{0.5} \cdot \left(Sc_{O2_j}\right)^{\frac{1}{3}} \cdot \frac{D_{O2_j}}{d_{h_{i,j}}} \qquad ksa_{O2_{i,j}} = k_{O2_{i,j}} \cdot a_t$$

$$k_{EtOH_{i,j}} = 0.75 \cdot \left(Re_{i,j}\right)^{0.5} \cdot \left(Sc_{EtOH_j}\right)^{\frac{1}{3}} \cdot \frac{D_{EtOH_j}}{d_{h_{i,j}}} \qquad ksa_{EtOH_{i,j}} = k_{EtOH_{i,j}} \cdot a_t$$

$$k_{Urea_{i,j}} = 0.75 \cdot \left(Re_{i,j}\right)^{0.5} \cdot \left(Sc_{Urea_j}\right)^{\frac{1}{3}} \cdot \frac{D_{Urea_j}}{d_{h_{i,j}}} \qquad ksa_{Urea_{i,j}} = k_{Urea_{i,j}} \cdot a_t$$

$$k_{CB_{i,j}} = 0.75 \cdot \left(Re_{i,j}\right)^{0.5} \cdot \left(Sc_{CB_j}\right)^{\frac{1}{3}} \cdot \frac{D_{CB_j}}{d_{h_{i,j}}} \qquad ksa_{CB_{i,j}} = k_{CB_{i,j}} \cdot a_t$$

$$k_{DMSO_{i,j}} = 0.75 \cdot \left(Re_{i,j}\right)^{0.5} \cdot \left(Sc_{DMSO_j}\right)^{\frac{1}{3}} \cdot \frac{D_{DMSO_j}}{d_{h_{i,j}}} \qquad ksa_{DMSO_{i,j}} = k_{DMSO_{i,j}} \cdot a_t$$

$$k_{Form_{i,j}} = 0.75 \cdot \left(Re_{i,j}\right)^{0.5} \cdot \left(Sc_{Form_j}\right)^{\frac{1}{3}} \cdot \frac{D_{Form_j}}{d_{h_{i,j}}} \qquad ksa_{Form_{i,j}} = k_{Form_{i,j}} \cdot a_t$$

$$ksa_{O2} = \begin{pmatrix} 0.258 & 0.294 & 0.332 & 0.351 & 0.392 \\ 0.261 & 0.298 & 0.336 & 0.356 & 0.397 \\ 0.266 & 0.303 & 0.343 & 0.363 & 0.405 \end{pmatrix} \cdot sec^{-1}$$

Temperature - across
Flow - Down

$$ksa_{EtOH} = \begin{pmatrix} 0.165 & 0.189 & 0.213 & 0.225 & 0.251 \\ 0.167 & 0.191 & 0.215 & 0.228 & 0.254 \\ 0.17 & 0.195 & 0.22 & 0.233 & 0.26 \end{pmatrix} \cdot sec^{-1}$$

$$ksa_{Urea} = \begin{pmatrix} 0.145 & 0.165 & 0.187 & 0.198 & 0.22 \\ 0.147 & 0.167 & 0.189 & 0.2 & 0.223 \\ 0.149 & 0.171 & 0.193 & 0.204 & 0.228 \end{pmatrix} \cdot sec^{-1}$$

$$ksa_{CB} = \begin{pmatrix} 0.068 & 0.079 & 0.09 & 0.096 & 0.109 \\ 0.069 & 0.08 & 0.091 & 0.097 & 0.11 \\ 0.07 & 0.081 & 0.093 & 0.099 & 0.113 \end{pmatrix} \cdot sec^{-1}$$

$$ksa_{DMSO} = \begin{pmatrix} 0.101 & 0.116 & 0.133 & 0.142 & 0.161 \\ 0.102 & 0.118 & 0.135 & 0.144 & 0.163 \\ 0.104 & 0.12 & 0.138 & 0.147 & 0.166 \end{pmatrix} \cdot sec^{-1}$$

$$ksa_{Form} = \begin{pmatrix} 0.128 & 0.148 & 0.169 & 0.18 & 0.203 \\ 0.13 & 0.15 & 0.171 & 0.182 & 0.205 \\ 0.132 & 0.153 & 0.174 & 0.186 & 0.21 \end{pmatrix} \cdot sec^{-1}$$

Determination of Dimensionless Henry's Constants fot Oxygen (Himmelblau, 1960)

$i := 1..5$

$T_{F_i} =$

200
220
240
250
270

$$T_{1_i} := \left(\frac{T_{F_i} - 32}{1.8} - 273.15\right)\cdot\frac{1}{1000} \qquad T_i := \left(\frac{T_{F_i} - 32}{1.8} - 273.15\right)$$

T_{1_i}
0.366
0.378
0.389
0.394
0.405

T_i
366.483
377.594
388.706
394.261
405.372

$A := -0.0005943$

$B := -0.1470$

$C := -0.05120$

$D := -0.1076$

$E := 0.8447$

Initial Guess : $H := 1$

$$H_i := \text{root}\left(A\cdot(\log(H))^2 - B\cdot\left(\frac{1}{T_{1_i}}\right)^2 - C\cdot\frac{\log(H)}{T_{1_i}} - D\cdot\log(H) - \frac{E}{T_{1_i}} - 1, H\right)\cdot 10^4$$

H_i
$7.052\cdot10^4$
$6.995\cdot10^4$
$6.826\cdot10^4$
$6.706\cdot10^4$
$6.409\cdot10^4$

$\frac{atm}{mole}$

$$H_{dim_i} := H_i\cdot\frac{18}{(1000\cdot0.0821\cdot T_i)}$$

H_{dim_i}
42.189
40.616
38.501
37.292
34.661

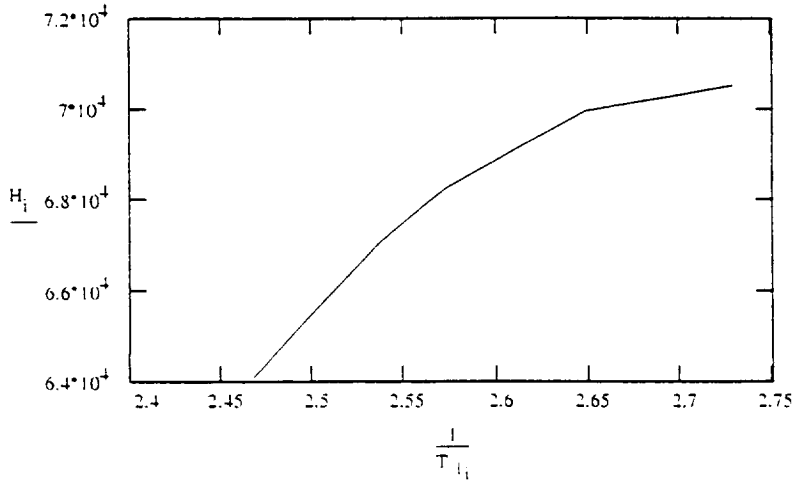

Analysis for Plug Flow vs. Axial Dispersion for VRA

Given:

$$d_p := \frac{1.68 - 0.7}{\ln\left(\frac{1.68}{0.7}\right)} \cdot mm$$ (Log mean average of the particle diameter)

$$d_p = 1.119 \cdot mm$$

$L := 0.5 \cdot m$ (Length of reactor)

$n := 2$ (Reaction order - 1st in OC and Oxygen)

$Pe_r := 4.67$ (Average reactor Peclet number)

$v_l := 120 \cdot \frac{cm^3}{min}$ (Volumetric flow of liquid thorugh VRA

$d_r := 6.043 \cdot cm$ (Diameter of VRA)

$$U := \frac{v_l}{\frac{\pi}{4} \cdot d_r^2}$$ $U = 6.973 \cdot 10^{-4} \cdot m \cdot sec^{-1}$ (Superficial velocity through VRA)

First, we must calculate the axial dispersion coefficient from the reactor Peclet number:

$$D_a := U \cdot \frac{L}{Pe_r}$$ $D_a = 7.466 \cdot 10^{-5} \cdot m^2 \cdot sec^{-1}$ (Axial dispersion coefficient)

From this, we can calculate the fluid Peclet number:

$$Pe_f := d_p \cdot \frac{U}{D_a}$$ $Pe_f = 0.01046$ (Fluid Peclet number)

This number can be used in the criterion listed in Satterfield (1975) to determine if plug flow is a valid assumption. In order to assume plug flow, the following criterion must be satisfied :

$$\frac{L}{d_p} > 20 \cdot \frac{n}{Pe_f} \cdot \ln\left(\frac{1}{1 - X}\right)$$

Assuming best case scenario : $X := 0.999$

$$\frac{L}{d_p} = 446.668$$ $$20 \cdot \frac{n}{Pe_f} \cdot \ln\left(\frac{1}{1 - X}\right) = 2.643 \cdot 10^{4}$$

$i := 0..999 \qquad x_i := \frac{i}{1000}$

$$f(L, d_p, Pe_f, n, X) := \frac{d_p}{L} \cdot \frac{20}{Pe_f} \cdot n \cdot \ln\left(\frac{1}{1 - X}\right)$$

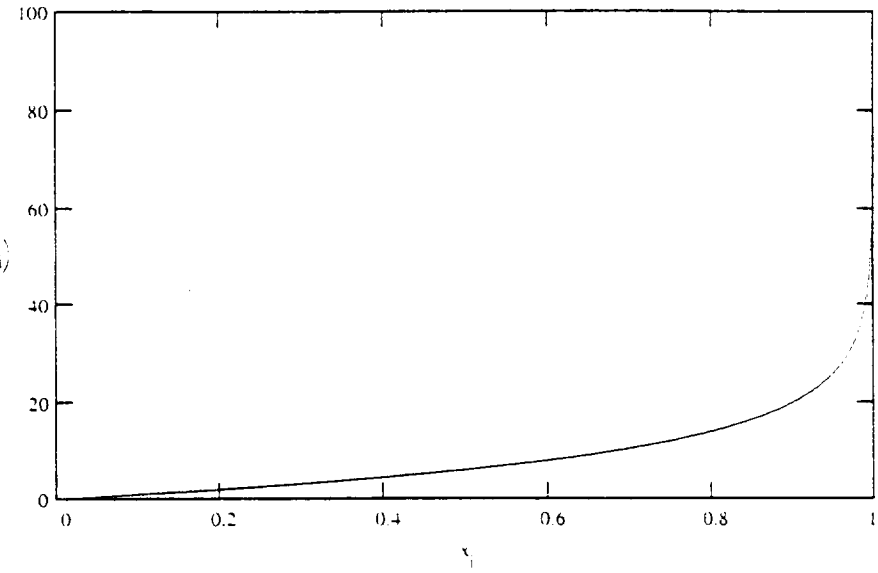

$Pe_{min} := 0.1$

Given

$f(L, d_p, Pe_{min}, n, 0.999) = 1$

$Pe_{min} := \text{find}(Pe_{min})$

$Pe_{min} = 0.619$

Therefore, we must have a fluid Peclet number above 0.619 for plug flow to be assumed. The fluid Peclet number for the VRA is well below this limit and axial dispersion must be taken into account

APPENDIX B - Calibration Curves

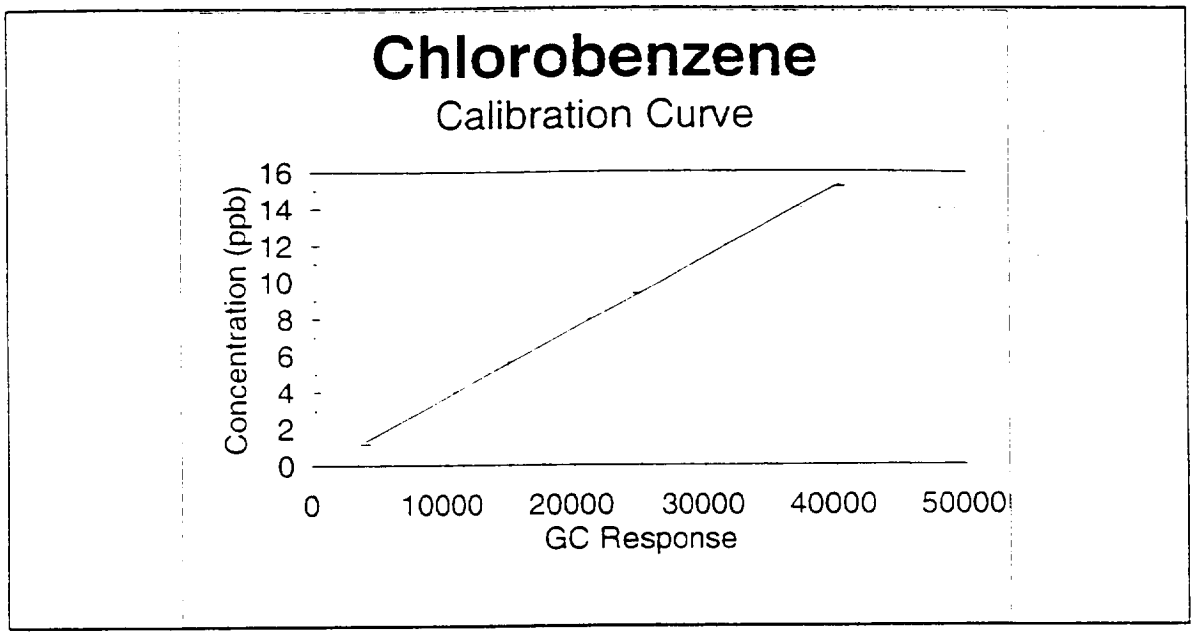
Chlorobenzene
Calibration Curve
Concentration (ppb)
16
14
12
10
8
6
4
2
0
0
10000
20000
30000
40000
50000
GC Response

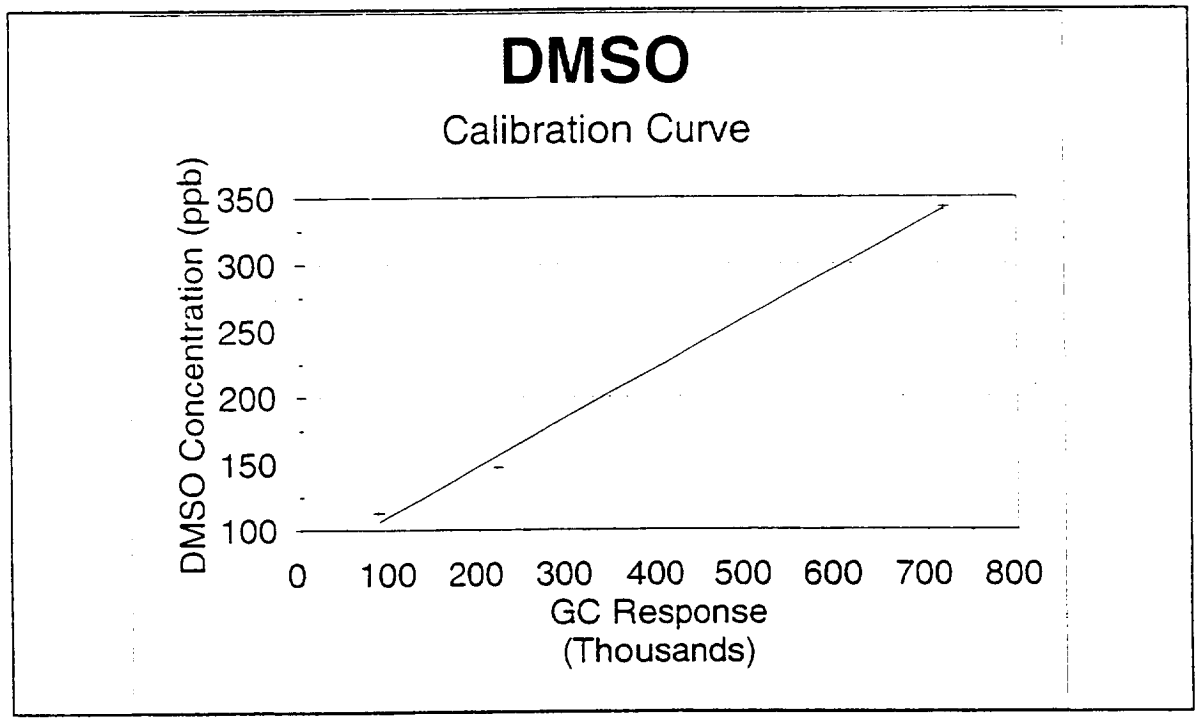
DMSO
Calibration Curve
DMSO Concentration (ppb)
350
300
250
200
150
100
0
100
200
300
400
500
600
700
800
GC Response
(Thousands)

```
          DO 18 I=J+1,N
            A(I,J)=A(I,J)*DUM
18        CONTINUE
        ENDIF
19      CONTINUE
        RETURN
        END
```

APPENDIX C - Spreadsheet Data

Chlorobenzene

thru test RXR

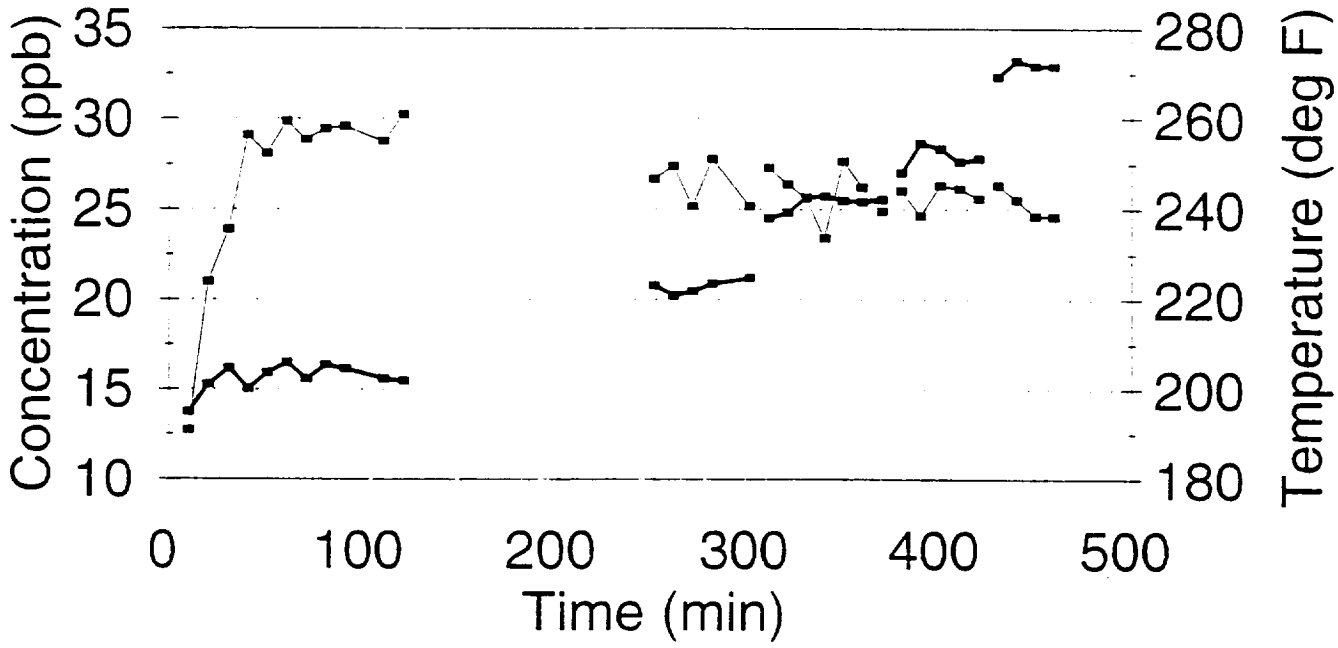

Date : 4/6/95
Experiment : Chlorobenzene thru Test Column w/ raW catalyst
File . tcb3.wb1
Operator : Louis Kindt

Chlorobenzene	Slope	Intercept	GC Response	Co (ppm, ppb)
Sample A	0.000333	-0.012839	92280	30.69578
Sample B	0.000333	-0.012839	85080	28.29979

Time (min)	Column Temp (deg F)	System Pressure (psig)	Liquid Flow Rate (ml/min)	pH	Chloro-benzene GC Response	Chloro-benzene Conc. (ppb)	CONVERSION									
10.1	195.068	67.969	98.871	4.679	38280	12.72585	0.58542									
20.1	201.172	67.852	100.048	4.775	63150	21.002	0.315802									
30.1	204.834	68.159	103.823	4.905	71860	23.90048	0.221376									
40.1	200.195	67.881	101.503	4.932	87460	29.0918	0.052254									
50.1	203.857	67.676	94.335	4.988	84460	28.09347	0.084778									
60.1	206.055	67.72	98.351	5.056	89760	29.85718	0.02732									
70.1	202.393	68.086	97.174	4.957	86800	28.87217	0.059409									
80.1	205.566	67.427	97.901	5.074	88560	29.45785	0.040329									
90.1	204.59	67.749	104.377	5.164	88920	29.57765	0.036426									
110.1	202.393	67.588	98.732	5.015	86380	28.7324	0.063963									
120.1	201.904	67.617	97.624	5.166	90860	30.22324	0.015394									
130.1	202.393	67.529	84.258	5.053	90020	29.94371		0.024501								
140.1	204.102	67.09	80.033	5.541	86640	28.81892		0.061144								
150.1	199.707	67.251	79.756	5.362	83900	27.90711		0.090849								
160.1	201.172	67.354	79.722	5.576	85560	28.45952		0.072852								
170.1	202.881	67.617	80.449	4.994	80000	26.60928		0.133129								
180.1	203.857	67.163	76.744	5.095	83180	27.66751		0.098654								
190.1	200.928	67.017	58.183	5.091	66480	22.11015			0.279701							
200.1	203.125	66.899	60.538	5.449	71900	23.91379			0.220942							
210.1	201.416	66.899	58.287	5.127	79320	26.383			0.140501							
220.1	199.463	66.855	61.092	5.165	78840	26.22326			0.145705							
230.1	225.342	67.075	59.499	5.014	79240	26.35637			0.141368							
240.1	205.078	66.914	60.884	5.265	72700	24.18002			0.212269							
250.1	223.145	67.075	94.716	5.09	80160	26.66253				0.057854						
260.1	220.947	67.207	101.156	5.101	82380	27.40129				0.031749						
270.1	221.924	67.441	96.482	5.114	75640	25.15838				0.111005						
280.1	223.633	67.822	96.897	5.034	83540	27.78731				0.018109						
300.1	224.854	67.5	101.018	5.281	75760	25.19831				0.109594						
310.1	238.037	67.749	96.482	5.369	82080	27.30146					0.035277					
320.1	239.258	67.061	95.651	5.428	79380	26.40296					0.067026					
330.1	242.676	67.588	100.464	5.205	77060	25.63092					0.094307					
340.1	242.92	67.544	94.646	5.409	70380	23.40797					0.172857					
350.1	241.943	67.749	94.577	5.239	83280	27.70079					0.021166					
360.1	241.699	67.061	100.533	5.44	78780	26.2033					0.074082					
370.1	242.187	67.646	99.044	5.279	74820	24.8855					0.120647					
380.1	248.047	67.471	94.404	5.289	78260	26.03025						0.080196				
390.1	254.639	67.632	97.174	5.487	74080	24.63925						0.129349				
400.1	253.418	67.632	100.983	5.197	79160	26.32975						0.069613				
410.1	250.488	67.573	99.252	5.21	78620	26.15005						0.075963				
420.1	251.221	67.5	98.005	5.466	76940	25.59099						0.095718				
430.1	269.451	67.69	99.806	5.228	79180	26.33641							0.069378			
440.1	272.949	67.646	102.299	5.496	76720	25.51778							0.098305			
450.1	271.729	68.203	99.979	5.456	73960	24.59931							0.13076			
460.1	271.729	67.778	97.347	5.295	73860	24.56604							0.131936			

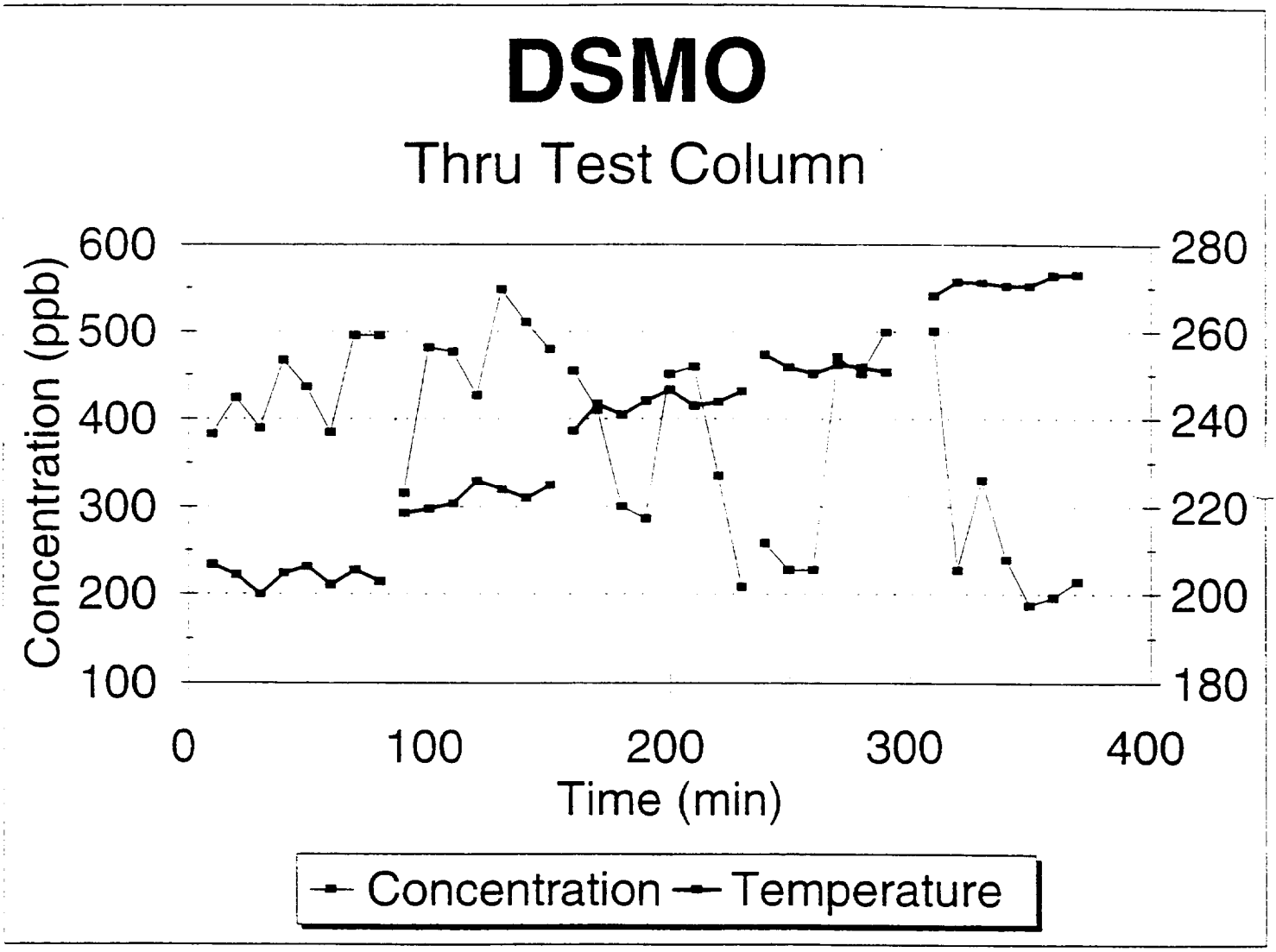
DSMO
Thru Test Column
Concentration (ppb)
600
500
400
300
200
100
280
260
240
220
200
180
0
100
200
300
400
Time (min)
Concentration
Temperature

Date : 3/27/95
Experiment : DMSO thru Test column w/raw catalyst
File : tdmso1.wb1
erator : Louis Kindt

	Slope	Intercept	GC Response	Co (ppm, ppb)
DMSO	0.000371	74.18412	929400	419.23514

Time (min)	Column Temp (deg F)	System Pressure (psig)	Liquid Flow Rate (ml/min)	pH	DSMO Response	DMSO Conc. (ppb)	Conversion				AVG FLOW
9.75	206.787	66.929	101.156	4.201	830400	382.48019	0.0876714				99.7574
19.75	204.346	66.782	98.317	4.182	944000	424.65557	-0.012929				101.2803
29.75	199.951	67.002	92.049	3.833	849600	389.60842	0.0706685				100.3384
39.75	204.834	66.87	98.871	4.299	1058000	466.97945	-0.113884				98.16667
49.75	206.299	66.577	97.867	4.479	975200	436.23895	-0.040559				100.4589
59.75	202.148	66.768	99.806	4.574	837400	385.07903	0.0814725				
69.75	205.566	66.987	102.368	4.193	1134000	495.19537	-0.181188				
79.75	202.881	67.354	99.875	4.591	1134000	495.19537	-0.181188				
89.75	218.506	67.207	100.672	4.605	649200	315.20749		0.248137			
99.75	219.482	67.251	101.226	4.473	1097000	481.45867		-0.14842			
109.75	220.703	67.324	108.29	4.102	1083000	476.261		-0.13602			
119.75	225.83	67.163	98.802	5.021	949800	426.80889		-0.01807			
129.75	223.877	67.134	98.317	5.146	1279000	549.02838		-0.3096			
139.75	221.924	67.617	100.083	4.682	1174000	510.04586		-0.21661			
149.75	224.854	66.885	101.572	4.562	1091000	479.2311		-0.14311			
159.75	237.305	67.075	101.849	5.031	1025000	454.7278			-0.08466		
169.75	243.408	67.28	100.325	4.8	904800	410.10209			0.021785		
179.75	240.967	67.163	98.975	4.777	609200	300.35701			0.28356		
189.75	244.141	67.441	101.814	4.886	570500	285.98917			0.317831		
199.75	246.582	67.705	100.672	4.84	1014000	450.64392			-0.07492		
209.75	242.92	67.69	102.334	4.667	1038000	459.55421			-0.09617		
219.75	243.896	67.383	96.932	4.807	702800	335.10714			0.20067		
229.75	246.338	66.724	99.806	4.814	362400	208.72952			0.502118		
239.75	254.639	66.636	94.785	4.72	496500	258.51577				0.383363	
249.75	251.709	66.929	97.797	4.806	412600	227.36688				0.457663	
259.75	250.244	67.573	95.997	4.796	414500	228.07227				0.45598	
269.75	252.441	66.943	99.217	4.903	1068000	470.69207				-0.12274	
279.75	251.709	67.061	100.152	4.882	1016000	451.38644				-0.07669	
289.75	250.732	66.68	101.052	4.738	1146000	499.65052				-0.19181	
309.75	268.311	67.178	100.464	4.991	1148000	500.39304					-0.19359
319.75	271.484	67.749	97.451	4.847	411700	227.03274					0.45846
329.75	271.24	67.192	101.399	4.808	690200	330.42924					0.211828
339.75	270.508	67.002	104.896	5.13	444900	239.35864					0.429059
349.75	270.508	67.09	98.351	4.402	305400	187.56758					0.552596
359.75	272.949	66.826	100.637	4.77	329400	196.47787					0.531342
369.75	273.193	67.163	100.014	4.671	377700	214.40983					0.488569

Date : 4/4/95
Experiment : Ethanol thru differential column over freash raw catalyst
File : tetoh4.wb1
Operator : Louis Kindt

	Slope	Intercept	GC Response	Co (ppm. ppb)
Ethanol (A)	0.000259	0.153773	96005	25.00021
Ethanol (B)	0.000259	0.153773	65488	17.102301

Time (min)	Column Temp (deg F)	System Pressure (psig)	Liquid Flow Rate (ml/min)	pH	Ethanol GC Response	Ethanol Conc. (ppm)	Conversion							
9.95	200.439	67.808	96.447	5.075	41227	10.82347	0.5670649					99.49914	3.024134	204.2063
19.95	204.59	68.364	98.767	4.866	59610	15.58105	0.3767631					97.4994	1.099015	223.8282
29.95	204.834	67.69	105.727	4.981	66318	17.31711	0.3073215					97.52617	1.544443	240.1123
39.95	201.66	67.983	103.961	4.944	78845	20.55914	0.1776413					98.61975	2.263881	250.8545
49.95	208.008	68.057	103.857	4.845	82690	21.55424	0.1378376					98.8778	0.959067	271.3526
59.95	206.543	68.086	94.508	5.186	84280	21.96574	0.1213779							
69.95	202.148	68.232	96.966	4.945	85559	22.29675	0.1081376							
79.95	202.637	68.159	101.087	4.808	86070	22.429	0.1028477							
89.95	203.125	67.559	102.507	4.828	85283	22.22532	0.1109947							
99.95	200.928	68.086	98.04	4.757	86003	22.41166	0.1035413							
109.95	206.055	68.013	99.529	4.549	85951	22.3982	0.1040796							
119.95	205.811	67.544	86.024	4.679	86470	22.53252		0.098707						
129.95	202.148	67.28	80.587	4.728	84877	22.12024		0.115198						
139.95	196.777	67.749	78.96	4.701	85158	22.19297		0.112289						
149.95	200.928	67.646	80.83	4.612	85228	22.21108		0.111564						
159.95	200.684	67.529	78.717	4.988	85813	22.36248		0.105508						
169.95	200.684	67.559	78.96	4.878	84929	22.1337		0.114659						
179.95	201.172	67.441	79.202	4.831	84573	22.04157		0.118345						
189.95	205.566	67.397	79.133	4.832	85221	22.20927		0.111637						
199.95	198.242	67.28	59.776	4.746	84289	21.96807			0.121285					
209.95	199.219	67.603	57.975	4.761	83684	21.81149			0.127548					
219.95	204.346	67.324	61.681	4.826	81705	21.29932			0.148034					
229.95	201.172	67.397	59.811	4.493	82051	21.38887			0.144453					
239.95	201.172	67.236	61.854	4.589	83354	21.72609			0.130964					
249.95	221.68	67.822	95.373	3.994	57863	15.12892				0.115387				
259.95	225.586	67.441	98.074	3.892	58368	15.25962				0.107745				
269.95	224.365	67.529	97.936	3.985	58179	15.21071				0.110605				
279.95	225.098	67.28	97.624	4.207	57929	15.14601				0.114388				
289.95	222.412	67.72	98.49	3.983	57941	15.14911				0.114206				
299.95	237.305	67.603	100.533	3.877	53611	14.02849					0.179731			
309.95	241.455	67.852	98.421	4.469	54178	14.17523					0.171151			
319.95	239.99	67.661	97.07	4.137	54043	14.14029					0.173193			
329.95	242.92	67.295	96.135	3.756	52990	13.86777					0.189128			
339.95	238.037	67.441	96.828	3.813	53133	13.90478					0.186964			
349.95	240.967	67.866	96.17	4.551	51859	13.57507					0.206243			
359.95	249.512	67.91	99.39	4.481	50957	13.34163						0.219893		
369.95	248.291	67.793	96.482	4.745	51691	13.53159						0.208786		
379.95	251.953	67.925	96.62	4.575	52374	13.70835						0.19845		
389.95	253.662	67.5	101.987	4.457	51612	13.51114						0.209981		
399.95	269.52	67.5	99.148	4.573	48331	12.66201							0.259631	
409.95	271.569	67.397	98.317	4.502	48134	12.61102							0.262612	
419.95	272.461	67.866	98.005	4.586	48579	12.72619							0.255878	
429.95	271.484	67.661	100.637	4.473	48186	12.62448							0.261826	
439.95	271.729	67.91	98.282	4.423	48228	12.63535							0.26119	

Ethanol

thru test column

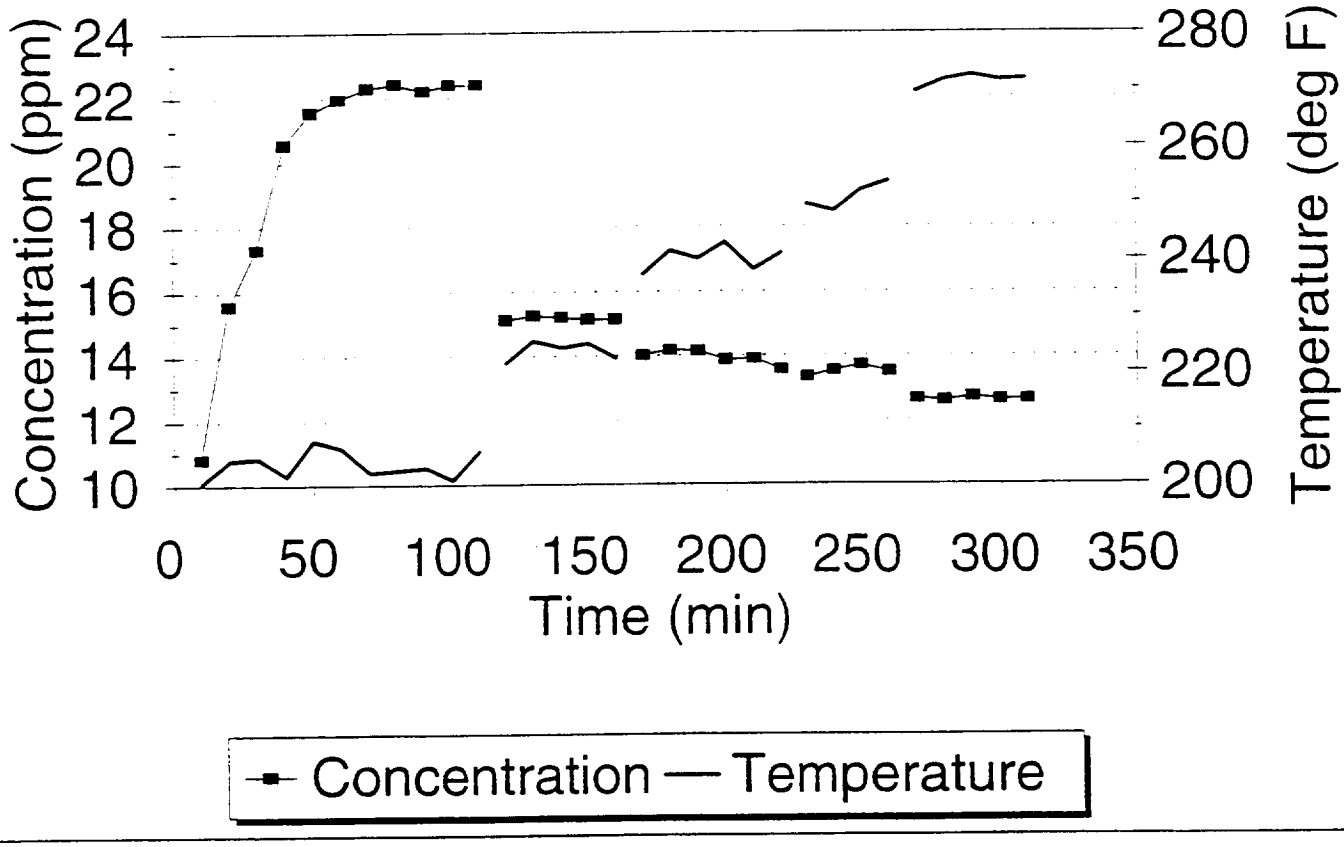

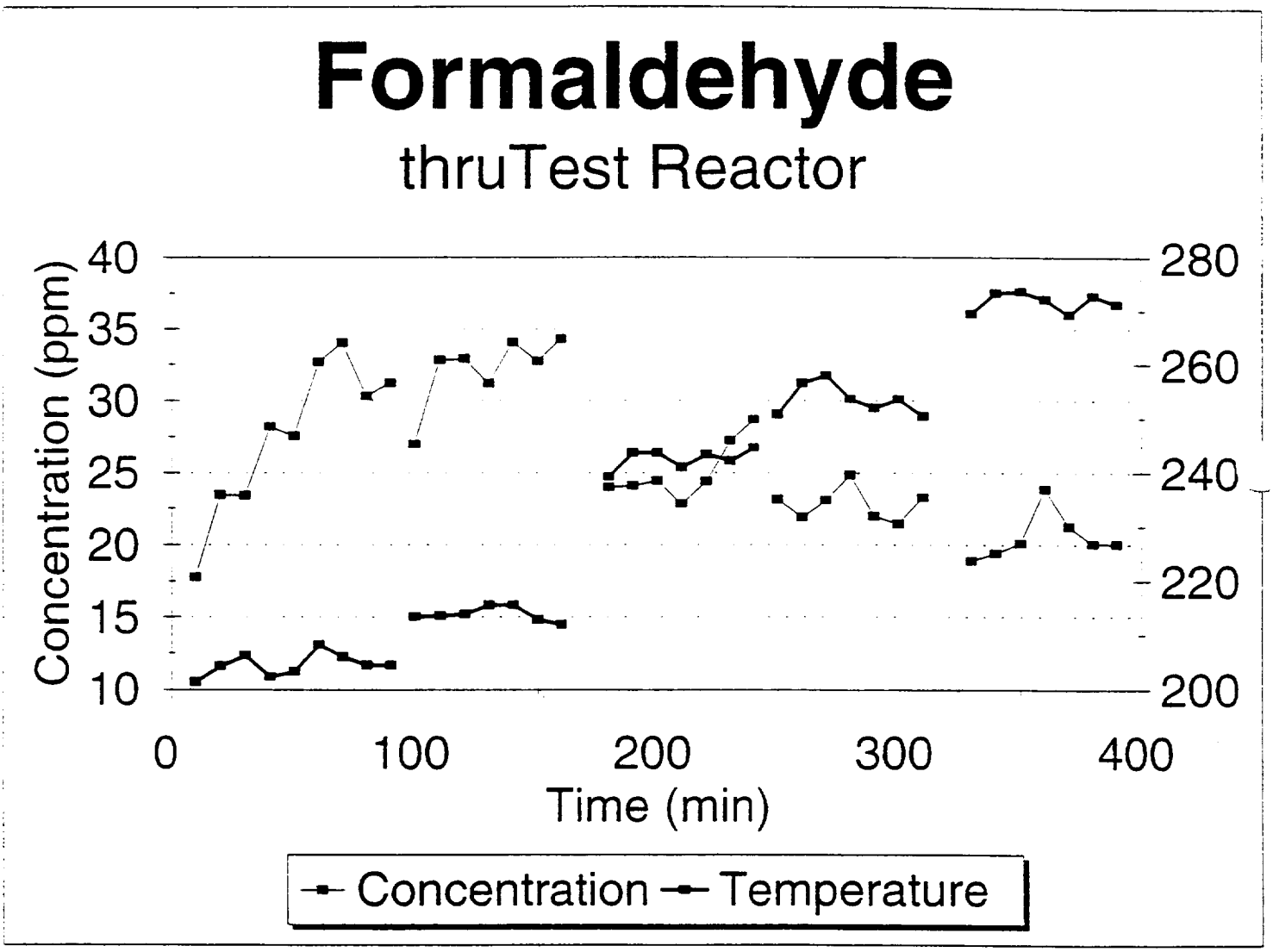
Formaldehyde
thruTest Reactor
Concentration (ppm)
40
35
30
25
20
15
10
280
260
240
220
200
0
100
200
300
400
Time (min)
Concentration
Temperature

Date : 3/16/95
Experiment Formaldehyde thru test column w/raw catalyst
File : tform1.wb1
rator : Louis Kindt

Formaldehyde Background Correction (GC Response)		IS Conc. (ppb)	IS Response	Form Response	Corrected Response	Co (ppb)
16039	F.aldehyde	21.32	154204	3213093	3197054	110.5049

Time (min)	(deg F)	System Pressure (psig)	Liquid Flow Rate (ml/min)	pH	F.Aldehyde IS Response	F.Aldehyde GC Response	Corrected Form GC Response	F.Aldehyde Conc. (ppb)	F.Aldehyde Coversion				
9.85	201.416	66.855	95.373	3.818	154296	529963	513924	17.752987	0.8393466				
19.85	204.346	67.324	98.975	3.94	151616	682893	666854	23.442986	0.7878557				
29.85	206.299	67.324	100.221	4.281	154043	692665	676626	23.411752	0.7881383				
39.85	202.393	67.397	96.689	3.8	153163	826429	810390	28.201189	0.7447969				
49.85	203.369	67.295	99.425	3.852	152153	802337	786298	27.544434	0.7507402				
59.85	208.252	67.925	99.252	3.958	153779	959481	943442	32.699822	0.7040871				
69.85	206.055	67.646	101.953	3.911	153972	999947	983908	34.059632	0.6917817				
79.85	204.59	68.027	100.637	3.58	152887	885641	869602	30.316369	0.7256559				
89.85	204.59	67.529	100.845	3.545	153771	917016	900977	31.229604	0.7173917				
99.85	213.379	67.397	99.737	3.539	155591	802878	786839	26.954335		0.75608			
109.85	213.623	68.027	98.213	3.431	152048	952009	935970	32.810166		0.703089			
119.85	213.867	67.617	99.46	3.603	152167	956207	940168	32.931552		0.70199			
129.85	215.576	67.749	101.987	3.543	153966	916709	900670	31.179423		0.717846			
139.85	215.576	67.617	101.503	3.165	152295	989587	973548	34.072102		0.691669			
149.85	212.891	67.5	97.382	3.611	153791	960808	944769	32.74326		0.703694			
159.85	211.914	67.617	96.759	3.555	155690	1018182	1002143	34.308062		0.689534			
179.85	239.258	67.925	101.503	3.552	152740	702362	686323	23.94986			0.783269		
189.85	243.652	67.969	102.818	3.463	155304	717838	701799	24.085591			0.782041		
199.85	243.652	67.793	99.148	3.579	152606	714920	698881	24.409497			0.779109		
209.85	240.967	68.188	99.737	3.78	152286	668308	652269	22.829372			0.793409		
219.85	243.408	67.427	103.511	3.711	151870	710836	694797	24.38446			0.779336		
229.85	242.187	67.852	100.879	3.521	152367	794168	778129	27.219986			0.753676		
239.85	244.629	68.057	101.745	3.779	152445	836132	820093	28.673264			0.740525		
249.85	250.732	67.471	101.018	3.701	152492	678587	662548	23.157811				0.790436	
259.85	256.592	67.559	99.252	3.578	152438	642476	626437	21.903392				0.801788	
269.85	258.057	67.412	100.879	3.632	153510	681153	665114	23.093333				0.79102	
279.85	253.662	67.705	100.395	3.682	154356	734961	718922	24.824783				0.775351	
289.85	251.953	67.954	102.126	3.876	152700	645272	629233	21.963405				0.801245	
299.85	253.662	67.559	100.498	3.914	153326	633063	617024	21.449317				0.805897	
309.85	250.488	67.749	100.775	3.974	153975	688185	672146	23.267012				0.789448	
329.85	269.531	67.632	98.732	3.819	153709	561115	545076	18.901008					0.828958
339.85	273.437	67.573	97.209	3.624	155081	581126	565087	19.421552					0.824247
349.85	273.682	67.881	102.576	3.756	152710	592134	576095	20.107304					0.818042
359.85	272.217	67.456	99.91	3.942	153116	701273	685234	23.853139					0.784144
369.85	269.287	67.456	102.576	3.7	153373	627562	611523	21.251574					0.807687
379.85	272.949	67.822	104.204	3.665	155238	600894	584855	20.080632					0.818283
389.85	271.24	67.954	100.187	3.739	150062	580372	564333	20.044348					0.818611

Date : 3/21/95
Experiment : Urea thru Test Column
File : turea1.wb1
Operator : Louis Kindt

	Slope	Intercept	HPLC Response	Co (ppm))
Urea	0.028588	-0.220178	184.9033	5.065851

Time (min)	Column Temp (deg F)	System Pressure (psig)	Liquid Flow Rate (ml/min)	pH	HPLC Response	Urea Conc. (ppm)	Conversion				
9.95	199.463	69.741	101.503	5.238	110.4729	2.938029	0.420032				
19.95	205.078	68.73	100.637	4.67	148.3733	4.021529	0.206149				
29.95	204.346	68.613	94.404	4.768	115.2921	3.075799	0.392837				
39.95	201.904	69.097	99.286	4.692	125.7067	3.373532	0.334064				
49.95	203.369	65.947	102.645	4.827	147.5692	3.998541	0.210687				
59.95	205.811	67.148	100.568	4.598	126.0453	3.383214	0.332153				
69.95	200.928	67.573	101.191	4.781	166.6467	4.543928	0.103028				
79.95	203.125	67.31	96.239	4.465	200.9067	5.523355	-0.090311				
89.95	205.078	66.973	95.131	4.656	124.4353	3.337186	0.341239				
99.95	218.262	66.65	95.131	4.319	174.9367	4.780923		0.056245			
109.95	222.656	67.427	98.559	4.361	165.3067	4.50562		0.11059			
119.95	218.262	66.797	93.4	4.367	143.5133	3.882591		0.233576			
129.95	224.121	67.148	96.655	4.493	156.5133	4.254235		0.160213			
139.95	223.877	67.368	94.889	4.718	159.77	4.347337		0.141835			
149.95	221.191	67.09	95.616	4.691	152.0033	4.125303		0.185664			
159.95	223.389	67.251	97.382	4.642	114.4867	3.052774		0.397382			
169.95	222.9	66.958	98.144	4.682	82.8695	2.148901		0.575807			
179.95	238.525	67.119	95.547	4.64	161.47	4.395937			0.132241		
189.95	241.455	67.266	99.598	4.656	113.7327	3.03122			0.401637		
199.95	242.432	67.734	99.806	4.64	180.67	4.944828			0.02389		
209.95	243.652	67.266	98.455	4.962	189.2567	5.190304			-0.02457		
219.95	238.77	67.002	94.75	4.632	127.8133	3.433758			0.322175		
229.95	239.746	67.192	100.464	4.723	177.98	4.867926			0.03907		
239.95	244.141	67.471	96.689	4.367	182.45	4.995715			0.013845		
249.95	247.07	67.588	101.884	4.447	143.9078	3.893869				0.23135	
259.95	251.709	67.28	97.486	4.909	176.7	4.831333				0.046294	
269.95	252.686	67.09	98.802	4.521	110.9459	2.951551				0.417363	
279.95	251.221	67.075	99.944	4.913	126.8133	3.40517				0.327819	
289.95	250.488	67.148	99.737	4.644	150.5333	4.083279				0.19396	
299.95	250.244	66.973	92.499	4.749	87.1124	2.270197				0.551863	
319.95	268.799	66.943	97.486	4.594	102.3699	2.70638					0.46576
329.95	269.531	67.075	101.191	4.504	113.2933	3.018659					0.404116
339.95	272.949	67.207	95.997	4.418	90.85887	2.377301					0.53072
349.95	270.752	67.119	97.382	4.34	163.7391	4.460806					0.119436
359.95	270.996	66.577	97.001	4.3	129.3721	3.47832					0.313379
369.95	269.531	67.456	98.421	4.517	62.3077	1.561078					0.691843

Urea thru Test RXR

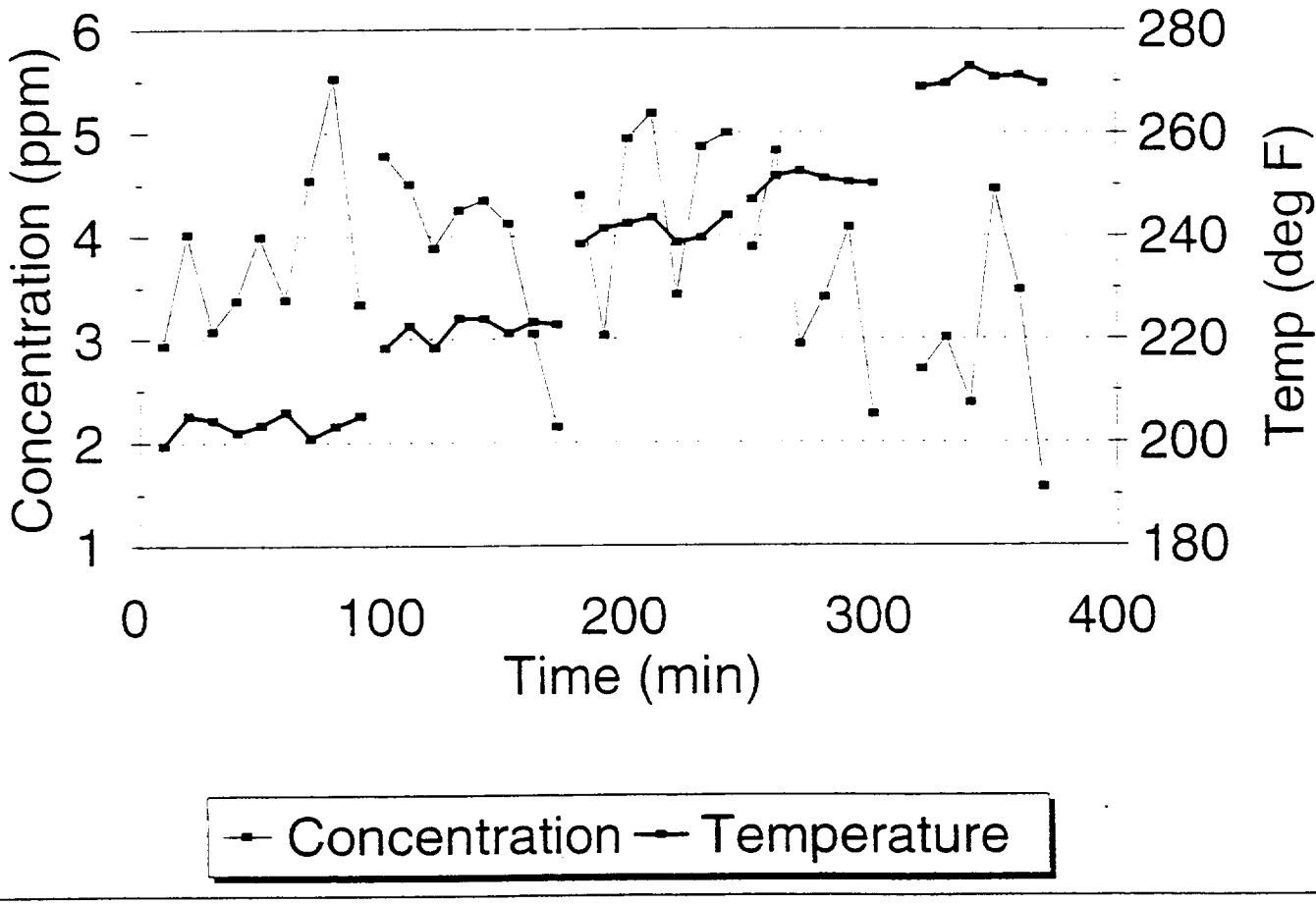

APPENDIX D - Modeling Program Printouts

```
      PROGRAM MASST
      EXTERNAL GOLDSEC

      CHARACTER * 20 GFN, RFN

      DOUBLE PRECISION KSAO2, KSAS(10),ALPHA(10),KLAO2,RHO,T,P,DIA,VL,
     +VGSTP,HL, CONCG, K(10)
      INTEGER CHOICE, NORGCONT

      COMMON/TEMP/TK
      DOUBLE PRECISION DP,PSTP,VG,TR,EPSILON,TSTP,MUG,RHOL, ETA,R,TK,
     +NU,AT,AREA,UG,UL,AP, DPE,DH,MU25, DO2,DETOH,DUREA, VCB, VDMSO,
     +VFORM,ECB,EDMSO,EFORM , DO2T, DETOHT, DUREAT,DCBT,DDMSOT,DFORMT,
     +RE,RELC, RELS, SC(15), SCO2, ALP, B, Y, RHOO2,VVG,VVL, PI,DFLT,
     +TOL, A, OBJ,H, MU
      PARAMETER (PI = 3.14159265359)

      RFN = 'MASS-P.OUT'
      GFN = 'MASST.OUT'

      OPEN (UNIT=4, FILE = RFN, ACCESS='sequential',STATUS='old')
      READ (4,*) T
      READ (4,*) P
      READ (4,*) DIA
      READ (4,*) VL
      READ (4,*) VGSTP
      READ (4,*) NORGCONT
      READ (4,*) CHOICE

      CLOSE (UNIT=4)


C     CATALYST PROPERTIES AND OTHER CONSTANTS
      EPSILON = 0.6076
      RHO = 1.022
      ETA = 0.07
      DP = 0.112
      AT = 6*(1.0-EPSILON)/DP
      R = 10.73
      TR = T+459
      TK = ((T-32)/1.8)+273.15
      PSTP = 14.7
      TSTP = 298.15
      RHOL = 1.0
      MUG = 0.000258
      MU25 = 0.009
      DO2 = 3.25D-5
      DETOH = 1.699D-5
      DUREA = 1.37D-5
      VDMSO = 174.5
      VFORM = 99.5
      VCB = 308.1

C     CALCULATE GAS PHASE VOLUMETRIC FLOW RATE
      VG = (TK*PSTP*VGSTP)/(TSTP*P)

C     CALUCLATE VISCOSITY OF WATER

      MU = 0.01*EXP(-24.71+(4209.0/TK)+(0.04527*TK)-0.00003376*(TK)**2.)
      NU = MU/RHOL

C     CALCULATE COLUMN AREA AND LIQUID AND GAS VELOCITIES
```

```
      AREA = PI*(DIA/2.0)**2.0
      UG = VG/(AREA*EPSILON)
      UL = VL/(AREA*EPSILON)
      HL = VL/(VL+VG)

C     CALCULATE PARAMETERS FOR KSA CORRELATIONS
      AP = PI*0.75*4.0*(DP/2.0)**2.0
      DPE = DSQRT(AP/PI)
      DH = HL*DPE/(1.5*(1.0-HL))

C     CALCULATE TEMPERATURE DEPENTDENT DIFFUSIVITIES
      DO2T=DO2*MU25*TK/(298.15*MU)
      DETOHT = DETOH*MU25*TK/(298.15*MU)
      DUREAT = DUREA*MU25*TK/(298.15*MU)
      ECB = 9.58/VCB-1.12
      EDMSO = 9.58/VDMSO-1.12
      EFORM = 9.58/VFORM-1.12
      DCBT = 1.25D-8*(VCB**(-0.19)-0.292)*(MU/0.01)**ECB*(TK)**1.52
      DDMSOT = 1.25D-8*(VDMSO**(-0.19)-0.292)*(MU/0.01)**EDMSO*(TK)**1.52
      DFORMT = 1.25D-8*(VFORM**(-0.19)-0.292)*(MU/0.01)**EFORM*(TK)**1.52

C     CALCULATE RENOLDS NUMBER

      DH = 0.617
      RE = DH*UL/(HL*NU)
      RELC = 0.312*EXP(0.341*DPE)
      RELS = 7.77*EXP(0.334*DPE)

C     CALCULATE SCHMIDT NUMBER
      SCO2 = MU/(RHOL*DO2T)
      DO 10 I=1,NORGCONT
      IF(CHOICE .EQ. 1) SC(I) = MU/(RHOL*DETOHT)
      IF(CHOICE .EQ. 2) SC(I) = MU/(RHOL*DCBT)
      IF(CHOICE .EQ. 3) SC(I) = MU/(RHOL*DDMSOT)
      IF(CHOICE .EQ. 4) SC(I) = MU/(RHOL*DFORMT)
      IF(CHOICE .EQ. 5) SC(I) = MU/(RHOL*DUREAT)
      IF(CHOICE .EQ. 6 .AND. I .EQ. 1) SC(I) = MU/(RHOL*DETOHT)
      IF(CHOICE .EQ. 6 .AND. I .EQ. 2) SC(I) = MU/(RHOL*DCBT)
      IF(CHOICE .EQ. 6 .AND. I .EQ. 3) SC(I) = MU/(RHOL*DDMSOT)
      IF(CHOICE .EQ. 6 .AND. I .EQ. 4) SC(I) = MU/(RHOL*DFORMT)
      IF(CHOICE .EQ. 6 .AND. I .EQ. 5) SC(I) = MU/(RHOL*DUREAT)
10    CONTINUE

CALCULATE MASS TRANSFER COEFFICIENTS

      IF(RE.GT.RELS) THEN

      KSAO2 = AT*0.75*DSQRT(RE)*(SCO2**(1.0/3.0))*DO2T/DH
      DO 20 I=1,NORGCONT
      IF(CHOICE.EQ.1) KSAS(I)=AT*0.75*DSQRT(RE)*(SC(I)**(1./3.))
     +*DETOHT/DH
      IF(CHOICE.EQ.2) KSAS(I)=AT*0.75*DSQRT(RE)*(SC(I)**(1./3.))
     +*DCBT/DH
      IF(CHOICE.EQ.3) KSAS(I)=AT*0.75*DSQRT(RE)*(SC(I)**(1./3.))
     +*DDMSOT/DH
      IF(CHOICE.EQ.4) KSAS(I)=0.4013
      IF(CHOICE.EQ.5) KSAS(I)=AT*0.75*DSQRT(RE)*(SC(I)**(1./3.))
     +*DUREAT/DH
      IF(CHOICE.EQ.6.AND.I.EQ.1) KSAS(I)=AT*0.75*DSQRT(RE)*
     +(SC(I)**(1./3.))*DETOHT/DH
      IF(CHOICE .EQ. 6 .AND. I .EQ. 2) KSAS(I)=AT*0.75*DSQRT(RE)*
     +(SC(I)**(1./3.))*DCBT/DH
```

```
      IF(CHOICE .EQ. 6 .AND. I .EQ. 3) KSAS(I)=AT*0.75*DSQRT(RE)*
     +(SC(I)**(1./3.))*DDMSOT/DH
      IF(CHOICE .EQ. 6 .AND. I .EQ. 4) KSAS(I)=3.135*AT*0.75*DSQRT(RE)*
     +(SC(I)**(1./3.))*DFORMT/DH
      IF(CHOICE .EQ. 6 .AND. I .EQ. 5) KSAS(I)=AT*0.75*DSQRT(RE)*
     +(SC(I)**(1./3.))*DUREAT/DH
20    CONTINUE

      ELSE IF(RE.GT.RELC.AND.RE.LT.RELS) THEN

      KSAO2 = AT*0.55*DPE*(RE**0.14)*SCO2**(1./3.)*
     + DO2T/DH
      DO 30 I=1,NORGCONT
      IF(CHOICE .EQ. 1) KSAS(I)=AT*0.55*DPE*(RE**0.14)*SC(I)**(1./3.)*
     + DETOHT/DH
      IF(CHOICE .EQ. 2) KSAS(I)=AT*0.55*DPE*(RE**0.14)*SC(I)**(1./3.)*
     +DCBT/DH
      IF(CHOICE .EQ. 3) KSAS(I)=AT*0.55*DPE*(RE**0.14)*SC(I)**(1./3.)*
     +DDMSOT/DH
      IF(CHOICE .EQ. 4) KSAS(I)=AT*0.55*DPE*(RE**0.14)*SC(I)**(1./3.)*
     +DFORMT/DH
      IF(CHOICE .EQ. 5) KSAS(I)=AT*0.55*DPE*(RE**0.14)*SC(I)**(1./3.)*
     +DUREAT/DH
      IF(CHOICE.EQ.6.AND.I.EQ.1) KSAS(I)=AT*0.55*DPE*(RE**0.14)*
     +SC(I)**(1./3.)*DETOHT/DH
      IF(CHOICE .EQ. 6 .AND. I .EQ. 2) KSAS(I)=AT*0.55*DPE*(RE**0.14)*
     +SC(I)**(1./3.)*DCBT/DH
      IF(CHOICE .EQ. 6 .AND. I .EQ. 3) KSAS(I)=AT*0.55*DPE*(RE**0.14)*
     +SC(I)**(1./3.)*DDMSOT/DH
      IF(CHOICE .EQ. 6 .AND. I .EQ. 4) KSAS(I)=AT*0.55*DPE*(RE**0.14)*
     +SC(I)**(1./3.)*DFORMT/DH
      IF(CHOICE .EQ. 6 .AND. I .EQ. 5) KSAS(I)=AT*0.55*DPE*(RE**0.14)*
     +SC(I)**(1./3.)*DUREAT/DH
30    CONTINUE

      ELSE

      PRINT *, 'PAST LIMITATIONS OF CORRELATIONS - MUST FIND A MORE
     + SUITABLE CORRELATION'
      END IF

C     CALCULATER KLA FOR OXYGEN
      CONCG = 0.0160169*P/(R*TR)
      ALP = 0.06371
      B = 0.3014
      Y = 0.4484
      RHOO2 = CONCG*32.0
      VVG = RHOO2*UG*10
      VVL = RHOL*UL*10
      KLAO2 = ALP*((VVL)**B)*((VVG)**Y)

C     CALCULATE HENRY'S CONSTANT

      A = 1.00
      MAXIT = 10000
      DFLT = 0.00
      TOL = 1.0E-6
      H = 0.0
      OBJ = 0.0
      CALL GOLDSEC(A, MAXIT, TOL, DFLT, H, OBJ)
      H = H*1.D4*18/(1000*0.0821*TK)
```

```
C CALCULATE RATE CONSTANTS AND EFFECTIVESS FACTORS

      ETA = 1.0
      DO 55 I=1, NORGCONT
      IF(CHOICE .EQ. 1) ALPHA(I) = 3.0
      IF(CHOICE .EQ. 2) ALPHA(I) = 7.0
      IF(CHOICE .EQ. 3) ALPHA(I) = 4.5
      IF(CHOICE .EQ. 4) ALPHA(I) = 1.0
      IF(CHOICE .EQ. 5) ALPHA(I) = 1.5
      IF(CHOICE .EQ. 6 .AND. I .EQ. 1) ALPHA(I) = 3.0
      IF(CHOICE .EQ. 6 .AND. I .EQ. 2) ALPHA(I) = 7.0
      IF(CHOICE .EQ. 6 .AND. I .EQ. 3) ALPHA(I) = 4.5
      IF(CHOICE .EQ. 6 .AND. I .EQ. 4) ALPHA(I) = 1.0
      IF(CHOICE .EQ. 6 .AND. I .EQ. 5) ALPHA(I) = 1.5
      IF(CHOICE .EQ. 1) K(I) = 4.063954D13*DEXP(-6763.7/TK)
      IF(CHOICE .EQ. 2) K(I) = 1.051855D9*DEXP(-1115.0/TK)
      IF(CHOICE .EQ. 3) K(I) = 7.753002D34*DEXP(-26194.9/TK)
      IF(CHOICE .EQ. 4) K(I) = 1.0D15
      IF(CHOICE .EQ. 5) K(I) = 3.461048D17*DEXP(-10533/TK)
      IF(CHOICE .EQ. 6 .AND.I.EQ.1) K(I)=4.063954D13*DEXP(-6763.7/TK)
      IF(CHOICE .EQ. 6 .AND.I.EQ.2) K(I)=1.051855D9*DEXP(-1115.0/TK)
      IF(CHOICE .EQ. 6 .AND.I.EQ.3) K(I)=7.753002D34*DEXP(-26194.9/TK)
      IF(CHOICE .EQ. 6 .AND.I.EQ.4) K(I)=1.00D15
      IF(CHOICE .EQ. 6 .AND.I.EQ.5) K(I)=3.461048D17*DEXP(-10533/TK)
55    CONTINUE

      OPEN (UNIT=3, FILE = GFN,ACCESS='sequential',STATUS='unknown')
      ENDFILE 3
      REWIND 3

113   FORMAT(d20.12)
      WRITE(3,113) KSAO2
      WRITE(3,113) KLAO2
      WRITE(3,113) RHO
      WRITE(3,113) VG
      WRITE(3,113) CONCG
      WRITE(3,113) AREA
      WRITE(3,113) H
      WRITE(3,113) ETA
      WRITE(3,113) VL
      WRITE(3,113) HL
      WRITE(3,113) T
      WRITE(3,113) P
      WRITE(3,113) DIA

      DO 114 I=1, NORGCONT
         WRITE(3,113) KSAS(I)
         WRITE(3,113) ALPHA(I)
         WRITE(3,113) K(I)
114   CONTINUE

      CLOSE (UNIT=3)

      RETURN
      END



      REAL*8 FUNCTION OBJFCN(H)
      IMPLICIT REAL*8(A-H,O-Z)
      COMMON/TEMP/TK
```

```
      TD=TK/1000
      A=-0.0005943
      B=-0.1470
      C=-0.05120
      D=-0.1076
      E=0.8447
      OBJFCN=A*(DLOG10(H))**2+B*(1./TD)**2-C*(DLOG10(H))/TD-D*DLOG10(H)+
     +E/TD-1
      RETURN
      END
C
C
      REAL*8 FUNCTION SECT(XVAL,UNC)
      IMPLICIT REAL*8(A-H,O-Z)
      SECT = XVAL - 0.618 * UNC
      RETURN
      END
C
      SUBROUTINE GOLDSEC(A,MAXIT,TOL,DFLT,X,FX)
      IMPLICIT REAL*8(A-H,O-Z)
      EXTERNAL OBJFCN,SECT
      COMMON /GOLD/ RA
      KFLAG = 0
      N = 0
      B = 50
C     F1 = OBJFCN(A)
C     IF(F1.GT.0.0) GOTO 998
C      DO 5 I=1,MAXIT
C          B = B + 0.001
C          F2 = OBJFCN(B)
C          IF(F2.GE.0.0) GOTO 10
C          A = B
C          F1 = F2
C   5  CONTINUE
C      GOTO 998
10    CONTINUE
      UNC = B - A
      IF(UNC.LE.TOL) GOTO 45
      IF(N.EQ.MAXIT) GOTO 999
      IF(N.EQ.0) GOTO 15
      IF(KFLAG.EQ.1) GOTO 30
      GOTO 40
15    CONTINUE
      X1 = SECT(B,-UNC)
      FX1 = OBJFCN(X1)**2
      IF(N.GT.0) GOTO 25
20    CONTINUE
      X2 = SECT(A,UNC)
      FX2 = OBJFCN(X2)**2
25    CONTINUE
      N = N + 1
      IF(FX1.GT.FX2) GOTO 35
      KFLAG = 1
      B = X2
      GOTO 10
30    CONTINUE
      X2 = X1
      FX2 = FX1
      GOTO 15
35    CONTINUE
      KFLAG = 2
      A = X1
```

```
      GOTO 10
40    CONTINUE
      X1 = X2
      FX1 = FX2
      GOTO 20
45    CONTINUE
      FA = OBJFCN(A)**2
      FB = OBJFCN(B)**2
      IF(FA.LE.FB) THEN
        X = A
        FX = FA
      ELSE
        X = B
        FX = FB
      ENDIF
      RETURN

998   WRITE(6,801)
999   WRITE(6,802) N
      X = DFLT
      FX = OBJFCN(X)**2
      RETURN
C
801   FORMAT(//,1X,'** ERROR : ROOT NOT BRACKETED !',//)
802   FORMAT(//,1X,'** ERROR : SUBROUTINE GOLDEN DID NOT FIND THE ROOT A
     &FTER ',I6,'  ITERATIONS;',/,12X,'DEFAULT VALUE IS RETURNED',//)
      END
```

```
      PROGRAM SOLVE

      EXTERNAL DERIVS
      DOUBLE PRECISION Z, ZADD, ZOUT, Y(15),RTOL,ATOL(15),YF(15),
     +RWORK(382)
      CHARACTER * 20 AFN, QFN, GFN, SFN, TFN
      INTEGER NORGCONT,ZSTEPS,IWORK(35)

      COMMON /CNST/ KLAO2,KSAO2,KSAS,A,VL,VG,HL,K,RHO,ETA,ALPHA
      DOUBLE PRECISION KLAO2,KSAO2,KSAS(10),A,VL,VG,HL,K(10),RHO,ETA
      DOUBLE PRECISION ALPHA(10)

      COMMON /CNST1/ TEMP,NTOL,NSTEPS
      DOUBLE PRECISION TEMP(10),NTOL(2)
      INTEGER NSTEPS

      COMMON /CNST2/ CHOICE
      INTEGER CHOICE

      COMMON /CNST3/ H
      DOUBLE PRECISION H

      SFN = 'SOLVE-P.OUT'
      TFN = 'SOLVE.OUT'
      OPEN (UNIT=5, FILE=SFN, ACCESS='sequential', STATUS='old')

      READ (5,*) AFN
      READ (5,*) QFN
      READ (5,*) Z
      READ (5,*) ZF
      READ (5,*) ZSTEPS
      READ (5,*) NORGCONT
      READ (5,*) CHOICE
      READ (5,*) Y(1)

      DO 809 I=1, NORGCONT
         READ (5,*) Y(I+2)
809   CONTINUE
      READ (5,*) RTOL

      DO 811 I=1, NORGCONT+2
         READ (5,*) ATOL(I)
811   CONTINUE

      READ (5,*) NTOL(1)
      READ (5,*) NTOL(2)
      READ (5,*) NSTEPS

      ENDFILE (UNIT=5)
      CLOSE (UNIT=5)


      OPEN( UNIT=1, FILE=AFN, FORM='formatted', ACCESS='sequential'
     +, STATUS='UNKNOWN')
      ENDFILE 1
      REWIND 1

      OPEN( UNIT=2, FILE=QFN, FORM='formatted', ACCESS='sequential'
     +, STATUS='UNKNOWN')
      ENDFILE 2
      REWIND 2
```

```
      GFN = 'MASST.OUT'

      OPEN(UNIT=3, FILE=GFN,ACCESS='sequential', STATUS='old')

      READ(3,*) KSAO2
      READ(3,*) KLAO2
      READ(3,*) RHO
      READ(3,*) VG
      READ(3,*) CONCG
      READ(3,*) A
      READ(3,*) H
      READ(3,*) ETA
      READ(3,*) VL
      READ(3,*) HL
      READ(3,*) T
      READ(3,*) P
      READ(3,*) DIA
      DO 19 I=1, NORGCONT
         READ(3,*) KSAS(I)
         READ(3,*) ALPHA(I)
         READ(3,*) K(I)
19    CONTINUE

      CLOSE (UNIT = 3)

      ZADD = (ZF-Z)/ZSTEPS
      Y(2) = CONCG
      NEQ = 2+NORGCONT
      ZOUT = Z+ZADD
      ITOL = 2
      ITASK = 1
      ISTATE = 1
      IOPT = 1
      LRW = 382
      LIW = 35
      MF = 22

9     FORMAT (1X,A40,E14.6)
      WRITE (1,'(1x,a)') 'Input Parameters'
      WRITE (1,'(1x,a)') '================'
      WRITE (1,9) 'T (degrees F) = ', T
      WRITE (1,9) 'P (psia) = ', P
      WRITE (1,9) 'Diameter (cm) = ',DIA
      WRITE (1,9) 'Initial Time (sec) = ',Z
      WRITE (1,9) 'Final Time (sec) = ',Z+ZSTEPS*ZADD
      WRITE (1,'(1x,a27,i4)') 'No. of steps = ',ZSTEPS
      WRITE (1,9) 'Liquid Phase Oxygen (gmole/cubic cm) = ',Y(1)
      WRITE (1,9) 'Gas Phase Oxygen (gmole/cubic cm) = ',Y(2)
      WRITE (1,'(1x,a,i1)') 'No. of Org. Contaminants = ', NORGCONT
      WRITE (1,'(1x,a)') ' '

      DO 91 I=1,NORGCONT
      IF (CHOICE .EQ. 1) WRITE (1,'(1x,a)') 'Ethanol'
      IF (CHOICE .EQ. 2) WRITE (1,'(1x,a)') 'Chlorobenzene'
      IF (CHOICE .EQ. 3) WRITE (1,'(1x,a)') 'DMSO'
      IF (CHOICE .EQ. 4) WRITE (1,'(1x,a)') 'Formaldehyde'
      IF (CHOICE .EQ. 5) WRITE (1,'(1x,a)') 'Urea'
      IF (CHOICE.EQ.6 .AND. I.EQ.1) WRITE (1,'(1x,a)') 'Ethanol'
      IF (CHOICE.EQ.6 .AND. I.EQ.2) WRITE (1,'(1x,a)') 'Chlorobenzene'
      IF (CHOICE.EQ.6 .AND. I.EQ.3) WRITE (1,'(1x,a)') 'DMSO'
      IF (CHOICE.EQ.6 .AND. I.EQ.4) WRITE (1,'(1x,a)') 'Formaldehyde'
      IF (CHOICE.EQ.6 .AND. I.EQ.5) WRITE (1,'(1x,a)') 'Urea'
```

```
      WRITE (1,'(1x,a)') '==========='
      WRITE (1,9) 'C(t=0) (gmole/cubic cm) = ',Y(I+2)
      WRITE (1,9) 'ksas (1/s) = ',KSAS(I)
      WRITE (1,9) 'k (cm^(6)/gmole gcat s)= ',K(I)
      WRITE (1,9) 'alpha = ',ALPHA(I)
91    WRITE (1,'(1x,a)') '-----------'

      WRITE (1,'(1x,a)') ' '
      WRITE (1,9) 'H = ', H
      WRITE (1,9) 'klao2 (1/s) = ',KLAO2
      WRITE (1,9) 'ksao2 (1/s)= ',KSAO2
      WRITE (1,9) 'area (squared cm)= ',A
      WRITE (1,9) 'vl (ml/sec) = ',VL
      WRITE (1,9) 'vg (ml/s)= ',VG
      WRITE (1,9) 'hl = ',HL
      WRITE (1,9) 'rho (gcat/cubic cm)= ',RHO
      WRITE (1,9) 'eta = ',ETA

      WRITE (1,'(1x,a)') ' '
      WRITE (1,'(1x,a)') 'Tolerance parameters for LSODE routine'
      WRITE (1,'(1x,a)') '======================================'
      WRITE (1,'(1x,a)') ' '
      WRITE (1,9) 'rtol = ',RTOL
      DO 92 I=1,NEQ
92    WRITE (1,'(1x,a22,i1,a,d14.6)') 'atol(',I,') = ',ATOL(I)

      WRITE (1,'(1x,a)') ' '
      WRITE (1,'(1x,a)') 'Tolerance parameters for MNEWT routine'
      WRITE (1,'(1x,a)') '======================================'
      WRITE (1,'(1x,a)') ' '
      WRITE (1,9) 'tolx = ',NTOL(1)
      WRITE (1,9) 'tolf = ',NTOL(2)
      WRITE (1,'(1x,a27,i4)') 'No. of steps = ',NSTEPS


      WRITE (1,'(1x,a)') ' '
      WRITE (1,'(1x,a)') ' '
      WRITE (1,'(1x,a)') ' '
      WRITE (1,'(1x,a)') 'Results'
      WRITE (1,'(1x,a)') '======='
      WRITE (1,'(1x,48A)') '--------------------------------',
     +  '------------------------------------------------',
     +  '----------------------------------------'
2     FORMAT(1X,15A,15A,15A,15A,15A,15A,15A,15A)
      IF (CHOICE .EQ. 1) THEN
      WRITE (1,2) '     t          ','    o21          ',
     +  '    o2g        ','      Ethanol     ','                '
      ELSE IF (CHOICE .EQ. 2) THEN
      WRITE (1,2) '     t          ','    o21          ',
     +  '    o2g        ','  Chlorobenzene  ','                '
      ELSE IF (CHOICE .EQ. 3) THEN
      WRITE (1,2) '     t          ','    o21          ',
     +  '    o2g        ','      DMSO        ','                '
      ELSE IF (CHOICE .EQ. 4) THEN
      WRITE (1,2) '     t          ','    o21          ',
     +  '    o2g        ','  Formaldehyde   ','                '
      ELSE IF (CHOICE .EQ. 5) THEN
      WRITE (1,2) '     t          ','    o21          ',
     +  '    o2g        ','      Urea        ','                '
      ELSE
      WRITE (1,2) '     t          ','    o21          ',
     +  '    o2g        ','      Ethanol     ','  Chlorobenzene  ',
```

```
     +  '     DMSO      ','  Formaldehyde  ','     Urea      '
      ENDIF
      WRITE (1,2) '    (sec)       ','      g-mol/cc     ',
     +  '    g-mol./cc      ','    g-mol./cc   ','    g-mol./cc   ',
     +  '    g-mol./cc      ','    g-mol./cc   ','    g-mol./cc   '
      WRITE (1,'(1x,48A)') '-----------------------------------------',
     + '-------------------------------------------------------------',
     + '----------------------'
      DO 40  IOUT = 1,ZSTEPS
      CALL XSETUN(1)
      CALL LSODE(DERIVS, NEQ, Y, Z, ZOUT, ITOL,RTOL,ATOL,ITASK,
     +  ISTATE, IOPT, RWORK, LRW, IWORK, LIW, JAC,MF,*911)
      IF (ISTATE .LT. 0 ) GOTO 80
      IF (NORGCONT .EQ. 5) THEN
            WRITE (1,20)  Z, Y(1), Y(2), Y(3), Y(4), Y(5), Y(6), Y(7)
            WRITE (2,10) Z,',',Y(1),',',Y(2),',',Y(3),',',Y(4),',',Y(5),
     + ',',Y(6),',',Y(7)
10          FORMAT(1X,E14.6,1A,E14.6,1A,E14.6,1A,E14.6,1A,E14.6,
     +   1A,E14.6,1A,E14.6,1A,E14.6)
20          FORMAT(1X,E14.6,1X,E14.6,1X,E14.6,1X,E14.6,1X,E14.6,
     +   1X,E14.6,1X,E14.6,1X,E14.6)

      ELSE
            WRITE (1,21)  Z, Y(1), Y(2), Y(3)
            WRITE (2,11) Z,',',Y(1),',',Y(2),',',Y(3)
11          FORMAT(1X,E14.6,1A,E14.6,1A,E14.6,1A,E14.6)
21          FORMAT(1X,E14.6,1X,E14.6,1X,E14.6,1X,E14.6)
      END IF
40    ZOUT = ZOUT+ZADD
      DO 69 I = 1, NEQ
         YP(I) = Y(I)
69    CONTINUE

      OPEN(UNIT=7, FILE=TFN, ACCESS='sequential', STATUS='unknown')
      ENDFILE 7
      REWIND 7

      DO 813 I=1, NORGCONT
         WRITE (7,*) Y(I)
813   CONTINUE

      CLOSE (UNIT = 7)


      ENDFILE (UNIT=1)
      CLOSE (UNIT=1)
      ENDFILE (UNIT=2)
      CLOSE (UNIT=2)
      RETURN
80    WRITE (1,90)  ISTATE
90    FORMAT(///22H ERROR HALT.. ISTATE =,I3)
911   WRITE (1,*)
      ENDFILE (UNIT=1)
      CLOSE (UNIT=1)
      ENDFILE (UNIT=2)
      CLOSE (UNIT=2)
      RETURN
      END

      SUBROUTINE DERIVS(NEQ, Z, Y, YDOT,*)
      INTEGER NEQ
      DOUBLE PRECISION Z, Y(NEQ), YDOT(NEQ)
```

```
      COMMON /CNST/ KLAO2,KSAO2,KSAS,A,VL,VG,HL,K,RHO,ETA,ALPHA
      DOUBLE PRECISION KLAO2,KSAO2,KSAS(10),A,VL,VG,HL,K(10),RHO
      DOUBLE PRECISION ETA,ALPHA(10)

      COMMON /CNST1/ X,NTOL,NSTEPS
      DOUBLE PRECISION X(10),NTOL(2)
      INTEGER NSTEPS

      COMMON /CNST3/ H
      DOUBLE PRECISION H

      DO 3 I=1,NEQ-1
3           X(I)=0.D0
      CALL MNEWT(NSTEPS,X,NEQ-1,NTOL(1),NTOL(2),NEQ,Y,*911)
      DO 31 I=1,NEQ-1
31          X(I)=ABS(X(I))
      YDOT(1) = KLAO2*(Y(2)/H-Y(1) - KSAO2*(Y(1)-X(1)))
      YDOT(2) = KLAO2*(Y(1)-Y(2)/H)
      DO 1 I=3,NEQ
1           YDOT(I) = KSAS(I-2)*(X(I-1)-Y(I))
      RETURN
911   RETURN 1
      END


C ============================================================
C THE FOLLOWING SUBROUTINES ARE BASED ON SUBROUTINES GIVEN IN
C "NUMERICAL RECIPIES" BY WILLIAM H. PRESS, SAUL A. TEUKOLSKY
C WILLIAM T. VETTERLING, BRIAN P. FLANNERY. THE PURPOSE OF
C THESE ROUTINES IS TO COMPUTE THE SOLUTION VECTOR OF A SET OF
C NON-LINEAR ALGEBRAIC EQUATIONS.
C ============================================================

      SUBROUTINE MNEWT(NTRIAL,X,N,TOLX,TOLF,M,Y,*)
      INTEGER N,M,NTRIAL,NP
      DOUBLE PRECISION TOLF,TOLX,X(N),Y(M)
      PARAMETER (NP=15)
CU    USES LUBKSB,LUDCMP,USRFUN
      INTEGER I,K,INDX(NP)
      DOUBLE PRECISION D,ERRF,ERRX,FJAC(NP,NP),FVEC(NP),P(NP)
      DO 14  K=1,NTRIAL
      CALL USRFUN(X,N,NP,FVEC,M,Y)
      CALL FDJAC(X,N,FVEC,NP,FJAC,M,Y)
      ERRF=0.D0
      DO 11 I=1,N
        ERRF=ERRF+ABS(FVEC(I))
11    CONTINUE
      IF(ERRF.LE.TOLF)RETURN
      DO 12 I=1,N
        P(I)=-FVEC(I)
12    CONTINUE
      CALL LUDCMP(FJAC,N,NP,INDX,D,*911)
      CALL LUBKSB(FJAC,N,NP,INDX,P)
      ERRX=0.D0
      DO 13 I=1,N
        ERRX=ERRX+ABS(P(I))
        X(I)=X(I)+P(I)
13    CONTINUE
      IF(ERRX.LE.TOLX)RETURN
14    CONTINUE
      WRITE(1,'(a)') 'PROGRAM HALTED DUE TO GREATER THAN MAX.'
```

```
      WRITE(1,'(a)') 'ITERATIONS IN CALCULATING ROOTS  OF THE'
      WRITE(1,'(a)') 'GIVEN SET OF NONLINEAR ALGEBRAIC EQUATIONS...'
  911 RETURN 1
      END



      SUBROUTINE USRFUN(X,N,J,F,M,Y)
      INTEGER N,J,M
      DOUBLE PRECISION X(N),F(J),Y(M)

      COMMON /CNST/ KLAO2,KSAO2,KSAS,A,VL,VG,HL,K,RHO,ETA,ALPHA
      DOUBLE PRECISION KLAO2,KSAO2,KSAS(10),A,VL,VG,HL,K(10),RHO
      DOUBLE PRECISION ETA,ALPHA(10)

      COMMON /CNST2/ CHOICE
      INTEGER CHOICE

      DOUBLE PRECISION TOT1

      IF (CHOICE .EQ. 1) THEN
      TOT1=K(1)*ABS(X(2))*ABS(X(1))
      F(1)=(RHO*HL*ETA*TOT1+KSAO2*ABS(X(1)))-KSAO2*Y(1)
      F(2)=ABS(X(2))*((RHO/ALPHA(1))*ETA*HL*K(1)*ABS(X(1))+
     +KSAS(1))-KSAS(1)*Y(3)
      ENDIF

      IF (CHOICE .EQ. 2) THEN
      TOT1=K(1)*ABS(X(2))*ABS(X(1))
      F(1)=(RHO*HL*ETA*TOT1+KSAO2*ABS(X(1)))-KSAO2*Y(1)
      F(2)=ABS(X(2))*((RHO/ALPHA(1))*ETA*HL*K(1)*ABS(X(1))+
     +KSAS(1))-KSAS(1)*Y(3)
      ENDIF

      IF (CHOICE .EQ. 3) THEN
      TOT1=K(1)*ABS(X(2))*ABS(X(1))
      F(1)=(RHO*HL*ETA*TOT1+KSAO2*ABS(X(1)))-KSAO2*Y(1)
      F(2)=ABS(X(2))*((RHO/ALPHA(1))*ETA*HL*K(1)*ABS(X(1))+
     +KSAS(1))-KSAS(1)*Y(3)
      ENDIF

      IF (CHOICE .EQ. 4) THEN
      TOT1=K(1)*ABS(X(2))*ABS(X(1))
      F(1)=(RHO*HL*ETA*TOT1+KSAO2*ABS(X(1)))-KSAO2*Y(1)
      F(2)=ABS(X(2))*((RHO/ALPHA(1))*ETA*HL*K(1)*ABS(X(1))+
     +KSAS(1))-KSAS(1)*Y(3)
      ENDIF

      IF (CHOICE .EQ. 5) THEN
      TOT1=K(1)*ABS(X(2))*ABS(X(1))
      F(1)=(RHO*HL*ETA*TOT1+KSAO2*ABS(X(1)))-KSAO2*Y(1)
      F(2)=ABS(X(2))*((RHO/ALPHA(1))*ETA*HL*K(1)*ABS(X(1))+
     +KSAS(1))-KSAS(1)*Y(3)
      ENDIF

      IF (CHOICE .EQ. 6) THEN
      TOT1=K(1)*ABS(X(2))*ABS(X(1))+K(2)*ABS(X(3))*ABS(X(1))+
     +K(3)*ABS(X(4))*ABS(X(1))+K(4)*ABS(X(5))*ABS(X(1))+
     +K(5)*ABS(X(6))*ABS(X(1))
      F(1)=(RHO*HL*ETA*TOT1+KSAO2*ABS(X(1)))-KSAO2*Y(1)
```

```
      F(2)=ABS(X(2))*((RHO/ALPHA(1))*ETA*HL*K(1)*ABS(X(1))+
     +KSAS(1))-KSAS(1)*Y(3)
      F(3)=ABS(X(3))*((RHO/ALPHA(2))*ETA*HL*K(2)*ABS(X(1))+
     +KSAS(2))-KSAS(2)*Y(4)
      F(4)=ABS(X(4))*((RHO/ALPHA(3))*ETA*HL*K(3)*ABS(X(1))+
     +KSAS(3))-KSAS(3)*Y(5)
      F(5)=ABS(X(5))*((RHO/ALPHA(4))*ETA*HL*K(4)*ABS(X(1))+
     +KSAS(4))-KSAS(4)*Y(6)
      F(6)=ABS(X(6))*((RHO/ALPHA(5))*ETA*HL*K(5)*ABS(X(1))+
     +KSAS(5))-KSAS(5)*Y(7)
      ENDIF

      RETURN
      END



      SUBROUTINE FDJAC(X,N,FVEC,L,DF,M,Y)
      INTEGER N,M,L,NP
      DOUBLE PRECISION DF(L,L),FVEC(L),X(N),Y(M),EPS
      PARAMETER (NP=15,EPS=1.D-8)
CU    USES USRFUN
      INTEGER I,J
      DOUBLE PRECISION H,TEMP,F(NP)
      DO 12 J=1,N
      TEMP=X(J)
      H=EPS*ABS(TEMP)
      IF(H.EQ.0.D0)H=EPS
      X(J)=TEMP+H
      H=X(J)-TEMP
      CALL USRFUN(X,N,NP,F,M,Y)
      X(J)=TEMP
      DO 11 I=1,N
        DF(I,J)=(F(I)-FVEC(I))/H
11    CONTINUE
12    CONTINUE
      RETURN
      END


      SUBROUTINE LUBKSB(A,N,NP,INDX,B)
      INTEGER N,NP,INDX(N)
      DOUBLE PRECISION A(NP,NP),B(N)
      INTEGER I,II,J,LL
      DOUBLE PRECISION SUM
      II=0
      DO 12 I=1,N
      LL=INDX(I)
      SUM=B(LL)
      B(LL)=B(I)
      IF (II.NE.0)THEN
        DO 11 J=II,I-1
          SUM=SUM-A(I,J)*B(J)
11      CONTINUE
      ELSE IF (SUM.NE.0.D0) THEN
        II=I
      ENDIF
      B(I)=SUM
12    CONTINUE
      DO 14 I=N,1,-1
      SUM=B(I)
      DO 13 J=I+1,N
```

```
        SUM=SUM-A(I,J)*B(J)
13    CONTINUE
      B(I)=SUM/A(I,I)
14    CONTINUE
      RETURN
      END



      SUBROUTINE LUDCMP(A,N,NP,INDX,D,*)
      INTEGER N,NP,INDX(N),NMAX
      DOUBLE PRECISION D,A(NP,NP),TINY
      PARAMETER (NMAX=500,TINY=1.0D-20)
      INTEGER I,IMAX,J,K
      DOUBLE PRECISION AAMAX,DUM,SUM,VV(NMAX)
      D=1.D0
      DO 12 I=1,N
      AAMAX=0.D0
      DO 11 J=1,N
        IF (ABS(A(I,J)).GT.AAMAX) AAMAX=ABS(A(I,J))
11    CONTINUE
      IF (AAMAX.EQ.0.D0) THEN
        WRITE (1,'(a)') 'SINGULAR MATRIX IN LUDCMP'
        RETURN 1
      ENDIF
      VV(I)=1.D0/AAMAX
12    CONTINUE
      DO 19 J=1,N
      DO 14 I=1,J-1
        SUM=A(I,J)
        DO 13 K=1,I-1
          SUM=SUM-A(I,K)*A(K,J)
13      CONTINUE
        A(I,J)=SUM
14    CONTINUE
      AAMAX=0.D0
      DO 16 I=J,N
        SUM=A(I,J)
        DO 15 K=1,J-1
          SUM=SUM-A(I,K)*A(K,J)
15      CONTINUE
        A(I,J)=SUM
        DUM=VV(I)*ABS(SUM)
        IF (DUM.GE.AAMAX) THEN
          IMAX=I
          AAMAX=DUM
        ENDIF
16    CONTINUE
      IF (J.NE.IMAX)THEN
        DO 17 K=1,N
          DUM=A(IMAX,K)
          A(IMAX,K)=A(J,K)
          A(J,K)=DUM
17      CONTINUE
        D=-D
        VV(IMAX)=VV(J)
      ENDIF
      INDX(J)=IMAX
      IF(A(J,J).EQ.0.D0)A(J,J)=TINY
      IF(J.NE.N)THEN
        DUM=1.D0/A(J,J)
```

```
            DO 18 I=J+1,N
              A(I,J)=A(I,J)*DUM
18          CONTINUE
          ENDIF
19        CONTINUE
          RETURN
          END
```